

# Estimation and HAC-based Inference for Machine Learning Time Series Regressions\*

Andrii Babii<sup>†</sup>      Eric Ghysels<sup>‡</sup>      Jonas Striaukas<sup>§</sup>

October 18, 2021

## Abstract

Time series regression analysis in econometrics typically involves a framework relying on a set of mixing conditions to establish consistency and asymptotic normality of parameter estimates and HAC-type estimators of the residual long-run variances to conduct proper inference. This article introduces structured machine learning regressions for high-dimensional time series data using the aforementioned commonly used setting. To recognize the time series data structures we rely on the sparse-group LASSO estimator. We derive a new Fuk-Nagaev inequality for a class of  $\tau$ -dependent processes with heavier than Gaussian tails, nesting  $\alpha$ -mixing processes as a special case, and establish estimation, prediction, and inferential properties, including convergence rates of the HAC estimator for the long-run variance based on LASSO residuals. An empirical application to nowcasting US GDP growth indicates that the estimator performs favorably compared to other alternatives and that the text data can be a useful addition to more traditional numerical data.

**Keywords:** high-dimensional time series, tau-dependence, sparse-group LASSO, Fuk-Nagaev inequality, HAC estimator, Granger causality, text data, mixed frequency data.

**JEL Classifications:** C52, C55, C58

---

\*We thank participants at the Financial Econometrics Conference at the TSE Toulouse, the JRC Big Data and Forecasting Conference, the Big Data and Machine Learning in Econometrics, Finance, and Statistics Conference at the University of Chicago, the Nontraditional Data, Machine Learning, and Natural Language Processing in Macroeconomics Conference at the Board of Governors and the AI Innovations Forum organized by SAS and the Kenan-Flagler Business School as well as Jianqing Fan, Michele Lenza and Dacheng Xiu for comments. All remaining errors are ours.

<sup>†</sup>Department of Economics, University of North Carolina–Chapel Hill - Gardner Hall, CB 3305 Chapel Hill, NC 27599-3305. Email: babii.andrii@gmail.com

<sup>‡</sup>Department of Economics and Kenan-Flagler Business School, University of North Carolina–Chapel Hill. Email: eghysels@unc.edu.

<sup>§</sup>LIDAM UC Louvain and FRS–FNRS Research Fellow. Email: jonas.striaukas@gmail.com.

# 1 Introduction

Time series regression analysis in econometrics typically involves a framework relying on a set of mixing conditions to establish consistency and asymptotic normality of parameter estimates and Heteroskedasticity Autocorrelation Consistent or HAC-type estimators of the residual long-run variances to conduct proper inference. The increased use of machine learning methods by economists does not fall within this framework. The bulk of the machine learning methods assumes i.i.d. regressors and residuals. There have been a number of recent attempts to expand the asymptotic theory to settings involving time series dependent data, mostly for the LASSO estimator. For instance, [Kock and Callot \(2015\)](#) establish oracle inequalities for VAR with i.i.d. errors, [Wong, Li, and Tewari \(2019\)](#) consider  $\beta$ -mixing series with exponential tails, [Wu and Wu \(2016\)](#), [Han and Tsay \(2017\)](#), and [Chernozhukov, Härdle, Huang, and Wang \(2019\)](#) allow for polynomial tails under the functional dependence measure of [Wu \(2005\)](#). They also develop the partialling-out type inference in systems of regression equations.

Despite these efforts, there is no complete asymptotic estimation and HAC-based inference framework for high-dimensional time series regression models under assumptions comparable to the classical GMM and QML estimators. To the best of our knowledge, no existing work provides sharp results for mixing time series with commonly encountered polynomial tails and no existing work provides a complete theory of the HAC estimation of the residual long-run variance. We provide a general asymptotic theory framework for parameter estimation using a class of regularized regressions under weaker than mixing and polynomial tail conditions.<sup>1</sup> [Chernozhukov, Härdle, Huang, and Wang \(2019\)](#) consider the HAC estimator with a Bartlett kernel without developing the supporting theory, while [Feng, Giglio, and Xiu \(2019\)](#) look at HAC estimation for a specific application but do not provide a general asymptotic theory. Our paper develops the debiased inference based on the explicit bias correction and considers the HAC-based estimators of the residual long-run variance, characterizing how the optimal choice of the bandwidth parameter depends on the number of regressors, their dependence properties, as well as the tail features of the DGP.

The regularized regression is particularly attractive for prediction in the big data environment. First, it is directly linked to the objective of minimizing the empirical MSE. At the same time, regularization and shrinkage allow us to improve upon the inadmissible OLS estimator with high-dimensional data. Lastly, LASSO-type esti-

---

<sup>1</sup>Our weak dependence conditions allow for commonly used  $\alpha$ -mixing processes that are not covered by the functional dependence of [Wu \(2005\)](#).

mators solve elegantly the variable selection problem that might be computationally challenging with traditionally used Akaike and Bayesian information criteria.

Several novel contributions are required to achieve our goal. We aim to improve the prediction and estimation accuracy of the classical LASSO estimator incorporating additional structure available for time series data. We consider a general setting where the time series data are not necessarily sampled at the same frequency because in many high dimensional applications one typically encounters such a situation. Indeed, economists increasingly rely on non-standard data, such as textual and imaging data. This type of data is obviously voluminous, think of real-time news as an example, but also most invariably poses challenges in terms of dealing with mixed frequency time series. The object of interest is usually a low-frequency data series, say observed quarterly or monthly, whereas the information flow is both voluminous and high-frequency. For this reason, we present a general regression framework able to handle mixed frequency data, with standard same frequency sampling as a special case.<sup>2</sup>

The time series regressions involve the sparse-group LASSO (sg-LASSO) regularization. The structure represented by groups covers lagged dependent variables and groups of lags for a single (high-frequency) covariate.<sup>3</sup> We establish a new Fuk-Nagaev inequality for  $\tau$ -dependent processes under finite moment conditions. The inequality allows for  $\alpha$ -mixing processes with heavier than Gaussian tails that are commonly used in econometric applications. Building on this inequality, we characterize the non-asymptotic and asymptotic estimation and prediction properties of the sg-LASSO estimator with dependent data, which to the best of our knowledge are new. We also derive the debiased central limit theorem with the explicit bias correction and establish convergence rates of the HAC estimator for the long-run variance based on LASSO residuals.<sup>4</sup> Our results cover the LASSO and the group LASSO

---

<sup>2</sup>Relatively little is known about handling high-dimensional mixed frequency data. Among the exceptions is [Andreou, Gagliardini, Ghysels, and Rubin \(2019\)](#) who study principal component analysis with large dimensional panels and focus on mixed frequency data.

<sup>3</sup>The sparse-group LASSO was introduced by [Simon, Friedman, Hastie, and Tibshirani \(2013\)](#). The idea to apply group structures to time series covariates is novel. In contrast to group LASSO, the sparse-group LASSO promotes sparsity *between* and *within* groups (i.e. lags of time series covariates).

<sup>4</sup>Inference for variations of the LASSO with i.i.d. data have previously been treated by [Belloni, Chernozhukov, and Hansen \(2010\)](#), [Belloni, Chen, Chernozhukov, and Hansen \(2012\)](#), [Belloni, Chernozhukov, and Hansen \(2014\)](#), [van de Geer, Bühlmann, Ritov, and Dezeure \(2014\)](#), [Caner and Kock \(2018\)](#), and [Cai, Zhang, and Zhou \(2019\)](#) among others, see also [Chiang and Sasaki \(2019\)](#) for LASSO with exchangeable arrays, and the excellent review paper [Belloni, Chernozhukov, Chetverikov, Hansen, and Kato \(2018\)](#) for further references on high-dimensional methods in econo-

estimators as a special case. Building on the debiased CLT, we can construct tests for low-dimensional groups of coefficients, including the (mixed-frequency) Granger causality test. The notion of Granger causality is commonly used in the time series analysis and can be formalized in terms of the conditional independence, see [Florens and Mouchart \(1982\)](#) for its comparison to other dynamic notions of causality.<sup>5</sup>

Throughout the paper, we recognize that sub-Gaussian tails and the exact sparsity are overly restrictive and rely on moment restrictions and the approximate sparsity instead. The sg-LASSO estimator also allows us to combine effectively sparse and dense signals, see e.g., [Carrasco and Rossi \(2016\)](#) for ill-posed dense time series regressions. In our treatment, we do not rely on high-level restricted eigenvalue conditions imposed on the sample covariance matrix and characterize directly the impact of its estimation on convergence rates of the sg-LASSO estimator.

An empirical application of great interest to central banks around the world is provided.<sup>6</sup> We study nowcasting low-frequency series – focusing on the key example of US GDP growth – in a data-rich environment, where our data not only includes conventional high-frequency series but also non-standard data generated by textual analysis. The latter type of data is shown to be statistically significant using the newly proposed HAC-based inference. Our nowcasts are superior to those posted by the Federal Reserve Bank of New York which involves proprietary information whereas our models exclusively rely on public domain data, and most importantly involve high dimensional non-conventional data sources.

The rest of the paper is organized as follows. In Section 2 we present the generic regression setting used in the paper. Section 3 we establish non-asymptotic bounds and convergence rates for the estimation and prediction accuracy of the sg-LASSO estimator imposing dependence over time with  $\tau$ -dependence coefficients which can be understood as dependence measures weaker than  $\alpha$ -mixing coefficients in addition to some mild moment restrictions which do not require sub-Gaussianity. Next we cover inference in Section 4. We start with the large sample approximation to the distribution of the sg-LASSO estimator (and as a consequence of the LASSO and the group LASSO) with  $\tau$ -dependent data. We also cover the estimation of the precision

---

metrics.

<sup>5</sup>There exists an extensive literature on the causal inference with machine learning methods within the Rubin Causal Model (static) framework involving a potential outcomes ([Rubin \(1974\)](#)), see [Athey and Imbens \(2019\)](#) for the excellent review and further references.

<sup>6</sup>Recent applications of the LASSO to dependent data include estimation of the global bank connectedness, see [Demirer, Diebold, Liu, and Yilmaz \(2018\)](#); estimation of the structure of social interactions, see [Manresa \(2013\)](#); asset pricing, see [Bryzgalova \(2016\)](#) and [Feng, Giglio, and Xiu \(2019\)](#); estimation of the vector error correction models, see [Liao and Phillips \(2015\)](#) and [Liang and Schienle \(2019\)](#); testing Granger network causality, see [Basu, Shojaie, and Michailidis \(2015\)](#).

matrix, derive the HAC estimator for the LASSO and show that the optimal choice of the bandwidth parameter for the HAC estimator depends on the number of covariates and the weak dependence as well as tail features of the DGP. We report on a Monte Carlo study in Section 5 which provides insights about the validity of the asymptotic analysis in finite sample settings typically encountered in empirical applications. Section 6 covers the empirical application. Conclusions appear in Section 7.

## 2 Time series regressions and sparse-group LASSO

Let  $(y_t)_{t \in [T]}$  be the target variable measured at discrete time points  $t \in [T] = \{1, \dots, T\}$ . Predictions of  $y_t$  can involve lagged y's as well as a large set of covariates and lags thereof. In the interest of generality, but more importantly because of empirical relevance we allow the covariates to be sampled at higher frequencies - with same frequency being a special case. More specifically, let there be  $K$  covariates  $\{x_{t-j/m, k}, j \in [m], t \in [T], k \in [K]\}$  possibly measured at some higher frequency with  $m$  observations every  $t$  and the following regression model

$$\phi(L)y_t = \sum_{k=1}^K \psi(L^{1/m}; \beta_k)x_{t,k} + u_t, \quad t \in [T], \quad (1)$$

where  $\phi(L)y_t = y_t - \rho_0 - \sum_{j=1}^J \rho_j y_{t-j}$  is the low-frequency lag polynomial and  $\psi(L^{1/m}; \beta_k)x_{t,k} = 1/m \sum_{j=1}^m \beta_{j,k} x_{t-j/m, k}$  is the high-frequency lag polynomial. When we set  $m = 1$  we have a standard autoregressive distributed lag (ARDL) model, which is the workhorse regression model of the time series econometrics literature.<sup>7</sup>

The ARDL-MIDAS model (using the terminology of Andreou, Ghysels, and Kourtellos (2013)) features  $J + 1 + m \times K$  parameters. In the big data setting with a large number of covariates sampled at high-frequency, the total number of parameters may be large compared to the effective sample size or even exceed it. This leads to poor estimation and out-of-sample prediction accuracy in finite samples. For instance, with  $m = 3$  (quarterly/monthly setting), 4 lagged quarters, and 35 covariates, we need to estimate  $m \times K = 420$  parameters. At the same time, say post-WWII quarterly GDP growth series has less than 300 observations.

The LASSO estimator, see Tibshirani (1996), offers an appealing convex relaxation of a difficult non-convex best subset selection problem. By construction, it

---

<sup>7</sup>Note that the polynomial  $\psi(L^{1/m}; \beta_k)x_{t,k}$  only involves  $m$  lags, which is done for the sake of simplicity and without loss of generality. In addition, regression (1) involves high-frequency lags  $t - j/m$ . In some applications lags  $t - 1 - j/m$  might be more suitable, or a combination of both, again without loss of generality.

produces sparse parsimonious models zeroing-out a large number of the estimated parameters. The model selection is not free and comes at a price that can be high in the low signal-to-noise environment with heavy-tailed dependent data. In this paper, we focus on the structured sparsity with additional dimensionality reductions that aim to improve upon the unstructured LASSO estimator.

First, we parameterize the high-frequency lag polynomial following the MIDAS regression or the distributed lag econometric literatures (see [Ghysels, Santa-Clara, and Valkanov \(2006\)](#)) as

$$\psi(L^{1/m}; \beta_k)x_{t,k} = \frac{1}{m} \sum_{j=1}^m \omega(j/m; \beta_k)x_{t-j/m,k}, \quad (2)$$

where  $\dim(\beta_k) = L < m$ . The weight function  $\omega : [0, 1] \times \mathbf{R}^L \rightarrow \mathbf{R}$  is approximated as follows

$$\omega(t; \beta_k) \approx \sum_{l=1}^L \beta_{k,l} w_l(t), \quad t \in [0, 1], \quad (3)$$

where  $\{w_l : l = 1, \dots, L\}$  is a collection of functions, called the *dictionary*. The simplest example of the dictionary consists of algebraic power polynomials, also known as [Almon \(1965\)](#) polynomials in the time series analysis. More generally, the dictionary may consist of arbitrary approximating functions, including classical orthonormal bases.<sup>8</sup>

The size of the dictionary  $L$  and the number of covariates  $K$  can still be large and the *approximate sparsity* is a key assumption imposed throughout the paper. With the approximate sparsity, we typically recognize that assuming that most of the estimated coefficients are zero is overly restrictive and that the approximation error should be taken into account. For instance, the weight function may have an infinite series expansion, nonetheless, most can be captured by a relatively small number of orthogonal basis functions. Similarly, there can be a large number of economically relevant predictors, nonetheless, it might be sufficient to select only a smaller number of the most relevant ones to achieve good out-of-sample forecasting performance. Both model selection goals can be achieved with the LASSO estimator. However, the LASSO does not recognize that covariates at different (high-frequency) lags are temporally related.

---

<sup>8</sup>See Appendix Section [A.2](#) for more examples. Using orthogonal polynomials typically reduces the multicollinearity and leads to better finite sample performance. The specification in (2) deviates from the standard MIDAS polynomial specification as it results in a linear regression model - a subtle but key innovation as it maps MIDAS regressions in the standard regression framework.

In the baseline model, all high-frequency lags (or approximating functions once we parametrize the lag polynomial) of a single covariate constitute a group. We can also assemble all lag dependent variables into a group. Other group structures could be considered, for instance combining various covariates into a single group, but we will work with the simplest group setting of the aforementioned baseline model. The sparse-group LASSO (sg-LASSO), see [Simon, Friedman, Hastie, and Tibshirani \(2013\)](#), allows us to incorporate such structure into the estimation procedure. In contrast to the group LASSO, see [Yuan and Lin \(2006\)](#), the sg-LASSO promotes sparsity *between* and *within* groups, and allows us to capture the predictive information from each group, such as approximating functions from the dictionary or specific covariates from each group.<sup>9</sup>

Let  $\mathbf{y} = (y_1, \dots, y_T)^\top$ ,  $\mathbf{X} = (\iota, \mathbf{y}_1, \dots, \mathbf{y}_J, Z_1 W, \dots, Z_K W)$ , where  $\iota$  is a vector of ones,  $Z_k = (x_{k,t-j/m})_{t \in [T], j \in [m]}$  with  $k \in [K]$ , and  $W = \left(\frac{1}{m} w_l(j/m)\right)_{j \in [m], l \in [L]}$ . In addition, put  $\beta = (\rho_0, \rho_1, \dots, \rho_J, \beta_1^\top, \dots, \beta_K^\top)^\top$  and  $\mathbf{y}_j = (y_{1-j}, \dots, y_{T-j})^\top$ . Then, the sparse-group LASSO estimator, denoted  $\hat{\beta}$ , solves the penalized least-squares problem

$$\min_{\beta \in \mathbf{R}^p} \|\mathbf{y} - \mathbf{X}\beta\|_T^2 + 2\lambda\Omega(\beta) \quad (4)$$

with a penalty function that interpolates between the  $\ell_1$  LASSO penalty and the  $\ell_2$  group LASSO penalty

$$\Omega(\beta) = \alpha|\beta|_1 + (1 - \alpha) \sum_{k=0}^K |\beta_k|_2.$$

The amount of penalization is controlled by the regularization parameter  $\lambda > 0$  while  $\alpha \in [0, 1]$  is a weight parameter that determines the relative importance of the sparsity and the group structure. Setting  $\alpha = 1$ , we obtain the LASSO estimator while setting  $\alpha = 0$ , leads to the group LASSO estimator. Note also that with a single group ( $K = 0$ ), the penalty resembles the elastic net penalty with the only difference that we have  $|\beta|_2$  instead of  $|\beta|_2^2$ . Therefore, with a single group, the sg-LASSO achieves similar to the elastic net regularization goals. In practice, groups are defined by a particular problem, while  $\alpha$  can be fixed or selected in a data-driven way. Figure 1 illustrates the geometry of the unit ball under the  $\Omega(\cdot)$  norm for different

---

<sup>9</sup>Selecting the most important elements from the dictionary to approximate the MIDAS weights is superior to selecting, e.g., the polynomial of a fixed degree, see [DeVore \(1998\)](#) for the comparison between the linear and nonlinear approximation. It should also be noted that [Marsilli \(2014\)](#), and [Uematsu and Tanaka \(2019\)](#) are recent examples extending the MIDAS regression setting to a penalized regression setting. None of these existing papers provide an asymptotic theory supporting the proposed methods.

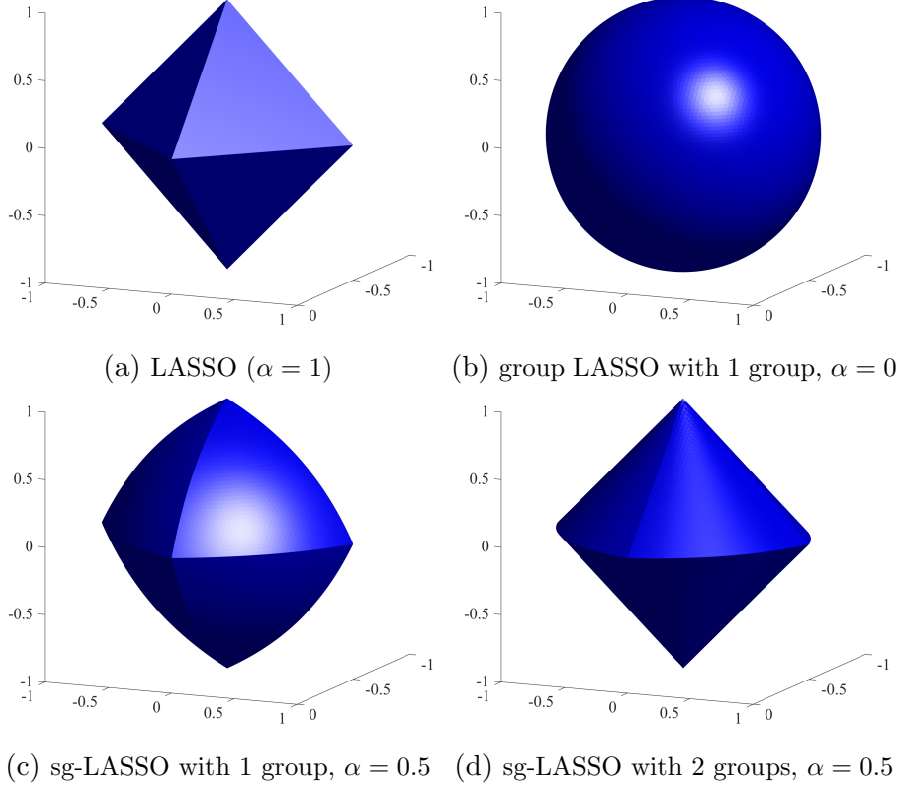


Figure 1: Geometry of  $\{\beta : \Omega(\beta) \leq 1\}$  for different groupings and values of  $\alpha$ .

groupings and different values of  $\alpha$ . [Simon, Friedman, Hastie, and Tibshirani \(2013\)](#) provide a computationally efficient variation of the coordinate descent algorithm.

### 3 Oracle inequalities and convergence rates

In this section, we establish non-asymptotic bounds and convergence rates for the estimation and prediction accuracy of the sg-LASSO estimator. We focus on the generic dynamic linear regression model

$$y_t = \mathbb{E}[y_t | \mathcal{F}_t] + u_t, \quad \mathbb{E}[u_t | \mathcal{F}_t] = 0,$$

where  $(y_t)_{t \in \mathbf{Z}}$  is a real-valued stochastic process and  $(\mathcal{F}_t)_{t \in \mathbf{Z}}$  is a filtration. In the most general case, the filtration is generated by some covariates, all lags of covariates, as well as all lags of the dependent variable. We approximate the conditional mean function with the best linear approximation, denoted  $X_t^\top \beta^0$ , where  $X_t \in \mathbf{R}^p$  may

include covariates, lags of covariates up to a certain order, as well as lags of the dependent variable.<sup>10</sup>

Using the setting of equation (4), in the vector notation, we write

$$\mathbf{y} = \mathbf{m} + \mathbf{u},$$

where  $\mathbf{y} = (y_1, \dots, y_T)^\top$ ,  $\mathbf{m} = (\mathbb{E}[y_1|\mathcal{F}_1], \dots, \mathbb{E}[y_T|\mathcal{F}_T])^\top$ , and  $\mathbf{u} = \mathbf{y} - \mathbf{m}$ . The best linear approximation is denoted  $\mathbf{X}\beta^0$ , where  $\mathbf{X}$  is  $T \times p$  design matrix and  $\beta^0 \in \mathbf{R}^p$ .

**Notation.** For a random variable  $X \in \mathbf{R}$ , let  $\|X\|_q = (\mathbb{E}|X|^q)^{1/q}$  be its  $L_q$  norm with  $q \geq 1$ . For a vector  $\delta \in \mathbf{R}^p$  and a subset  $J \subset [p] = \{1, \dots, p\}$ , let  $\delta_J$  be a vector in  $\mathbf{R}^p$  with the same coordinates as  $\delta$  on  $J$  and zero coordinates on  $J^c$ . Let  $\mathbf{G} = \{G_g : g \geq 1\}$  be a partition of  $[p]$  and  $\bar{G} = \max_{G \in \mathbf{G}} |G|$ , where  $|G|$  is the cardinality of  $G$ . The sparse-group structure is described by a pair  $(S_0, \mathcal{G}_0)$ , where  $S_0 = \{j \in [p] : \beta_j^0 \neq 0\}$  is a support of  $\beta^0$  and  $\mathcal{G}_0 = \{G \in \mathbf{G} : \beta_G^0 \neq 0\}$  is a group support. We denote  $\ell_p, p \geq 1$  norm as  $|\beta|_p = \left(\sum_{j=1}^p |\beta_j|^p\right)^{1/p}$  and  $|\beta|_\infty = \max_{1 \leq j \leq p} |\beta_j|$ . For  $u, v \in \mathbf{R}^T$ , the empirical inner product is defined as  $\langle \mathbf{u}, \mathbf{v} \rangle_T = \frac{1}{T} \sum_{t=1}^T u_t v_t$  with the induced empirical norm  $\|\cdot\|_T^2 = \langle \cdot, \cdot \rangle_T = \|\cdot\|_2^2 / T$ . We also use  $\|A\|_\infty = \max_j \sum_k |A_{j,k}|$  to denote the matrix norm. For a symmetric matrix  $A$ , let  $\text{vech}(A) \in \mathbf{R}^{p(p+1)/2}$  be its vectorization consisting of the lower triangular and the diagonal part. Lastly, for  $a, b \in \mathbf{R}$ , we put  $a \vee b = \max\{a, b\}$ .

### 3.1 Non-asymptotic bounds and convergence rates

We measure the dependence over time with  $\tau$ -dependence coefficients. These coefficients can be understood as dependence measures weaker than  $\alpha$ -mixing coefficients, see Appendix Section A.1 for more details.

**Assumption 3.1** (Data). *Let  $(y_t, X_t)_{t \in \mathbf{Z}}$  be a stationary stochastic process in  $\mathbf{R}^{1+p}$  such that (i)  $\max_{j \in [p]} \mathbb{E}|u_t X_{t,j}|^q = O(1)$  for some  $q > 2$ ; (ii)  $\max_{j,k \in [p]} \mathbb{E}|X_{t,j} X_{t,k}|^{\tilde{q}} = O(1)$  for some  $\tilde{q} > 2$ ; (iii)  $(u_t X_t)_{t \in \mathbf{Z}}$  have  $\tau$ -dependence coefficients  $\tau_k \leq dk^{-a}$  with  $a > (q-1)/(q-2)$ ; (iv)  $(X_t X_t^\top)_{t \in \mathbf{Z}}$  have  $\tau$ -dependence coefficients  $\tilde{\tau}_k \leq \tilde{d}k^{-\tilde{a}}$  with  $\tilde{a} > (\tilde{q}-1)/(\tilde{q}-2)$ .*

Assumption 3.1 imposes some mild weak dependence and moment restrictions on the data-generating process. As it is usually the case, stationarity is not crucial and can

---

<sup>10</sup>In the correctly specified case,  $\mathbf{m} = \mathbf{X}\beta^0$  and the regression score is a martingale difference sequence which simplifies the theoretical treatment. We consider a more realistic setting which requires probabilistic tools for serially correlated processes.

be relaxed at the costs of introducing heavier notation and assumptions. We require only  $q > 2$  finite moments for stochastic processes and do not require sub-Gaussianity which could be particularly restrictive for financial and economic data.<sup>11</sup>

Identification in the linear model is achieved whenever the population covariance matrix  $\Sigma = \mathbb{E}[\mathbf{X}^\top \mathbf{X}/T]$  is invertible or in other words whenever the smallest eigenvalue of  $\Sigma$  is bounded away from zero.<sup>12</sup> This condition is also known as the completeness condition. Interestingly, sparse vectors can be identified and accurately estimated even when the covariance matrix is singular. The only requirement is that  $\Sigma$  is well-behaved on a certain cone, see Babii and Florens (2017) for a related discussion in the context of ill-posed econometric models.

**Assumption 3.2** (Restricted eigenvalue). *There exists some universal constants  $\gamma_1, \gamma_2 > 0$  such that for all  $\delta$  in  $\mathcal{C}(c_0) = \{\delta \in \mathbf{R}^p : \Omega_1(\delta) \leq c_0 \Omega_0(\delta)\}$  with  $\Omega_0, \Omega_1$  as in Eq. A.6 and  $c_0 = \frac{c+1}{c-1}$  for some  $c > 1$*

$$|\Sigma^{1/2}\delta|_2^2 \geq \gamma_1 |\delta_{S_0}|_2^2 \quad \text{and} \quad |\Sigma^{1/2}\delta|_2^2 \geq \gamma_2 \sum_{G \in \mathcal{G}_0} |\delta_G|_2^2.$$

Assumption 3.2 is a population counterpart to the frequently used restricted eigenvalue or compatibility condition imposed on the sample covariance matrix. The regularization parameter is determined by the new Fuk-Nagaev concentration inequality, appearing in the Appendix equation (A.3).

**Assumption 3.3** (Regularization parameter). *Under Assumptions 3.1 and 3.2, suppose that the regularization parameter satisfies*

$$\lambda = \Lambda \left( \frac{p}{\delta T^{\kappa-1}} \right)^{1/\kappa} \vee \sqrt{\frac{\log(8p/\delta)}{T}}$$

with  $\Lambda = c(\alpha + (1-\alpha)\bar{G}^{1/2})C$ ,  $\kappa = \frac{(a+1)q-1}{a+q-1}$ , and some  $C > 0$ .

The regularization parameter depends on the temporal dependence, measured by  $a$  and heaviness of tails, measured by  $q$ . This dependence is reflected in the *dependence-tails exponent*  $\kappa$ . Under maintained assumptions, we obtain the following bound on

---

<sup>11</sup>Note also that even if  $u_t$  and  $X_t$  were sub-Gaussian, their products and cross-products are not sub-Gaussian.

<sup>12</sup>We call loosely  $\Sigma$  the covariance matrix as it coincides with the covariance matrix of a zero-mean random vector  $X \in \mathbf{R}^p$ . Likewise, we refer to  $\hat{\Sigma} = \mathbf{X}^\top \mathbf{X}/T$  as the sample covariance matrix.

the estimation and prediction accuracy of the sg-LASSO estimator (proofs appear in Appendix Section A.3).<sup>13</sup>

**Theorem 3.1.** *Suppose that Assumptions 3.1, 3.2, and 3.3 are satisfied. Then for every  $\delta \in (0, 1)$  with probability at least  $1 - \delta - A_1 \frac{s_\alpha^{\tilde{\kappa}} p^2}{T^{\tilde{\kappa}-1}} - 2p(p+1) \exp(-A_2 T/s_\alpha^2)$*

$$\|\mathbf{X}(\hat{\beta} - \beta^0)\|_T^2 \leq C_1 s_\alpha \lambda^2 + 4\|\mathbf{m} - \mathbf{X}\beta^0\|_T^2$$

and

$$\Omega(\hat{\beta} - \beta^0) \leq C_2 s_\alpha \lambda + C_3 \lambda^{-1} \|\mathbf{m} - \mathbf{X}\beta^0\|_T^2 + C_4 s_\alpha^{1/2} \|\mathbf{m} - \mathbf{X}\beta^0\|_T.$$

with  $s_\alpha^{1/2} = \alpha \sqrt{\frac{|S_0|}{\gamma_1}} + (1 - \alpha) \sqrt{\frac{|\mathcal{G}_0|}{\gamma_2}}$ , and universal constants  $A_1, A_2, C_j, j \in [4]$ .

In the special case of the LASSO estimator,  $\alpha = 1$ , we obtain the counterpart to the result of Belloni, Chen, Chernozhukov, and Hansen (2012) for the LASSO with i.i.d. data. For another extreme  $\alpha = 0$ , we obtain non-asymptotic bounds for the group LASSO reflecting the approximation error. We call the constant  $s_\alpha$  the *effective sparsity*. The effective sparsity is a linear combination of sparsity and group sparsity constants weighted by restricted eigenvalue constants.

An immediate consequence of the bounds stated in Theorem 3.1 is the asymptotic guarantee for the sg-LASSO estimator presented in the following corollary which we state under the assumption that the approximation error is negligible and the dimension/sparsity increase at a certain rate.

**Assumption 3.4.** *Suppose that (i)  $\|\mathbf{m} - \mathbf{X}\beta^0\|_T^2 = O_P(s_\alpha \lambda^2)$ ; (ii)  $s_\alpha^{\tilde{\kappa}/2} p = o(T^{(\tilde{\kappa}-1)/2})$  and  $p^2 \exp(-A_2 T/s_\alpha^2) = o(1)$ .*

**Corollary 3.1.** *Suppose that Assumptions 3.1, 3.2, 3.3, and 3.4 are satisfied. Then*

$$\|\mathbf{X}(\hat{\beta} - \beta^0)\|_T^2 = O_P\left(\frac{s_\alpha p^{2/\kappa}}{T^{2-2/\kappa}} \vee \frac{s_\alpha \log p}{T}\right).$$

and

$$\Omega(\hat{\beta} - \beta^0) = O_P\left(\frac{s_\alpha p^{1/\kappa}}{T^{1-1/\kappa}} \vee s_\alpha \sqrt{\frac{\log p}{T}}\right).$$

---

<sup>13</sup>Note that the sg-LASSO penalty is not decomposable with respect to the support or the group support of  $\beta^0$  and the results from the theory of decomposable regularizers are not directly applicable, see Negahban, Ravikumar, Wainwright, and Yu (2012) or Van de Geer (2016). However, our bounds rely on similar techniques.

If the effective sparsity constant is fixed, then  $p = o(T^{\kappa-1})$  is a sufficient condition for the prediction error and  $\Omega$ -norm to converge to zero, whenever  $\tilde{\kappa} \geq 2\kappa - 1$ . In this case Assumption 3.4 is vacuous. Convergence rates reflect a trade-off between tails, dependence, and the number of covariates. Note that, the number of covariates can increase at a faster rate than the sample size, provided that  $\kappa > 2$ . Assuming that tails of the data decrease exponentially fast so that all moments of the data exist, it is possible to get rid of the first polynomial tail. We avoid such assumptions since the economic and the financial time series are often believed to have heavier tails.

**Remark 3.1.** *Since  $\ell_1$ -norm is equivalent to the  $\Omega$ -norm whenever groups have fixed size, we automatically obtain the same convergence rate in the  $\ell_1$ -norm.*

**Remark 3.2.** *In the special case of the LASSO estimator, Caner and Kock (2018) obtain the convergence rate of order  $O_P\left(\frac{p^{1/q}}{T^{1/2}}\right)$  with  $q \geq 2$  under the i.i.d. assumption. Since  $\kappa \xrightarrow{a \rightarrow \infty} q$ , we recover the  $O_P\left(\frac{p^{1/q}}{T^{1-1/q}}\right)$  convergence rate that one would obtain in the case of independent data applying directly the Fuk and Nagaev (1971), Corollary 4.*

**Remark 3.3.** *Recognizing that the dependence and tails may affect the performance of the LASSO estimator is important, however, the polynomial dependence on the dimension should not necessarily be considered as a negative result. The dependence on the dimension is still better than for the classical OLS, ridge regression, and PCA regression estimators, especially if the data are not strongly dependent and/or more than two moments exist.<sup>14</sup>*

## 4 Inference

We start with the large sample approximation to the distribution of the bias-corrected sg-LASSO estimator (and as a consequence of the LASSO and the group LASSO) with  $\tau$ -dependent data. The bias of the sg-LASSO estimator is denoted  $b = \hat{\Theta}\mathbf{X}^\top(\mathbf{y} -$

---

<sup>14</sup>It may be possible to achieve better dependence on the dimension if one is willing to modify the MSE loss function and to introduce additional tuning parameters, see Fan, Li, and Wang (2017) and Lecué and Lerasle (2019) for estimators based on the Huber loss or the median-of-means loss in the i.i.d. case. Under the high-level restricted eigenvalue conditions imposed on the sample covariance matrix, one could also follow another approach based on introducing self-normalization in the penalty function and using concentration inequalities for self-normalized sums, see Belloni, Chen, Chernozhukov, and Hansen (2012) and Belloni, Chernozhukov, and Hansen (2014) for the i.i.d. case.

$\mathbf{X}\hat{\beta})/T$ , where  $\hat{\beta}$  is the sg-LASSO estimator of  $\beta^0$  and  $\hat{\Theta}$  is the nodewise LASSO estimator of the precision matrix  $\Theta = \Sigma^{-1}$  (assumed to exist) described in the next subsection. For any set of indices  $G \subset [p]$  and a  $p \times p$  matrix  $A$ , let  $A_G$  be its sub-matrix consisting of rows of  $A$  corresponding to indices in  $G$ . If  $G = \{j\}$  is a singleton, then we simply put  $A_G = A_j$ . We also put  $\xi_t = u_t \Theta_G X_t$ ,  $S = \max_{j \in G} S_j$ , and  $s = s_\alpha \vee S$ , where  $S_j$  is the number of non-zero coefficients in the  $j^{th}$  row of the precision matrix.<sup>15</sup> Let  $V_{t,j}$  be the regression error in  $j^{th}$  nodewise LASSO regression. The following assumption imposes several additional mild regularity conditions on the DGP.

**Assumption 4.1.** *Let  $G \subset [p]$  be a group of fixed size such that (i)  $\sup_x \mathbb{E}[u_0^2 | X_0 = x] \leq C$  for some universal constant  $C < \infty$ ; (ii)  $\|\Theta_G\|_\infty = O(1)$ ; (iii) each coordinate of  $(\xi_t)_{t \in \mathbf{Z}}$  and  $(\xi_t \xi_s^\top)_{t \in \mathbf{Z}}$  has tau-dependence coefficients satisfying  $\sum_{t=1}^{\infty} \tau_{T,t}^{\frac{q-2}{q-1}} = O(1)$  for  $q > 2$  as in Assumption 3.1 and  $\sum_{t=1}^{\infty} \tilde{\tau}_{T,t} = O(1)$  for all  $s \geq t$ ; (iv) for every  $j \in G$ , the long run variance of  $(V_{t,j}^2)_{t \in \mathbf{Z}}$  exists; (v)  $s \log p = o(T^{1/2})$  and  $s^{\kappa/2} p = o(T^{3\kappa/4-1})$ ; (vi)  $\|\mathbf{m} - \mathbf{X}\beta^0\|_T = o_P(T^{-1/2})$ .*

The following results gives the approximation to the large sample distribution of the debiased sg-LASSO estimator under weak dependence and tails conditions.

**Theorem 4.1.** *Suppose that Assumptions 3.1, 3.2, 3.3, and 3.4 are satisfied for the sg-LASSO regression and for each nodewise LASSO regression  $j \in G$  and that Assumption 4.1 holds. Then*

$$\sqrt{T}(\hat{\beta}_G + b_G - \beta_G^0) \xrightarrow{d} N(0, \Xi_G)$$

with  $\Xi_G = \lim_{T \rightarrow \infty} \text{Var} \left( \frac{1}{\sqrt{T}} \sum_{t=1}^T u_t \Theta_G X_t \right)$ .

Our debiased CLT result for the sg-LASSO should be compared to [van de Geer, Bühlmann, Ritov, and Dezeure \(2014\)](#), Theorem 2.4 that states an asymptotic expansion for the LASSO estimator that can be used subsequently to derive the debiased CLT with i.i.d. subexponential data under some additional restrictions. Having a consistent estimator of the long-run variance  $\Xi_G$  allows us immediately to construct valid t- and Wald tests for low-dimensional groups of coefficients.

---

<sup>15</sup>Note that the sparsity of the precision matrix is a naturally related to the conditional independence in the Gaussian graphical model, see [Meinshausen and Bühlmann \(2006\)](#) for more details. We find that in the high-dimensional settings, the sparsity of the precision matrix is strongly empirically supported in time series data.

## 4.1 Nodewise LASSO

The bias-correction term  $b$  and the expression of the long-run variance in Theorem 4.1 depend on the precision matrix  $\Theta = \Sigma^{-1}$ . There exist several approaches to the estimation of the precision matrix in the high-dimensional setting: the nodewise LASSO, see Bühlmann and Van De Geer (2011); the weighted graphical LASSO see Janková and van de Geer (2018); or the ridge regression. We focus on nodewise LASSO regressions introduced in Meinshausen and Bühlmann (2006) and used subsequently in van de Geer, Bühlmann, Ritov, and Dezeure (2014) in the i.i.d. setting. The estimator is based on the observation that the covariance matrix of the partitioned vector  $X = (X_j, X_{-j}^\top)^\top \in \mathbf{R} \times \mathbf{R}^{p-1}$  can be written as

$$\Sigma = \mathbb{E}[XX^\top] = \begin{pmatrix} \Sigma_{j,j} & \Sigma_{j,-j} \\ \Sigma_{-j,j} & \Sigma_{-j,-j} \end{pmatrix},$$

where  $\Sigma_{j,j} = \mathbb{E}[X_j^2]$  and all other elements defined similarly. Then by the partitioned inverse formula, the  $j^{\text{th}}$  row of the precision matrix  $\Theta = \Sigma^{-1}$  is computed as

$$\Theta_j = \sigma_j^{-2} (1 \ -\gamma_j^\top),$$

where  $\gamma_j = \Sigma_{-j,-j}^{-1} \Sigma_{-j,j}$  is the projection coefficient in the regression of  $X_j$  on  $X_{-j}$

$$X_j = X_{-j}^\top \gamma_j + v_j, \quad \mathbb{E}[X_{-j} v_j] = 0, \quad (5)$$

and  $\sigma_j^2 = \Sigma_{j,j} - \Sigma_{j,-j} \gamma_j = \mathbb{E}[v_j^2]$  is the variance of the regression error. This indicates that we can estimate the  $j^{\text{th}}$  row of the precision matrix as  $\hat{\Theta}_j = \hat{\sigma}_j^{-2} (1 \ -\hat{\gamma}_j^\top)$  with  $\hat{\gamma}_j$  solving

$$\min_{\gamma \in \mathbf{R}^{p-1}} \|\mathbf{X}_j - \mathbf{X}_{-j} \gamma\|_T^2 + 2\lambda_j |\gamma|_1$$

and

$$\hat{\sigma}_j^2 = \|\mathbf{X}_j - \mathbf{X}_{-j} \hat{\gamma}_j\|_T^2 + \lambda_j |\hat{\gamma}_j|,$$

where  $\mathbf{X}_j \in \mathbf{R}^T$  is the column vector of observations of  $X_j$  and  $\mathbf{X}_{-j}$  is the  $T \times (p-1)$  matrix of observations of  $X_{-j}^\top$ . The nodewise LASSO estimator of the precision matrix can be written then as  $\hat{\Theta} = \hat{B}^{-1} \hat{C}$  with

$$\hat{C} = \begin{pmatrix} 1 & -\hat{\gamma}_{1,1} & \dots & -\hat{\gamma}_{1,p-1} \\ -\hat{\gamma}_{2,1} & 1 & \dots & -\hat{\gamma}_{2,p-1} \\ \vdots & \vdots & \ddots & \vdots \\ -\hat{\gamma}_{p-1,1} & \dots & -\hat{\gamma}_{p-1,p-1} & 1 \end{pmatrix} \quad \text{and} \quad \hat{B} = \text{diag}(\hat{\sigma}_1^2, \dots, \hat{\sigma}_p^2).$$

More generally, we allow for the approximate sparsity in Eq. 5 and consider  $v_j$  as a non-degenerate random variable that does not change with the sample size.

## 4.2 HAC estimator

To the best of our knowledge the HAC estimator for the LASSO estimator has not been comprehensively treated in the relevant literature.<sup>16</sup> We focus on the HAC estimator for the sparse-group LASSO, covering the LASSO and the group LASSO as special cases. For a group  $G \subset [p]$  of a fixed size, the HAC estimator of the long-run variance is

$$\hat{\Xi}_G = \sum_{|k| < T} K\left(\frac{k}{M_T}\right) \hat{\Gamma}_k, \quad (6)$$

where  $\hat{\Gamma}_k = \hat{\Theta}_G \left( \frac{1}{T} \sum_{t=1}^{T-k} \hat{u}_t \hat{u}_{t+k} X_t X_{t+k}^\top \right) \hat{\Theta}_G^\top$ , and  $\hat{\Gamma}_{-k} = \hat{\Gamma}_k^\top$ , where the kernel function  $K : \mathbf{R} \rightarrow [-1, 1]$  with  $K(0) = 1$  gives less weight to more distant noisy covariances, and  $M_T$  is a truncation parameter, see [Newey and West \(1987\)](#) and [Andrews \(1991\)](#). In the empirical implementation we use the Parzen kernel:

$$K_{PR}(x) = \begin{cases} 1 - 6x^2 + 6|x|^3 & \text{for } 0 \leq |x| \leq 1/2, \\ 2(1 - |x|)^3 & \text{for } 1/2 \leq |x| \leq 1, \\ 0 & \text{otherwise.} \end{cases}$$

**Assumption 4.2.** Suppose that  $(u_t^2)_{t \in \mathbf{Z}}$  and  $(v_{t,j}^2)_{t \in \mathbf{Z}}$  for each  $j \in G$  have finite long run variances.

The following result derives the convergence rate of the HAC estimator for a group of coefficients  $G$  estimated using the LASSO to the long-run variance, which under the stationarity simplifies to

$$\Xi_G = \sum_{k \in \mathbf{Z}} \Gamma_k$$

with  $\Gamma_k = \Theta_G \mathbb{E}[u_t u_{t+k} X_t X_{t+k}^\top] \Theta_G^\top$  and  $\Gamma_{-k} = \Gamma_k^\top$ . Put  $s = s_\alpha \vee S$ , where  $S = \max_{j \in G} S_j$ , and  $S_j$  is the sparsity of  $\Theta_j$ .

**Theorem 4.2.** Suppose that Assumptions 3.1, 3.2, 3.3, 3.4, 4.2 are satisfied for the sg-LASSO and each nodewise LASSO regressions with  $\kappa \geq \tilde{q}$ . Suppose also

---

<sup>16</sup>Convergence rates of the HAC estimator for non-sparse high-dimensional least-squares under weak dependence conditions have been obtained previously, e.g., in [Li and Liao \(2019\)](#).

that Assumptions A.4.1, and A.4.2 are satisfied with  $V_t = (u_t v_{t,j} / \sigma_j^2)_{j \in G}$ . Then if  $s\sqrt{\frac{\log p}{T}} = o(1)$  and  $s^\kappa p = o(T^{4\kappa/5-1})$  as  $M_T \rightarrow \infty$  and  $T \rightarrow \infty$

$$\|\hat{\Xi}_G - \Xi_G\| = O_P \left( M_T \left( \frac{sp^{1/\kappa}}{T^{1-1/\kappa}} \vee s\sqrt{\frac{\log p}{T}} + \frac{s^2 p^{2/\kappa}}{T^{2-3/\kappa}} + \frac{s^3 p^{5/\kappa}}{T^{4-5/\kappa}} \right) + M_T^{-\varsigma} + T^{-(\varsigma \wedge 1)} \right).$$

The first term in the inner parentheses is of the same order as the estimation error of the maximum between the estimation errors of the sg-LASSO and the nodewise LASSO. We conjecture that it might be possible to get rid of the last two terms terms in the inner parentheses and to improve the dependence on the bandwidth from  $M_T$  to  $M_T^{1/2}$ , e.g., with sampling splitting and cross fitting. In any case, the optimal choice of the bandwidth parameter depends on the number of covariates  $p$  and the dependence-tails exponent  $\kappa$ .<sup>17</sup>

It is worth stressing that this result does not follow from e.g., Andrews (1991) who provide a comprehensive treatment of the kernel HAC estimation based on residuals in the fixed-dimensional case with  $\sqrt{T}$ -consistent estimators.

### 4.3 Inference for groups and Granger causality test

In the mixed-frequency setting, testing the statistical significance of a single covariate amounts to using the Wald test. Therefore, we are interested in testing

$$H_0 : R\beta_G^0 = 0 \quad \text{against} \quad H_1 : R\beta_G^0 \neq 0,$$

where  $R$  is  $r \times |G|$  matrix, e.g.,  $R = I_{|G|}$  if we want to test that all coefficients are jointly zero. Assuming that  $R$  is a full row rank matrix and that  $\hat{\Xi}_G$  is positive definite, it follows from the Theorem 4.1 that

$$W_T = T \left[ R(\hat{\beta}_G + b_G - \beta_G^0) \right]^\top \left( R\hat{\Xi}_G R^\top \right)^{-1} \left[ R(\hat{\beta}_G + b_G - \beta_G^0) \right] \xrightarrow{d} \chi_r^2.$$

Therefore, the Wald test rejects as usual when  $W_T > q_{1-\alpha}$ , where  $q_{1-\alpha}$  is the quantile of order  $1 - \alpha$  of  $\chi_r^2$ .

The Wald test can be easily extended to testing nonlinear restrictions by the usual Delta method argument. For groups described by lags of a single covariate, the test essentially reduces to the (mixed frequency) Granger causality test. To

---

<sup>17</sup>A comprehensive study of the optimal bandwidth choice based on higher-order asymptotic expansions is beyond the scope of this paper and is left for the future research, see, e.g., Lazarus, Lewis, Stock, and Watson (2018) for the recent literature review and practical recommendations.

test hypotheses on the increasing set of coefficients, it is preferable to use the non-pivotal sup-norm based statistics instead of the one based on the quadratic form, see e.g., [Ghysels, Hill, and Motegi \(2018\)](#). Such an extension for approximately sparse regression models is left for future research.

## 5 Monte Carlo experiments

In this section, we aim to assess the out-of-sample predictive performance (forecasting and nowcasting), the MIDAS weights recovery of the sg-LASSO with dictionaries, and the finite-sample performance of debiased HAC inferences. We benchmark the performance of our novel sg-LASSO setup against two alternatives: (a) unstructured, meaning standard, LASSO with MIDAS and (b) unstructured LASSO with unrestricted lag polynomial. The former allows us to assess the benefits of exploiting group structures, whereas the latter focuses on the advantages of using dictionaries in a high dimensional setting. Finally, we also study the small sample performance of HAC estimators in the high dimensional regime and conclude with practical recommendations for the HAC implementation.

The simulation design details appear in Appendix Section [A.5](#). We generate a process  $y_t$  thought to be sampled at a quarterly frequency and dependent on 2 lags and three monthly series each with 12 lags. The DGP only involves a few parameters due to the MIDAS regression polynomial restrictions. However, the researcher has 10 potential monthly series and does not know any of the lag structures. This means potentially  $10 \times 12$  covariates (assuming the lag order is known) plus 2 lagged dependent variables, adding up to 122 potential regressors. The sample sizes are  $T = 50, 100$  or  $200$ .

### 5.1 Forecasting, nowcasting, and weights recovery

In Table [A.1–A.2](#), we report the average mean squared forecast errors for one-step-ahead forecasts and nowcasts. The sg-LASSO with MIDAS weighting (sg-LASSO-MIDAS) outperforms all other methods in all simulation scenarios. Importantly, both sg-LASSO-MIDAS and unstructured LASSO-MIDAS with non-linear weight function approximation perform much better than all other methods in most of the scenarios when the sample size is small ( $T = 50$ ). In this case, sg-LASSO-MIDAS yields the largest improvements over alternatives, in particular, with a large number of noisy covariates (bottom-right block). The LASSO without MIDAS weighting has typically large forecast errors. The method performs better when half of the

high-frequency lags are included in the regression model. Lastly, forecasts using flow-aggregated covariates seem to perform better than other simple aggregation methods in all simulation scenarios, but significantly worse than the sg-LASSO-MIDAS.

In Table A.3–A.4 we report additional results for the estimation accuracy of the weight functions. In Figure A.1–A.3, we plot the estimated weight functions from several methods. Results indicate that the LASSO without MIDAS weighting can not recover accurately weights in small and samples and/or low signal-to-noise ratio. Using Legendre polynomials improves the performance substantially and the sg-LASSO seems to improve even more over the unstructured LASSO.

## 5.2 Inference for high-dimensional time series data

To assess the small sample properties of the HAC estimator for the low-dimensional parameter in a high dimensional data setting we simplify the DGP to a linear regression model with independently drawn AR(1) covariates  $\{x_{t,j}, j \in [p]\}$ . The simulation design details appear again in Appendix Section A.5. The vector of population regression coefficients  $\beta^0$  has the first five non-zero entries  $(5, 4, 3, 2, 1)$  and all remaining entries are zero. The sample size is  $T = 500$  and the number of covariates is  $p \in \{20, 200\}$ . We focus on the LASSO estimator to estimate coefficients  $\hat{\beta}$ .

We report the average coverage (av. cov) and the average length of confidence intervals for the nominal coverage of 0.95 and report results on a grid of values of the truncation parameter  $M_T \in \{10, 20, 40, \dots, 160\}$ , using the Parzen kernel. We estimate the long run covariance matrix  $\hat{\Xi}$  based on the LASSO residuals  $\hat{u}_t$  and the precision matrix  $\hat{\Theta}$  using nodewise LASSO regressions. The first step is to compute scores  $\hat{V}_t = \hat{u}_t X_t$ , where  $\hat{u}_t = y_t - X_t^\top \hat{\beta}$ , and  $\hat{\beta}$  is the LASSO estimator. Then we compute the high-dimensional HAC estimator using the formula in equation (6). We compute the pivotal statistics for each MC experiment  $i \in [N]$  and each coefficient  $j \in [p]$  as  $\text{pivot}_j^{(i)} \triangleq (\hat{\beta}_j^{(i)} + b_j^{(i)} - \beta^0) / \sqrt{\hat{\Xi}_{j,j}^{(i)} / T}$ , where  $b_j^{(i)} = \hat{\Theta}_j^{(i)} \mathbf{X}^{\top(i)} \hat{\mathbf{u}}^{(i)} / T$ ,  $\hat{\mathbf{u}} = \mathbf{y} - \mathbf{X} \hat{\beta}$ . We then compute the empirical coverage as

$$\text{av.cov}_j = \frac{1}{N} \sum_{i=1}^N \mathbf{1}\{\text{pivot}_j^{(i)} \in [-1.96, 1.96]\}$$

and the average confidence interval length as  $\text{length}_j = \frac{1}{N} \sum_{i=1}^N 2 \times 1.96 \times \sqrt{\hat{\Xi}_{j,j}^{(i)} / T}$ . The number of Monte Carlo experiments was set at  $N = 5000$ .

We report average results over the active and inactive sets of the vector of coefficients. Table 1 shows results for the Gaussian data and Table 2 for the student- $t(5)$

data. We find that the optimal bandwidth parameter  $M_T$  appears to be smaller when the number of regressors  $p$  is larger. Note that the number of lags in the HAC estimator equals  $M_T$ , hence, fewer lags should be taken into account as  $p$  increases. For Gaussian data and the active set of coefficients, the optimal bandwidth parameter is around 30 for  $p = 200$  and 80 for  $p = 20$ . A similar pattern is found for the inactive set, although with slightly smaller optimal bandwidth parameters – 20 for large  $p$  case and 60 for small  $p$ . For heavy-tailed data, the optimal bandwidth parameter is lower compared to the Gaussian data.<sup>18</sup> Overall, the simulation results confirm our theoretical findings.

| $M_T \setminus p$ | Average coverage (av. cov) |       |                           |       | Confidence interval length |       |                           |       |
|-------------------|----------------------------|-------|---------------------------|-------|----------------------------|-------|---------------------------|-------|
|                   | Active set of $\beta^0$    |       | Inactive set of $\beta^0$ |       | Active set of $\beta^0$    |       | Inactive set of $\beta^0$ |       |
|                   | 20                         | 200   | 20                        | 200   | 20                         | 200   | 20                        | 200   |
| 10                | 0.912                      | 0.930 | 0.918                     | 0.942 | 0.330                      | 0.320 | 0.321                     | 0.304 |
| 20                | 0.932                      | 0.944 | 0.940                     | 0.951 | 0.358                      | 0.340 | 0.344                     | 0.312 |
| 40                | 0.942                      | 0.956 | 0.947                     | 0.956 | 0.375                      | 0.364 | 0.350                     | 0.312 |
| 60                | 0.947                      | 0.965 | 0.950                     | 0.960 | 0.386                      | 0.384 | 0.349                     | 0.311 |
| 80                | 0.950                      | 0.971 | 0.952                     | 0.964 | 0.395                      | 0.402 | 0.348                     | 0.309 |
| 100               | 0.953                      | 0.976 | 0.954                     | 0.968 | 0.403                      | 0.419 | 0.346                     | 0.308 |
| 120               | 0.956                      | 0.980 | 0.957                     | 0.972 | 0.411                      | 0.435 | 0.344                     | 0.306 |
| 140               | 0.959                      | 0.983 | 0.958                     | 0.976 | 0.419                      | 0.451 | 0.342                     | 0.305 |
| 160               | 0.962                      | 0.984 | 0.960                     | 0.980 | 0.427                      | 0.465 | 0.340                     | 0.303 |

Table 1: HAC inference simulation results – The table reports average coverage (first four columns) and average length of confidence intervals (last four columns) for active and inactive sets of  $\beta^0$ . The data is generated using Gaussian distribution. We report results for a set of truncation parameter  $M_T$  values.

## 6 Nowcasting US GDP with textual news data

A term originated in meteorology, nowcasting pertains to the prediction of the present and very near future. It has been adopted in economics as standard economic activity measures such as gross domestic product (GDP), are only determined after a significant delay, and are even then subject to subsequent revisions. Nowcasting is intrinsically a mixed frequency data problem as the object of interest is a low-frequency data series - observed say quarterly - whereas real-time information - daily, weekly or monthly - during the quarter can be used to assess and potentially continuously

<sup>18</sup>We find similar results using Quadratic spectral kernel, which are reported in the Appendix Table A.5-A.6.

| $M_T \setminus p$ | Average coverage (av. cov) |       |                           |       | Confidence interval length |       |                           |       |
|-------------------|----------------------------|-------|---------------------------|-------|----------------------------|-------|---------------------------|-------|
|                   | Active set of $\beta^0$    |       | Inactive set of $\beta^0$ |       | Active set of $\beta^0$    |       | Inactive set of $\beta^0$ |       |
| 20                | 20                         | 200   | 20                        | 200   | 20                         | 200   | 20                        | 200   |
| 10                | 0.926                      | 0.951 | 0.928                     | 0.953 | 0.348                      | 0.347 | 0.332                     | 0.319 |
| 20                | 0.946                      | 0.963 | 0.948                     | 0.959 | 0.379                      | 0.369 | 0.355                     | 0.324 |
| 40                | 0.956                      | 0.972 | 0.955                     | 0.963 | 0.402                      | 0.397 | 0.361                     | 0.323 |
| 60                | 0.960                      | 0.978 | 0.959                     | 0.966 | 0.417                      | 0.423 | 0.361                     | 0.322 |
| 80                | 0.965                      | 0.983 | 0.962                     | 0.970 | 0.431                      | 0.446 | 0.359                     | 0.320 |
| 100               | 0.969                      | 0.986 | 0.965                     | 0.974 | 0.443                      | 0.467 | 0.357                     | 0.318 |
| 120               | 0.973                      | 0.988 | 0.968                     | 0.978 | 0.455                      | 0.487 | 0.355                     | 0.316 |
| 140               | 0.975                      | 0.991 | 0.972                     | 0.982 | 0.466                      | 0.506 | 0.353                     | 0.314 |
| 160               | 0.977                      | 0.992 | 0.974                     | 0.986 | 0.477                      | 0.524 | 0.351                     | 0.313 |

Table 2: HAC inference simulation results – The table reports average coverage (first four columns) and average length of confidence intervals (last four columns) for active and inactive sets of  $\beta^0$ . The data is generated using student-t(5) distribution. We report results for a set of truncation parameter  $M_T$  values.

update the state of the low-frequency series, or put differently, *nowcast* the series of interest.

One approach involves state space models featuring latent variables and is commonly used by central banks, such as the New York Fed which publishes its nowcasts used in this section.<sup>19</sup> Dealing with large data sets is challenging in a state space setting. Instead, we adopt a MIDAS regression-based approach which is more amenable to large dimensional data environments and extend in this paper the existing MIDAS nowcasting literature to a big data setting.<sup>20</sup>

The data used in our empirical analysis are described in Appendix Section A.7. For standard macro variables, we use a real-time FRED-MD monthly dataset. The data is available at the Federal Reserve Bank of St. Louis FRED database, see McCracken and Ng (2016) for more details on this dataset. For our main results, we use a subset of all available macro covariates which we list in Table A.7.<sup>21</sup> Next, we add data from the Survey of Professional Forecasters, namely, US GDP nowcasts and forecasts for several horizons, which we aggregate using Legendre polynomials. In addition, we augment predictive regression with news attention data based on

<sup>19</sup>State space models are estimated via maximum likelihood and using Kalman filtering or smoothing to nowcast the series of interest; see Baíbura, Giannone, Modugno, and Reichlin (2013) for a recent survey.

<sup>20</sup>See Andreou, Ghysels, and Kourtellos (2013) for nowcasting applications of MIDAS regressions.

<sup>21</sup>Additional set of results for the full set of FRED-MD monthly covariates with detailed implementation description is available in Appendix Section A.8.

textual analysis that has been recently made available by [Bybee, Kelly, Manela, and Xiu \(2019\)](#). Finally, we follow the literature on nowcasting real GDP and define our target variable to be the annualized growth rate. To measure forecast errors, we take 2019 February real GDP data vintage.

## 6.1 Models

Denote  $x_{t,k}$  the  $k$ -th high-frequency covariate at time  $t$ . The general ARDL-MIDAS predictive regression is

$$\phi(L)y_{t+1} = \mu + \sum_{k=1}^K \psi(L^{1/m}; \beta_k)x_{t,k} + u_{t+1}, \quad t = 1, \dots, T,$$

where  $\phi(L)$  is the low-frequency lag polynomial,  $\mu$  is the regression intercept and  $\sum_{k=1}^K \psi(L^{1/m}; \beta_k)x_{t,k}$  are high-frequency covariates. As discussed in Section 2, we parameterize the weight function as

$$\psi(L^{1/m}; \beta_k)x_{t,k} = \frac{1}{m} \sum_{j=1}^m \omega(j/m; \beta_k)x_{t+(h+1-j)/m,k},$$

where  $h$  indicates the number of leading months in the quarter  $t$ . For example, if  $h = 2$ , we shift high-frequency covariates two month in the quarter, and hence we nowcast the dependent variable one month ahead.

We benchmark our predictions with the simple random walk (RW) model, which is considered to be a reasonable benchmark for short-term GDP growth predictions. We focus on predictions of our method, sg-LASSO-MIDAS, with and without series based on textual analysis. One natural comparison is with Federal Reserve Bank of New York, denoted New York Fed, model implied nowcasts.<sup>22</sup> The latter are based on a dynamic factor model with thirty-seven predictors of different frequencies, see [Bok, Caratelli, Giannone, Sbordone, and Tambalotti \(2018\)](#) for more details. Note that some of the series used in their model are proprietary information not in the public domain. This means that on the one hand our methods may have an informational disadvantage, but on the other hand, are better at handling voluminous data sources.

## 6.2 Nowcasting results

Table 3 reports nowcasting results for US GDP growth rate real-time at one given instance, namely two months into a quarter (or put differently with one month left

---

<sup>22</sup>We downloaded the data from <https://www.newyorkfed.org/research/policy/nowcast>.

into the quarter). First, we observe from the table that the sg-LASSO-MIDAS model with standard macro information improves upon the New York Fed predictions in terms of smaller out-of-sample root mean squared errors - although the margin is slim reducing from .790 (ratio with respect to RW) to .761. Without text-based information, the improvement of sg-LASSO-MIDAS versus New York Fed nowcasts is therefore, not surprisingly, insignificant based on the [Diebold and Mariano \(1995\)](#) test statistic. We report similar findings using the full dataset of covariates in Appendix Section [A.8](#), where we also compare alternative machine learning methods with the sg-LASSO-MIDAS method and find that the latter outperforms all other alternatives.

Turning to results using additional text-based covariates, we see a significant improvement in terms of the quality of out-of-sample predictions. Relative to New York Fed nowcasts, sg-LASSO-MIDAS with textual data decrease prediction errors by 19%. The gain is also large relative to the sg-LASSO-MIDAS model that does not condition on news attention information, albeit slightly smaller. The [Diebold and Mariano \(1995\)](#) test statistic reveals that the increase in prediction accuracy is significant at 10% significance level when compared with New York Fed predictions as well as sg-LASSO-MIDAS model without textual data.

|                                    | Rel-RMSE | DM-stat-1 | DM-stat-2 |
|------------------------------------|----------|-----------|-----------|
| RW                                 | 2.606    | 3.624     | 3.629     |
| sg-LASSO-MIDAS (with textual data) | 0.639    | -1.687    |           |
| sg-LASSO-MIDAS (without)           | 0.761    |           | 1.687     |
| NY Fed                             | 0.790    | 0.490     | 1.727     |

Table 3: Nowcast real GDP comparison table – Forecast horizon is one month ahead. Column *Rel-RMSE* reports root mean squared forecasts error relative to the RW model. Column *DM-stat-1* reports the [Diebold and Mariano \(1995\)](#) test statistic for all models relative to sg-LASSO-MIDAS model without text-based information, while column *DM-stat-2* reports the Diebold Mariano test statistic relative to sg-LASSO-MIDAS model with text-based information. The out-of-sample period is 2002 Q1 to 2017 Q2.

In Figure [2](#), we plot a heat map of selected covariates through time for the sg-LASSO-MIDAS model which includes news attention data.<sup>23</sup> In addition to the heat map, which reveals sparsity patterns, we also plot the evolution of the number of selected covariates and the squared forecast errors across time. In general, the pattern is relatively sparse, with more covariates being selected after the Great Recession. Specifically, on average 14.93 covariates are selected before, while 19.63 after the crisis, and 17.58 for the entire out-of-sample exercise. Interestingly, after the crises the number of selected covariates is more stable - fourteen covariates are

<sup>23</sup>Figure [A.5](#) in the Appendix is a similar plot for the full-sample results using only macro data.

always selected. Three covariates are always selected throughout the out-of-sample period: Government budgets, All Employees: Financial Activities, and 3-Month AA Financial Commercial Paper Rate.<sup>24</sup>

In Figure 3, we plot the cumulative sum of loss differential (cumsfe), which is computed as

$$\text{cumsfe}_{t,t+k} = \sum_{q=t}^{t+k} e_{q,M1}^2 - e_{q,M2}^2 \quad (7)$$

for model  $M1$  versus  $M2$ . Positive value of  $\text{cumsfe}_{t,t+k}$  means model  $M1$  has larger squared forecast errors compared with model  $M2$  up to  $t+k$  point, and negative value imply the opposite. In our case,  $M1$  is the New York Fed prediction error, and  $M2$  is the sg-LASSO-MIDAS model either with or without news attention series. The plot in Figure 3 reveals that predictions based on sg-LASSO-MIDAS with or without news attention data yield smaller squared errors compared with New York Fed throughout the out-of-sample period. Interestingly, the largest gains are during the 2008-2009 recession period and at the beginning of 2011, which is around the period of the peak of European sovereign debt crises. The figure also shows marked improvements in prediction quality when using news attention series; notably, the largest gains are the two crises periods.<sup>25</sup>

### 6.3 Significance test

In this section, we test whether news attention series are significant predictors of real GDP growth rate. We estimate the same sg-LASSO-MIDAS model using real-time macro data and news attention series. As in nowcasting application, we use 4 quarters of lagged data; the effective sample starts from 1985 February and ends in 2017 May and the sample size is 126 quarters. We select the tuning parameter by using 10-fold cross-validation and set  $\alpha = 0.65$ . For real-time macro data, we take the 2017 May FRED-MD vintage and use real GDP values as of May 30<sup>th</sup>. To compute the precision matrix, we use nodewise LASSO regressions with a data-driven choice for the penalty parameter. Since news attention series are high-frequency, we test the restriction that all coefficients associated with each series are jointly zero.

---

<sup>24</sup>Note that without the news data, see Figure A.4, autoregressive lags are selected more often.

<sup>25</sup>As an aside, using the *cumsfe* plots, we also show in the Appendix that the choice for  $\alpha = 0.65$  is optimal, and yields the largest gains versus New York Fed nowcasts, see Figure A.6. The same figure also shows that favoring sparsity over group sparsity, i.e.  $\alpha \in (0.5, 1]$ , in general, improves predictions.



Figure 2: Sparsity pattern.

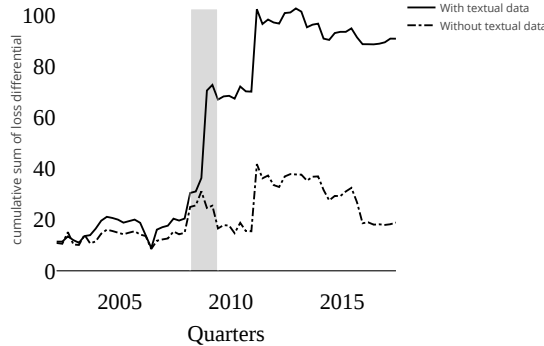


Figure 3: Cumulative sum of loss differential. Gray shaded area — NBER recession period.

Table 4 reports p-values of Wald test for each series where we use HAC estimator with Parzen kernel.<sup>26</sup> We report results for a grid of truncation parameter  $M_T$  values. Results indicate that Government budgets and Oil market are highly significant predictors. Government budgets is significant at 1%, while Oil market at 5% significance level for all truncation parameter values. In the nowcasting application, the former was always selected throughout the out-of-sample period, while the latter was always selected after the crisis.

|                    | $M_T$ | 10    | 20    | 30 |
|--------------------|-------|-------|-------|----|
| Commodities        | 0.533 | 0.514 | 0.554 |    |
| Government budgets | 0.002 | 0.009 | 0.008 |    |
| Oil market         | 0.024 | 0.044 | 0.017 |    |
| Recession          | 0.211 | 0.317 | 0.388 |    |
| Savings & loans    | 0.754 | 0.685 | 0.655 |    |
| Mortgages          | 0.750 | 0.604 | 0.553 |    |

Table 4: Significance test table – P-values for news attention series based on Wald test for a set of truncation parameter  $M_T$  values are reported. The number of lags in the HAC estimator correspond to  $M_T$ .

## 7 Conclusion

This paper offers a new perspective on the high-dimensional time series regressions with data sampled at the same or mixed frequencies and contributes more broadly to

---

<sup>26</sup>In the Appendix Table A.10 we report test statistic values.

the rapidly growing literature on estimation, inference, forecasting, and nowcasting with regularized machine learning methods. The first contribution of the paper is to introduce the sparse-group LASSO estimator for high-dimensional time series regressions. An attractive feature of the estimator is that it recognizes time series data structures and allows us to perform the hierarchical model selection within and between groups. At the same time, it nests the classical LASSO and the group LASSO as special cases.

To recognize that the economic and financial time series have typically heavier than Gaussian tails, we derive a new Fuk-Nagaev concentration inequality valid for a large class of  $\tau$ -dependent processes, including  $\alpha$ -mixing processes commonly used in econometrics. Building on this inequality, we establish non-asymptotic and asymptotic properties of the sparse-group LASSO estimator. We further derive the debiased central limit theorem with explicit bias-correction that leads to the valid t- and the Wald tests for the low-dimensional subset of parameters, including Granger causality tests. We also offer the first comprehensive treatment of the HAC estimators of the long-run variance for high-dimensional approximately sparse regressions characterizing how the convergence rate depends on the number of regressors.

The paper opens several directions for future research. First, since the high-dimensional regressions that recognize data structures typically outperform the unstructured LASSO estimator, it might be fruitful looking for such data structures in various applications. The problem of the optimal bandwidth choice for the HAC estimator in the sparse-group LASSO deserves more attention, c.f., [Sun, Phillips, and Jin \(2008\)](#) for the low-dimensional case. Lastly, it could be equally interesting to study alternative HAC estimators, especially for strongly autocorrelated time series and to compare those to kernel estimators, see [Müller \(2007\)](#) and [Müller \(2014\)](#).

Our empirical application provides new perspectives on applying machine learning methods to real-time forecasting, nowcasting and monitoring using time series data, including non-conventional data, sampled at different frequencies. To that end, we introduce a new class of MIDAS regressions with dictionaries linear in the parameters and based on orthogonal polynomials with lag selection using the sg-LASSO estimator.

## References

ALMON, S. (1965): “The distributed lag between capital appropriations and expenditures,” *Econometrica*, 33(1), 178–196.

ANDREOU, E., P. GAGLIARDINI, E. GHYSELS, AND M. RUBIN (2019): “Inference in group factor models with an application to mixed frequency data,” *Econometrica*, 87(4), 1267–1305.

ANDREOU, E., E. GHYSELS, AND A. KOURTELLOS (2013): “Should macroeconomic forecasters use daily financial data and how?,” *Journal of Business and Economic Statistics*, 31, 240–251.

ANDREWS, D. W. (1984): “Non-strong mixing autoregressive processes,” *Journal of Applied Probability*, 21(4), 930–934.

——— (1991): “Heteroskedasticity and autocorrelation consistent covariance matrix estimation,” *Econometrica*, 59(3), 817–858.

ATHEY, S., AND G. W. IMBENS (2019): “Machine learning methods that economists should know about,” *Annual Review of Economics*, 11, 685–725.

BABII, A., AND J.-P. FLORENS (2017): “Is completeness necessary? Estimation in nonidentified linear models,” Discussion paper, Mimeo-UNC Chapel Hill.

BAÑURA, M., D. GIANNONE, M. MODUGNO, AND L. REICHLIN (2013): “Nowcasting and the real-time data flow,” in *Handbook of Economic Forecasting, Volume 2 Part A*, ed. by G. Elliott, and A. Timmermann, pp. 195–237. Elsevier.

BASU, S., A. SHOJAIE, AND G. MICHAILIDIS (2015): “Network granger causality with inherent grouping structure,” *Journal of Machine Learning Research*, 16(13), 417–453.

BELLONI, A., D. CHEN, V. CHERNOZHUKOV, AND C. HANSEN (2012): “Sparse models and methods for optimal instruments with an application to eminent domain,” *Econometrica*, 80(6), 2369–2429.

BELLONI, A., AND V. CHERNOZHUKOV (2011): “High dimensional sparse econometric models: an introduction,” in *Inverse Problems and High-Dimensional Estimation*, pp. 121–156. Springer.

BELLONI, A., V. CHERNOZHUKOV, D. CHETVERIKOV, C. HANSEN, AND K. KATO (2018): “High-dimensional econometrics and generalized GMM,” *arXiv preprint arXiv:1806.01888*.

BELLONI, A., V. CHERNOZHUKOV, AND C. HANSEN (2010): “LASSO Methods for Gaussian Instrumental Variables Models,” *arXiv preprint arXiv:1012.1297*.

——— (2014): “Inference on treatment effects after selection among high-dimensional controls,” *Review of Economic Studies*, 81(2), 608–650.

BOK, B., D. CARATELLI, D. GIANNONE, A. M. SBORDONE, AND A. TAMBALOTTI (2018): “Macroeconomic nowcasting and forecasting with big data,” *Annual Review of Economics*, 10, 615–643.

BRYZGALOVA, S. (2016): “Spurious factors in linear asset pricing models,” .

BÜHLMANN, P., AND S. VAN DE GEER (2011): *Statistics for high-dimensional data: methods, theory and applications*. Springer Science & Business Media.

BYBEE, L., B. T. KELLY, A. MANELA, AND D. XIU (2019): “The structure of economic news,” Available at SSRN 3446225.

CAI, T. T., A. ZHANG, AND Y. ZHOU (2019): “Sparse group LASSO: optimal sample complexity, convergence rate, and statistical inference,” *arXiv preprint arXiv:1909.09851*.

CANER, M., AND A. B. KOCK (2018): “Asymptotically honest confidence regions for high dimensional parameters by the desparsified conservative lasso,” *Journal of Econometrics*, 203(1), 143–168.

CARRASCO, M., AND B. ROSSI (2016): “In-sample inference and forecasting in misspecified factor models,” *Journal of Business and Economic Statistics*, 34(3), 313–338.

CHERNOZHUKOV, V., C. HANSEN, AND M. SPINDLER (2016): “hdm: High-dimensional metrics,” *arXiv preprint arXiv:1608.00354*.

CHERNOZHUKOV, V., W. K. HÄRDLE, C. HUANG, AND W. WANG (2019): “Lasso-driven inference in time and space,” *Annals of Statistics* (forthcoming).

CHIANG, H. D., AND Y. SASAKI (2019): “Lasso under Multi-way Clustering: Estimation and Post-selection Inference,” *arXiv preprint arXiv:1905.02107*.

DEDECKER, J., AND P. DOUKHAN (2003): “A new covariance inequality and applications,” *Stochastic Processes and their Applications*, 106(1), 63–80.

DEDECKER, J., P. DOUKHAN, G. LANG, L. R. J. RAFAEL, S. LOUHICHI, AND C. PRIEUR (2007): “Weak dependence,” in *Weak dependence: With examples and applications*, pp. 9–20. Springer.

DEDECKER, J., AND C. PRIEUR (2004): “Coupling for  $\tau$ -dependent sequences and applications,” *Journal of Theoretical Probability*, 17(4), 861–885.

——— (2005): “New dependence coefficients. Examples and applications to statistics,” *Probability Theory and Related Fields*, 132(2), 203–236.

DEMIRER, M., F. X. DIEBOLD, L. LIU, AND K. YILMAZ (2018): “Estimating global bank network connectedness,” *Journal of Applied Econometrics*, 33(1), 1–15.

DEVORE, R. A. (1998): “Nonlinear approximation,” *Acta Numerica*, 7, 51–150.

DIEBOLD, F. X., AND R. S. MARIANO (1995): “Comparing predictive accuracy,” *Journal of Business and Economic Statistics*, 13(3), 253–263.

FAN, J., Q. LI, AND Y. WANG (2017): “Estimation of high dimensional mean regression in the absence of symmetry and light tail assumptions,” *Journal of the Royal Statistical Society: Series B (Statistical Methodology)*, 79(1), 247–265.

FENG, G., S. GIGLIO, AND D. XIU (2019): “Taming the factor zoo: A test of new factors,” *Journal of Finance* (forthcoming).

FLORENS, J.-P., AND M. MOUCHART (1982): “A note on noncausality,” *Econometrica*, 50(3), 583–591.

FORONI, C., M. MARCELLINO, AND C. SCHUMACHER (2015): “Unrestricted mixed data sampling (U-MIDAS): MIDAS regressions with unrestricted lag polynomials,” *Journal of the Royal Statistical Society: Series A (Statistics in Society)*, 178(1), 57–82.

FUK, D. K., AND S. V. NAGAEV (1971): “Probability inequalities for sums of independent random variables,” *Theory of Probability and Its Applications*, 16(4), 643–660.

GHYSELS, E., J. B. HILL, AND K. MOTEGI (2018): “Testing a large set of zero restrictions in regression models, with an application to mixed frequency granger causality,” *Journal of Econometrics* (forthcoming).

GHYSELS, E., AND H. QIAN (2019): “Estimating MIDAS regressions via OLS with polynomial parameter profiling,” *Econometrics and Statistics*, 9, 1–16.

GHYSELS, E., P. SANTA-CLARA, AND R. VALKANOV (2006): “Predicting volatility: getting the most out of return data sampled at different frequencies,” *Journal of Econometrics*, 131, 59–95.

GHYSELS, E., A. SINKO, AND R. VALKANOV (2006): “MIDAS regressions: Further results and new directions,” *Econometric Reviews*, 26, 53–90.

HAN, Y., AND R. S. TSAY (2017): “High-dimensional Linear Regression for Dependent Observations with Application to Nowcasting,” *arXiv preprint arXiv:1706.07899*.

HILL, J. B., AND E. RENAULT (2010): “Generalized method of moments with tail trimming,” *Dept. of Economics, University of North Carolina-Chapel Hill*.

JANKOVÁ, J., AND S. VAN DE GEER (2018): “Inference in high-dimensional graphical models,” in *Handbook of Graphical Models*, ed. by M. Maathuis, M. Drton, S. Lauritzen, and M. Wainwright, pp. 325–346. CRC Press.

KOCK, A. B., AND L. CALLOT (2015): “Oracle inequalities for high dimensional vector autoregressions,” *Journal of Econometrics*, 186(2), 325–344.

LAZARUS, E., D. J. LEWIS, J. H. STOCK, AND M. W. WATSON (2018): “HAR Inference: Recommendations for Practice,” *Journal of Business and Economic Statistics*, 36(4), 541–559.

LECUÉ, G., AND M. LERASLE (2019): “Robust machine learning by median-of-means: theory and practice,” *Annals of Statistics* (forthcoming).

LI, J., AND Z. LIAO (2019): “Uniform nonparametric inference for time series,” *Journal of Econometrics* (forthcoming).

LIANG, C., AND M. SCHIENLE (2019): “Determination of vector error correction models in high dimensions,” *Journal of Econometrics*, 208(2), 418–441.

LIAO, Z., AND P. C. PHILLIPS (2015): “Automated estimation of vector error correction models,” *Econometric Theory*, 31(3), 581–646.

MANRESA, E. (2013): “Estimating the structure of social interactions using panel data,” *Unpublished Manuscript. CEMFI, Madrid*.

MARSILLI, C. (2014): “Variable Selection in Predictive MIDAS Models,” Working papers 520, Banque de France.

MCCRACKEN, M. W., AND S. NG (2016): “FRED-MD: A monthly database for macroeconomic research,” *Journal of Business and Economic Statistics*, 34(4), 574–589.

MEINSHAUSEN, N., AND P. BÜHLMANN (2006): “High-dimensional graphs and variable selection with the LASSO,” *Annals of Statistics*, 34(3), 1436–1462.

MÜLLER, U. K. (2007): “A theory of robust long-run variance estimation,” *Journal of Econometrics*, 141(2), 1331–1352.

——— (2014): “HAC corrections for strongly autocorrelated time series,” *Journal of Business and Economic Statistics*, 32(3), 311–322.

NAGAEV, S. V. (1998): “Some refinements of probabilistic and moment inequalities,” *Theory of Probability and Its Applications*, 42(4), 707–713.

NEGAHBAN, S. N., P. RAVIKUMAR, M. J. WAINWRIGHT, AND B. YU (2012): “A unified framework for high-dimensional analysis of  $M$ -estimators with decomposable regularizers,” *Statistical Science*, 27(4), 538–557.

NEUMANN, M. H. (2013): “A central limit theorem for triangular arrays of weakly dependent random variables, with applications in statistics,” *ESAIM: Probability and Statistics*, 17, 120–134.

NEWHEY, W. K., AND K. D. WEST (1987): “A simple, positive semi-definite, heteroskedasticity and autocorrelation consistent covariance matrix,” *Econometrica*, 55(3), 703–708.

NZE, P. A., AND P. DOUKHAN (2004): “Weak dependence: models and applications to econometrics,” *Econometric Theory*, 20(6), 995–1045.

PARZEN, E. (1957): “On consistent estimates of the spectrum of a stationary time series,” *Annals of Mathematical Statistics*, 28(2), 329–348.

POLITIS, D. N. (2011): “Higher-order accurate, positive semidefinite estimation of large-sample covariance and spectral density matrices,” *Econometric Theory*, 27(4), 703–744.

RIO, E. (2017): *Asymptotic Theory of Weakly Dependent Random Processes*. Springer.

RUBIN, D. B. (1974): “Estimating causal effects of treatments in randomized and nonrandomized studies.,” *Journal of Educational Psychology*, 66(5), 688.

SILIVERSTOVS, B. (2017): “Short-term forecasting with mixed-frequency data: a MIDASSO approach,” *Applied Economics*, 49(13), 1326–1343.

SIMON, N., J. FRIEDMAN, T. HASTIE, AND R. TIBSHIRANI (2013): “A sparse-group LASSO,” *Journal of Computational and Graphical Statistics*, 22(2), 231–245.

SUN, Y., P. C. PHILLIPS, AND S. JIN (2008): “Optimal bandwidth selection in heteroskedasticity–autocorrelation robust testing,” *Econometrica*, 76(1), 175–194.

TIBSHIRANI, R. (1996): “Regression shrinkage and selection via the lasso,” *Journal of the Royal Statistical Society, Series B (Methodological)*, 58, 267–288.

UEMATSU, Y., AND S. TANAKA (2019): “High-dimensional macroeconomic forecasting and variable selection via penalized regression,” *Econometrics Journal*, 22, 34–56.

VAN DE GEER, S. (2016): *Estimation and testing under sparsity: École d’Été de Probabilités de Saint-Flour XLV–2015*, vol. 2159. Springer.

VAN DE GEER, S., P. BÜHLMANN, Y. RITOY, AND R. DEZEURE (2014): “On asymptotically optimal confidence regions and tests for high-dimensional models,” *The Annals of Statistics*, 42(3), 1166–1202.

WONG, K. C., Z. LI, AND A. TEWARI (2019): “LASSO guarantees for  $\beta$ -mixing heavy tailed time series,” *Annals of Statistics* (forthcoming).

WU, W. B. (2005): “Nonlinear system theory: Another look at dependence,” *Proceedings of the National Academy of Sciences*, 102(40), 14150–14154.

WU, W.-B., AND Y. N. WU (2016): “Performance bounds for parameter estimates of high-dimensional linear models with correlated errors,” *Electronic Journal of Statistics*, 10(1), 352–379.

YUAN, M., AND Y. LIN (2006): “Model selection and estimation in regression with grouped variables,” *Journal of the Royal Statistical Society: Series B (Statistical Methodology)*, 68(1), 49–67.

# APPENDIX

## A.1 Fuk-Nagaev inequality under $\tau$ -dependence

Mixing is by far the most commonly used weak dependence condition in econometrics. However, it is frequently criticized as there exist simple examples of Markov processes with discrete innovations that are not mixing, see, e.g., [Andrews \(1984\)](#). The widespread popularity of mixing has led to several efforts to develop alternative measures of the weak dependence that would include mixing conditions as a special case, see [Nze and Doukhan \(2004\)](#) and [Dedecker, Doukhan, Lang, Rafael, Louhichi, and Prieur \(2007\)](#) for a review.

The theoretical analysis of the LASSO-type estimators is crucially based on the concentration inequalities and the  $\tau$ -dependence introduced in [Dedecker and Prieur \(2004\)](#), which is the weakest known dependence concept for heavy-tailed data that does not suffer from [Andrews \(1984\)](#) criticism.<sup>27</sup> Let  $(\Omega, \mathcal{A}, \Pr)$  be a probability space,  $\mathcal{M}$  a  $\sigma$ -algebra of  $\mathcal{A}$ , and  $\xi$  some random element in the Banach space  $(E, |\cdot|)$ . For  $\xi \in \mathbf{R}$ , the  $\tau$  coefficient is defined as

$$\tau(\mathcal{M}, \xi) = \int \|F_{\xi|\mathcal{M}}(t) - F_{\xi}(t)\|_1 dt,$$

where  $F_{\xi}$  is the CDF of  $\xi$ ,  $F_{\xi|\mathcal{M}}$  is the conditional CDF of  $\xi$  given  $\mathcal{M}$ , and  $\|\cdot\|_1$  is the  $L_1$  norm. In the more general case, the  $\tau$  coefficient is defined as

$$\tau(\mathcal{M}, \xi) = \sup_{f \in \Lambda(E)} \int \|F_{f(X)|\mathcal{M}}(t) - F_{f(X)}(t)\|_1 dt,$$

where  $\Lambda(E) = \{f : |f(x) - f(y)| \leq |x - y|\}$  is the space of 1-Lipschitz functions on  $E$ .

It follows from [Dedecker and Prieur \(2004\)](#) and [Dedecker and Prieur \(2005\)](#), Lemma 1, that the  $\tau$  coefficient equals to the  $L_1$  coupling error implying that it is the weakest possible dependence concept for probabilistic results based on  $L_1$  coupling.

**Lemma A.1.1** ([Dedecker and Prieur \(2004\)](#)). *Let  $(\Omega, \mathcal{A}, \Pr)$  be a probability space,  $V$  an integrable real random variable, and  $\mathcal{M}$  a  $\sigma$ -algebra of  $\mathcal{A}$ . Let  $U \sim U[0, 1]$  be independent*

---

<sup>27</sup>There is no uniformly accepted definition of heavy-tailed data for LASSO-type estimators. For instance, [Wong, Li, and Tewari \(2019\)](#) defines heavy-tails as heavier than Gaussian, exponentially-decreasing tails, an assumption that implies that all moments exist. At the same time, the traditional time series analysis defines the data as heavy-tailed whenever the second moment does not exist, see, e.g., [Hill and Renault \(2010\)](#). In our treatment we refer to heavy-tailed distributions as distributions with finite  $q \geq 2$  moments only, an assumption widely accepted and commonly used in the asymptotic analysis of the GMM and QML estimators.

of  $\sigma(V) \vee \mathcal{M}$ . Then there exists  $V^* =_d V$ , measurable with respect to  $\mathcal{M} \vee \sigma(V) \vee \sigma(U)$ , independent of  $\mathcal{M}$ , and such that

$$\|V - V^*\|_1 = \tau(\mathcal{M}, V).$$

Let  $(\xi_t)_{t \in \mathbf{Z}}$  be a stochastic process on  $E$ . We endow the product space  $E^l = E \times E \times \cdots \times E$  with the following norm  $|x - y|_{E^l} = |x_1 - y_1| + \cdots + |x_l - y_l|$ . Put  $\mathcal{M}_t = \sigma(\xi_k : k \leq t)$ , and for  $J, k \geq 1$ , define

$$\tau_k(J) = \max_{1 \leq l \leq k} \frac{1}{l} \sup \{ \tau(\mathcal{M}_t, (\xi_{t_1}, \dots, \xi_{t_l})) : t_l > \cdots > t_1 \geq t + J, t \in \mathbf{Z} \}. \quad (\text{A.1})$$

The  $\tau$ -dependence coefficient is

$$\tau_J = \sup_{k \in \mathbf{N}} \tau_k(J). \quad (\text{A.2})$$

Dedecker and Prieur (2005) provide several examples of stochastic processes with bounds on  $\tau$ -dependence coefficients and compare  $\tau$ -dependence coefficients to various mixing conditions. This includes causal Bernoulli shifts, iterative random functions, and some other Markov chains. For instance, contractive autoregressive processes have geometrically decaying  $\tau$ -dependence coefficients, regardless of whether innovations are discrete or continuous.

**Example A.1.1.** Consider a stationary Markov chain  $(\xi_t)_{t \geq 0}$  generated as

$$\xi_t = F(\xi_{t-1}, \varepsilon_t),$$

where  $F$  is some measurable function and  $(\varepsilon_t)_{t \geq 0}$  are i.i.d. innovations, independent of  $X_0$ . Suppose that for some  $\rho \in (0, 1)$ ,  $\|F(x, \varepsilon_0) - F(y, \varepsilon_0)\|_1 \leq \rho \|x - y\|$ . Then  $\tau_J \leq \rho^J$ .

To obtain useful inequalities on tail probabilities, the dependence of the process should fade away sufficiently fast over time and there is usually a trade-off between the dependence and tails. We shall focus on polynomial tails or equivalently on finite polynomial moment conditions and obtain new Fuk-Nagaev inequality for  $\tau$ -dependent sequences. As emphasized in Nagaev (1998), the Fuk-Nagaev inequality delivers sharper estimates for tail probabilities in contrast with the Markov's bound in conjunction with the Rosenthal or Marcinkiewicz-Zygmund moment inequalities. Consequently, the Fuk-Nagaev inequality provides sharper estimates of convergence rates for LASSO-type estimators. In contrast to the previous work, our inequality reflects the mixture of the polynomial and the exponential tails in the spirit of the original inequality of Fuk and Nagaev (1971) for independent data.<sup>28</sup>

---

<sup>28</sup>Our inequality is sharper for our purposes than the inequality obtained in Dedecker and Prieur (2004), Theorem 2 for  $\tau$ -dependent processes, or Rio (2017), Theorem 6.2 for  $\alpha$ -mixing processes who are actually more interested in its application to moment inequalities.

**Theorem A.1.** Let  $(\xi_t)_{t \in \mathbf{Z}}$  be a real-valued centered stochastic process such that for some  $q \geq 2$ ,  $\mathbb{E}|\xi_t|^q < \infty$  for all  $t \in \mathbf{Z}$ . Then for every  $J \in [T]$  and  $x > 0$

$$\Pr \left( \left| \sum_{t=1}^T \xi_t \right| \geq 3x \right) \leq c_q^{(1)} A_{q,T} \frac{J^{q-1}}{x^q} + 4 \exp \left( -c_q^{(2)} x^2 / B_T^2 \right) + \frac{T \tau_{J+1}}{x},$$

where  $B_T^2 = \sum_{t=1}^T \sum_{k=1}^T |\text{Cov}(\xi_t, \xi_k)|$ ,  $c_q^{(1)} = 2 \left( 1 + \frac{2}{q} \right)^q$ ,  $c_q^{(2)} = \frac{2}{(q+2)^2 e^q}$ , and  $A_{q,T} = \sum_{t=1}^T \mathbb{E}|\xi_t|^q$ .

*Proof.* For  $a \in \mathbf{R}$ , let  $[a]$  denote its integer part. We split partial sums into blocks

$$\begin{aligned} V_1 &= \xi_1 + \cdots + \xi_J \\ V_2 &= \xi_{J+1} + \cdots + \xi_{2J} \\ &\vdots \\ V_{[T/J]} &= \xi_{([T/J]-1)J+1} + \cdots + \xi_{[T/J]J} \\ V_{[T/J]+1} &= \xi_{[T/J]J+1} + \cdots + \xi_T, \end{aligned}$$

where we set  $V_{[T/J]+1} = 0$  if  $T/J$  is an integer. Let  $(U_t)_{t=1}^{[T/J]+1}$  be i.i.d. random variables drawn from  $U[0, 1]$  independently of  $(V_t)_{t=1}^{[T/J]+1}$ . For every  $t = 3, \dots, [T/J] + 1$ , set  $\mathcal{M}_t = \sigma(V_1, \dots, V_{t-2})$ . Next, for  $t = 1, 2$ , we set  $V_t^* = V_t$ , while for  $t \geq 3$ , by Lemma A.1.1 there exist random variables  $V_t^* =_d V_t$  such that:

1.  $V_t^*$  is  $\sigma(V_1, \dots, V_{t-2}) \vee \sigma(V_t) \vee \sigma(U_t)$ -measurable, i.e.,  $V_t^* = f_t(V_1, \dots, V_{t-2}, V_t, U_t)$  for some measurable function  $f_t$ ;
2.  $V_t^* \perp\!\!\!\perp (V_1, \dots, V_{t-2})$ ;
3.  $\|V_t - V_t^*\|_1 = \tau(\mathcal{M}_t, V_t)$ .

It follows from properties 1. and 2. that  $(V_{2t}^*)_{t \geq 1}$  and  $(V_{2t-1}^*)_{t \geq 1}$  are sequences of independent random variables. Then

$$\begin{aligned} \left| \sum_{t=1}^T \xi_t \right| &\leq \left| \sum_{t \geq 1} V_{2t}^* \right| + \left| \sum_{t \geq 1} V_{2t-1}^* \right| + \sum_{t=3}^{[T/J]+1} |V_t - V_t^*| \\ &\triangleq I_T + II_T + III_T. \end{aligned}$$

By (Fuk and Nagaev, 1971, Corollary 4)

$$\begin{aligned} \Pr(I_T \geq x) &\leq \frac{c_q^{(1)}}{x^q} \sum_{t \geq 1} \mathbb{E}|V_{2t}^*|^q + 2 \exp \left( -\frac{c_q^{(2)} x^2}{\sum_{t \geq 1} \text{Var}(V_{2t}^*)} \right) \\ &\leq \frac{c_q^{(1)}}{x^q} \sum_{t \geq 1} \mathbb{E}|V_{2t}|^q + 2 \exp \left( -\frac{c_q^{(2)} x^2}{B_T^2} \right), \end{aligned}$$

where the second inequality follows since  $\sum_{t \geq 1} \text{Var}(V_{2t}^*) = \sum_{t \geq 1} \text{Var}(V_{2t}) \leq B_T^2$ . Similarly

$$\Pr(II_T \geq x) \leq \frac{c_q^{(1)}}{x^q} \sum_{t \geq 1} \mathbb{E}|V_{2t-1}|^q + 2 \exp\left(-\frac{c_q^{(2)}x^2}{B_T^2}\right).$$

Lastly, since  $\mathcal{M}_t$  and  $V_t$  are separated by  $J + 1$  lags of  $(\xi_t)_{t \geq 1}$ , we have  $\tau(\mathcal{M}_t, V_t) \leq J\tau_J(J + 1)$ . Then by Markov's inequality and property 3.

$$\begin{aligned} \Pr(III_T \geq x) &\leq \frac{1}{x} \sum_{t=3}^{[T/J]+1} \tau(\mathcal{M}_t, V_t) \\ &\leq \frac{T}{x} \tau_{J+1}. \end{aligned}$$

Combining all inequalities together, we obtain the result

$$\begin{aligned} \Pr\left(\left|\sum_{t=1}^T \xi_t\right| \geq 3x\right) &\leq \Pr(I_T \geq x) + \Pr(II_T \geq x) + \Pr(III_T \geq x) \\ &\leq \frac{c_q^{(1)}}{x^q} \sum_{t=1}^{[T/J]+1} \mathbb{E}|V_t|^q + 4 \exp\left(-\frac{c_q^{(2)}x^2}{B_T^2}\right) + \frac{T}{x} \tau_{J+1} \\ &\leq \frac{c_q^{(1)}}{x^q} J^{q-1} A_{q,T} + 4 \exp\left(-\frac{c_q^{(2)}x^2}{B_T^2}\right) + \frac{T}{x} \tau_{J+1}. \end{aligned}$$

□

Consequently, we obtain the following inequality for high-dimensional sums.

**Theorem A.2.** *Suppose that  $(\xi_t)_{t \in \mathbf{Z}}$  is a centered stochastic process in  $\mathbf{R}^p$  such that for every  $j \in [p]$ , (i)  $\mathbb{E}|\xi_{t,j}|^q < \infty$  for some  $q \geq 2$ ; (ii)  $\tau$ -dependence coefficients of  $\xi_{t,j}$  satisfy  $\tau_k^{(j)} \leq dk^{-a}$  for some universal constants  $d, a > 0$ . Then for every  $u > 0$*

$$\Pr\left(\left|\sum_{t=1}^T \xi_t\right|_{\infty} > u\right) \leq c_1(M_{q,T} \vee 1)pTu^{-\kappa} + 4p \exp\left(-\frac{c_2u^2}{B_T^2}\right),$$

where  $\kappa = \frac{(a+1)q-1}{a+q-1}$ ,  $M_{q,T} = \max_{j \in [p], t \in [T]} \mathbb{E}|\xi_{t,j}|^q$ ,  $B_T^2 = \max_{j \in [p]} \sum_{t=1}^T \sum_{k=1}^T |\text{Cov}(\xi_{t,j}, \xi_{k,j})|$ , and constants  $c_1 = 3^{\kappa} (c_q^{(1)} + d)$  and  $c_2 = c_q^{(2)}/9$ .

*Proof.* By Theorem A.1 for every  $j \in [p]$  and  $x > 0$

$$\Pr\left(\left|\sum_{t=1}^T \xi_{t,j}\right| \geq 3x\right) \leq c_q^{(1)} M_{q,T} T x^{-q} J^{q-1} + d T x^{-1} J^{-a} + 4 \exp\left(-c_q^{(2)} x^2 / B_T^2\right).$$

To balance the first two terms, we shall set  $J = x^{\frac{q-1}{q+a-1}}$ . Then by the union bound

$$\Pr \left( \left| \sum_{t=1}^T \xi_t \right|_{\infty} > u \right) \leq 3^{\kappa} \left( c_q^{(1)} + d \right) (M_{q,T} \vee 1) p T u^{-\kappa} + 4p \exp \left( -c_q^{(2)} u^2 / 9 B_T^2 \right).$$

□

The exponential tail depends on the sum of absolute values of covariances  $B_T^2$ , which can be controlled by the  $\tau$ -dependence coefficients. This follows from the fact that the covariance can be bounded by the  $L_1$  mixingale coefficient, which is bounded in turn by the  $\tau$ -dependence coefficient. For a real-valued stationary stochastic process  $(\xi_t)_{t \in \mathbf{Z}}$ , its  $L_1$  mixingale coefficient with respect to the filtration  $(\mathcal{M}_t)_{t \in \mathbf{Z}}$  is defined as

$$\gamma_t = \|\mathbb{E}(\xi_t | \mathcal{M}_0) - \mathbb{E}(\xi_t)\|_1.$$

The following covariance inequality follows from [Dedecker and Doukhan \(2003\)](#) and [Dedecker and Prieur \(2004\)](#) and provides a sharp way to control autocovariances with mixing and  $\tau$ -dependence coefficients. Note that  $\tau$ -dependence coefficients can be bounded by  $\alpha$ -mixing coefficient, see [Dedecker and Prieur \(2004\)](#), Lemma 6 and Remark 2.

**Proposition A.1.1.** *Let  $(\xi_t)_{t \in \mathbf{Z}}$  be a centered stationary stochastic process such that  $\mathbb{E}|\xi_0|^q < \infty$  for some  $q > 2$ , then*

$$|\text{Cov}(\xi_0, \xi_t)| \leq \gamma_t^{\frac{q-2}{q-1}} \|\xi_0\|_q^{q/(q-1)}$$

and  $\gamma_t \leq \tau_t$ .

*Proof.* Let  $Q$  be the quantile function of  $|\xi_0|$  and let  $G$  be the inverse of  $x \mapsto \int_0^x Q(u)du$ . By [Dedecker and Doukhan \(2003\)](#), Proposition 1

$$\begin{aligned} |\text{Cov}(\xi_0, \xi_t)| &\leq \int_0^{\gamma t} Q \circ G(u) du \\ &\leq \gamma_t^{\frac{q-2}{q-1}} \left( \int_0^{\|\xi_0\|_1} Q^{q-1} \circ G(u) du \right)^{1/(q-1)} = \gamma_t^{\frac{q-2}{q-1}} \|\xi_0\|_q^{q/(q-1)}, \end{aligned}$$

where the second line follows by Hölder's inequality and the last equality by the change of variables  $\int_0^{\|\xi_0\|_1} Q^{q-1} \circ G(u) du = \int_0^1 Q^q(u) du = \mathbb{E}|\xi_0|^q$ . The second statement follows from [Dedecker and Doukhan \(2003\)](#), Lemma 1 and [Dedecker and Prieur \(2004\)](#), Lemma 6. □

**Corollary A.1.1.** *Suppose that  $(\xi_t)_{t \in \mathbf{Z}}$  is a centered stationary stochastic process in  $\mathbf{R}^p$  such that for every  $j \in [p]$ , (i)  $\max_{j \in [p]} \mathbb{E}|\xi_{0,j}|^q = O(1)$  for some  $q > 2$ ; (ii)  $\tau$ -dependence coefficients of  $\xi_{t,j}$  satisfy  $\tau_k^{(j)} \leq dk^{-a}$  for some universal constants  $d > 0$  and  $a > \frac{q-1}{q-2}$ . Then there exists a universal constant  $C$  such that for every  $\delta \in (0, 1)$*

$$\Pr \left( \left| \frac{1}{T} \sum_{t=1}^T \xi_t \right|_{\infty} \leq C \left( \frac{p}{\delta T^{\kappa-1}} \right)^{1/\kappa} \vee \sqrt{\frac{\log(8p/\delta)}{T}} \right) \geq 1 - \delta. \quad (\text{A.3})$$

*Proof.* Under Assumptions (i)-(ii), by Proposition A.1.1

$$\begin{aligned}
B_T^2 &= \max_{j \in [p]} \sum_{t=1}^T \sum_{k=1}^T |\text{Cov}(\xi_{t,j}, \xi_{k,j})| \\
&= \max_{j \in [p]} \left\{ T\text{Var}(\xi_{0,j}) + 2 \sum_{t=1}^{T-1} (T-t) \text{Cov}(\xi_{0,j}, \xi_{t,j}) \right\} \\
&\leq \max_{j \in [p]} \left\{ T\text{Var}(\xi_{0,j}) + 2T \|\xi_{0,j}\|_q^{q/(q-1)} \sum_{t=1}^{T-1} (dt^{-a})^{\frac{q-2}{q-1}} \right\} = O(T).
\end{aligned}$$

Therefore, since  $M_{q,T} = O(1)$  and  $B_T^2 = O(T)$ , the result follows by inverting the inequality in Theorem A.2.  $\square$

## A.2 Dictionaries

It is possible to construct dictionaries using arbitrary sets of functions, including a mix of algebraic polynomials, trigonometric polynomials, B-splines, Haar basis, or wavelets. In this paper, we mostly focus on dictionaries generated by orthogonalized algebraic polynomials, though it might be interesting to tailor the dictionary for each particular application. The attractiveness of algebraic polynomials comes from their ability to generate a variety of functions with a relatively low number of parameters, which is especially desirable in the low signal-to-noise environments. The general family of appropriate orthogonal algebraic polynomials is given by Jacobi polynomial that nest Legendre, Gegenbauer, and Chebychev's polynomials as a special case.

**Example A.2.1** (Jacobi polynomials). *Applying the Gram-Schmidt orthogonalization procedure to  $\{1, x, x^2, x^3, \dots\}$  with respect to the measure*

$$d\mu(x) = (1-x)^\alpha (1+x)^\beta dx, \quad \alpha, \beta > -1,$$

*on  $[-1, 1]$ , we obtain Jacobi polynomials. In practice Jacobi polynomials can be computed through the well-known tree-term recurrence relation for  $n \geq 0$*

$$P_{n+1}^{(\alpha, \beta)}(x) = axP_n^{(\alpha, \beta)}(x) + bP_n^{(\alpha, \beta)}(x) - cP_{n-1}^{(\alpha, \beta)}(x)$$

*with  $a = \frac{(2n+\alpha+\beta+1)(2n+\alpha+\beta+2)}{2(n+1)(n+\alpha+\beta+1)}$ ,  $b = \frac{(2n+\alpha+\beta+1)(\alpha^2-\beta^2)}{2(n+1)(n+\alpha+\beta+1)(2n+\alpha+\beta)}$ ,  $c = \frac{(\alpha+n)(\beta+n)(2n+\alpha+\beta+2)}{(n+1)(n+\alpha+\beta+1)(2n+\alpha+\beta)}$ . To obtain the orthogonal basis on  $[0, 1]$ , we shift Jacobi polynomials with affine bijection  $x \mapsto 2x - 1$ .*

*For  $\alpha = \beta$ , we obtain Gegenbauer polynomials, for  $\alpha = \beta = 0$ , we obtain Legendre polynomials, while for  $\alpha = \beta = -1/2$  or  $\alpha = \beta = 1/2$ , we obtain Chebychev's polynomials of two kinds.*

In the mixed frequency setting, non-orthogonalized polynomials,  $\{1, x, x^2, x^3, \dots\}$ , are also called Almon polynomials. It is preferable to use orthogonal polynomials in practice due to better numerical properties. At the same time, orthogonal polynomials are available in Matlab, R, and Python packages. Legendre polynomials is our default recommendation, while other choices of  $\alpha$  and  $\beta$  are preferable if we want to accommodate heavier tails.

We noted in the main body of the paper that the specification in (2) deviates from the standard MIDAS polynomial specification as it results in a linear regression model - a subtle but key innovation as it maps MIDAS regressions in the standard regression framework. Moreover, casting the MIDAS regressions in a linear regression framework renders the optimization problem convex, something only achieved by [Siliverstovs \(2017\)](#) using the U-MIDAS of [Foroni, Marcellino, and Schumacher \(2015\)](#) which does not recognize the mixed frequency data structure, unlike our sg-LASSO.

### A.3 Proofs of main results

**Lemma A.3.1.** *Let  $|\cdot|_1$  and  $|\cdot|_2$  be two norms on  $\mathbf{R}^p$  and put  $\|\cdot\| = \alpha|\cdot|_1 + (1 - \alpha)|\cdot|_2$ . Then the dual norm of  $\|\cdot\|$ , denoted  $\|\cdot\|^*$ , satisfies*

$$\|z\|^* \leq \alpha|z|_1^* + (1 - \alpha)|z|_2^*, \quad \forall z \in \mathbf{R}^p,$$

where  $|\cdot|_1^*$  is the dual norm of  $|\cdot|_1$  and  $|\cdot|_2^*$  is the dual norm of  $|\cdot|_2$ .

*Proof.* Clearly,  $\|\cdot\|$  is a norm. By the convexity of  $x \mapsto x^{-1}$  on  $(0, \infty)$

$$\begin{aligned} \|z\|^* &= \sup_{\beta \neq 0} \frac{|\langle z, \beta \rangle|}{\|\beta\|} \leq \sup_{\beta \neq 0} \left\{ \alpha \frac{|\langle z, \beta \rangle|}{|\beta|_1} + (1 - \alpha) \frac{|\langle z, \beta \rangle|}{|\beta|_2} \right\} \\ &\leq \alpha \sup_{\beta \neq 0} \frac{|\langle z, \beta \rangle|}{|\beta|_1} + (1 - \alpha) \sup_{\beta \neq 0} \frac{|\langle z, \beta \rangle|}{|\beta|_2} = \alpha|z|_1^* + (1 - \alpha)|z|_2^*. \end{aligned}$$

□

*Proof of Theorem 3.1.* By Lemma A.3.1, using the fact that  $|\cdot|_\infty$  is the dual of  $|\cdot|_1$  and  $\max_k |z_k|_2$  is the dual of  $\sum_k |z_k|_2$

$$\begin{aligned} \Omega^*(\mathbf{X}^\top \mathbf{u}/T) &= \left\{ \alpha |\mathbf{X}^\top \mathbf{u}/T|_\infty + (1 - \alpha) \max_{G \in \mathbf{G}} |\mathbf{X}_G^\top \mathbf{u}/T|_2 \right\} \\ &\leq \left( \alpha + (1 - \alpha) \bar{G}^{1/2} \right) |\mathbf{X}^\top \mathbf{u}/T|_\infty \leq c^{-1} \lambda, \end{aligned} \tag{A.4}$$

where  $\mathbf{X}_G$  denotes the matrix with columns of  $\mathbf{X}$  corresponding to indices in  $G$  and we use the fact that under Assumptions 3.1 (i), (iii), by Corollary A.1.1 with probability at least  $1 - \delta$  :  $|\mathbf{X}^\top \mathbf{u}/T|_\infty \leq C \left( \frac{p}{\delta T^{\kappa-1}} \right)^{1/\kappa} \vee \sqrt{\frac{\log(8p/\delta)}{T}} = \frac{c^{-1} \lambda}{\alpha + (1 - \alpha) \bar{G}^{1/2}}$ , where the last line

follows by the choice of  $\lambda$  in Assumption 3.3. By Fermat's rule, the sg-LASSO satisfies  $\mathbf{X}^\top(\mathbf{X}\hat{\beta} - \mathbf{y})/T + \lambda z^* = 0$  for some  $z^* \in \partial\Omega(\hat{\beta})$ , where  $\partial\Omega(\hat{\beta})$  is the subdifferential of  $\beta \mapsto \Omega(\beta)$  at  $\hat{\beta}$ . Taking the inner product with  $\beta^0 - \hat{\beta}$

$$\langle \mathbf{X}^\top(\mathbf{X}\hat{\beta} - \mathbf{y}), \hat{\beta} - \beta^0 \rangle_T = \lambda \langle z^*, \beta^0 - \hat{\beta} \rangle \leq \lambda \left\{ \Omega(\beta^0) - \Omega(\hat{\beta}) \right\},$$

where the inequality follows by the definition of the subdifferential. Rearranging this inequality

$$\begin{aligned} \|\mathbf{X}(\hat{\beta} - \beta^0)\|_T^2 - \lambda \left\{ \Omega(\beta^0) - \Omega(\hat{\beta}) \right\} &\leq \langle \mathbf{u}, \mathbf{X}(\hat{\beta} - \beta^0) \rangle_T + \langle \mathbf{m} - \mathbf{X}\beta^0, \mathbf{X}(\hat{\beta} - \beta^0) \rangle_T \\ &\leq \Omega^* \left( \mathbf{X}^\top \mathbf{u} / T \right) \Omega(\hat{\beta} - \beta^0) + \|\mathbf{X}(\hat{\beta} - \beta^0)\|_T \|\mathbf{m} - \mathbf{X}\beta^0\|_T \\ &\leq c^{-1} \lambda \Omega(\hat{\beta} - \beta^0) + \|\mathbf{X}(\hat{\beta} - \beta^0)\|_T \|\mathbf{m} - \mathbf{X}\beta^0\|_T. \end{aligned}$$

where the second line follows by the dual norm inequality and the last by  $\Omega^*(\mathbf{X}^\top \mathbf{u} / T) \leq c^{-1} \lambda$  as shown in Eq. A.4. Therefore,

$$\begin{aligned} \|\mathbf{X}\Delta\|_T^2 &\leq c^{-1} \lambda \Omega(\Delta) + \|\mathbf{X}\Delta\|_T \|\mathbf{m} - \mathbf{X}\beta^0\|_T + \lambda \left\{ \Omega(\beta^0) - \Omega(\hat{\beta}) \right\} \\ &\leq (c^{-1} + 1) \lambda \Omega(\Delta) + \|\mathbf{X}\Delta\|_T \|\mathbf{m} - \mathbf{X}\beta^0\|_T \end{aligned} \quad (\text{A.5})$$

with  $\Delta = \hat{\beta} - \beta^0$ . Note that for arbitrary  $\beta \in \mathbf{R}^p$ , the sg-LASSO penalty can be decomposed as a sum of two seminorms  $\Omega(\beta) = \Omega_0(\beta) + \Omega_1(\beta)$  with

$$\Omega_0(\beta) = \alpha |\beta_{S_0}|_1 + (1 - \alpha) \sum_{G \in \mathcal{G}_0} |\beta_G|_2 \quad \text{and} \quad \Omega_1(\beta) = \alpha |\beta_{S_0^c}|_1 + (1 - \alpha) \sum_{G \in \mathcal{G}_0^c} |\beta_G|_2. \quad (\text{A.6})$$

Note also that  $\Omega_1(\beta^0) = 0$  and  $\Omega_1(\hat{\beta}) = \Omega_1(\Delta)$ . Then by the triangle inequality  $\Omega(\beta^0) - \Omega(\hat{\beta}) \leq \Omega_0(\Delta) - \Omega_1(\Delta)$ . If  $\|\mathbf{m} - \mathbf{X}\beta^0\|_T \leq \frac{1}{2} \|\mathbf{X}\Delta\|_T$ , then we obtain

$$\|\mathbf{X}\Delta\|_T^2 \leq 2c^{-1} \lambda \Omega(\Delta) + 2\lambda \{ \Omega_0(\Delta) - \Omega_1(\Delta) \}.$$

Since the left side of this equation is positive, this shows that  $\Omega_1(\Delta) \leq \frac{c+1}{c-1} \Omega_0(\Delta)$ , and whence  $\Delta$  belongs to  $\mathcal{C}(c_0)$ , c.f., Assumption 3.2. Then by Jensen's inequality and Assumption 3.2

$$\begin{aligned} \Omega(\Delta) &\leq (1 + c_0) \Omega_0(\Delta) \\ &\leq (1 + c_0) \left( \alpha \sqrt{|S_0|} |\Delta_{S_0}|_2 + (1 - \alpha) \sqrt{|\mathcal{G}_0|} \sqrt{\sum_{G \in \mathcal{G}_0} |\Delta_G|_2^2} \right) \\ &\leq (1 + c_0) s_\alpha^{1/2} |\Sigma^{1/2} \Delta|_2 \end{aligned} \quad (\text{A.7})$$

with  $s_\alpha^{1/2} = \alpha\sqrt{|S_0|\gamma_1^{-1}} + (1-\alpha)\sqrt{|\mathcal{G}_0|\gamma_2^{-1}}$ . Since  $|\Sigma^{1/2}\Delta|_2^2 = \Delta^\top \Sigma \Delta$ , by the inequality in Eq. A.5 and the dual norm inequality

$$\begin{aligned}\Omega^2(\Delta) &\leq (1+c_0)^2 s_\alpha |\Sigma^{1/2}\Delta|_2^2 \\ &= (1+c_0)^2 s_\alpha \left\{ \|\mathbf{X}\Delta\|_T^2 + \Delta^\top (\Sigma - \hat{\Sigma})\Delta \right\} \\ &\leq (1+c_0)^2 s_\alpha \left\{ 2(c^{-1}+1)\lambda\Omega(\Delta) + \Omega(\Delta)\Omega^* \left( (\hat{\Sigma} - \Sigma)\Delta \right) \right\} \\ &\leq (1+c_0)^2 s_\alpha \left\{ 2(c^{-1}+1)\lambda\Omega(\Delta) + \Omega^2(\Delta)\bar{G}|\text{vech}(\hat{\Sigma} - \Sigma)|_\infty \right\},\end{aligned}$$

where the last line follows by Lemma A.3.1 and elementary computations

$$\begin{aligned}\Omega^* \left( (\hat{\Sigma} - \Sigma)\Delta \right) &\leq \alpha|\hat{\Sigma} - \Sigma)\Delta|_\infty + (1-\alpha) \max_{G \in \mathbf{G}} |[(\hat{\Sigma} - \Sigma)\Delta]_G|_2 \\ &\leq \alpha|\Delta|_1|\text{vech}(\hat{\Sigma} - \Sigma)|_\infty + (1-\alpha)\bar{G}^{1/2}|\text{vech}(\hat{\Sigma} - \Sigma)|_\infty|\Delta|_1 \\ &\leq \bar{G}|\text{vech}(\hat{\Sigma} - \Sigma)|_\infty\Omega(\Delta).\end{aligned}$$

Therefore, on the event  $E = \left\{ |\text{vech}(\hat{\Sigma} - \Sigma)|_\infty \leq \frac{1}{2Gs_\alpha(1+2c_0)^2} \right\}$

$$\begin{aligned}\Omega(\Delta) &\leq 2(1+c_0)^2 s_\alpha (c^{-1}+1)\lambda + (1+c_0)^2 s_\alpha \bar{G}|\text{vech}(\hat{\Sigma} - \Sigma)|_\infty\Omega(\Delta) \\ &\leq 2(1+c_0)^2 s_\alpha (c^{-1}+1)\lambda + (1-A^{-1})\Omega(\Delta)\end{aligned}$$

with  $1-A^{-1} = \frac{(1+c_0)^2}{2(1+2c_0)^2} < 1$ . This observation in conjunction with the inequality in Eq. A.5 gives

$$\begin{aligned}\Omega(\Delta) &\leq 2A(1+c_0)^2 s_\alpha (c^{-1}+1)\lambda \\ \|\mathbf{X}\Delta\|_T^2 &\leq 4A(1+c_0)^2 s_\alpha (c^{-1}+1)^2\lambda^2.\end{aligned}$$

On the other hand, if  $\|\mathbf{m} - \mathbf{X}\beta^0\|_T > \frac{1}{2}\|\mathbf{X}\Delta\|_T$ , then

$$\|\mathbf{X}\Delta\|_T^2 \leq 4\|\mathbf{m} - \mathbf{X}\beta^0\|_T^2.$$

Therefore, on  $E$ , we always have

$$\|\mathbf{X}\Delta\|_T^2 \leq C_1 s_\alpha \lambda^2 + 4\|\mathbf{m} - \mathbf{X}\beta^0\|_T^2 \tag{A.8}$$

with  $C_1 = 4A(1+c_0)^2(c^{-1}+1)^2$ .

To establish the second statement, suppose first that  $\Delta \in \mathcal{C}(2c_0)$ . Then on  $E$

$$\begin{aligned}\Omega^2(\Delta) &\leq (1+2c_0)^2 s_\alpha |\Sigma^{1/2}\Delta|_2^2 \\ &= (1+2c_0)^2 s_\alpha \left\{ \|\mathbf{X}\Delta\|_T^2 + \Delta^\top (\Sigma - \hat{\Sigma})\Delta \right\} \\ &\leq (1+2c_0)^2 s_\alpha \left\{ C_1 s_\alpha \lambda^2 + 4\|\mathbf{m} - \mathbf{X}\beta^0\|_T^2 + \Omega^2(\Delta)\bar{G}|\text{vech}(\hat{\Sigma} - \Sigma)|_\infty \right\} \\ &\leq (1+2c_0)^2 s_\alpha \left\{ C_1 s_\alpha \lambda^2 + 4\|\mathbf{m} - \mathbf{X}\beta^0\|_T^2 \right\} + 2^{-1}\Omega^2(\Delta),\end{aligned}$$

where the first inequality follows by computations similar to Eq. A.7 and the second inequality from Eq. A.8. Therefore,

$$\Omega^2(\Delta) \leq 2(1+2c_0)^2 s_\alpha \{C_1 s_\alpha \lambda^2 + 4\|\mathbf{m} - \mathbf{X}\beta^0\|_T^2\}. \quad (\text{A.9})$$

On the other hand, if  $\Delta \notin \mathcal{C}(2c_0)$ , then  $\Delta \notin \mathcal{C}(c_0)$ , which as we've shown implies  $\|\mathbf{m} - \mathbf{X}\beta^0\|_T > \frac{1}{2}\|\mathbf{X}\Delta\|_T$ . In conjunction with Eq. A.5, this shows that

$$0 \leq \lambda c^{-1} \Omega(\Delta) + 2\|\mathbf{m} - \mathbf{X}\beta^0\|_T^2 + \lambda \{\Omega_0(\Delta) - \Omega_1(\Delta)\},$$

and whence

$$\begin{aligned} \Omega_1(\Delta) &\leq c_0 \Omega_0(\Delta) + \frac{2c}{\lambda(c-1)} \|\mathbf{m} - \mathbf{X}\beta^0\|_T^2 \\ &\leq 2^{-1} \Omega_1(\Delta) + \frac{2c}{\lambda(c-1)} \|\mathbf{m} - \mathbf{X}\beta^0\|_T^2. \end{aligned}$$

This shows that  $\Omega(\Delta) \leq (1+(2c_0)^{-1})\Omega_1(\Delta) \leq (1+(2c_0)^{-1})\frac{4c}{\lambda(c-1)}\|\mathbf{m} - \mathbf{X}\beta^0\|_T^2 = \lambda^{-1}\frac{2c(3c-1)}{c^2-1}\|\mathbf{m} - \mathbf{X}\beta^0\|_T^2$ . Combining this with inequality obtained in Eq. A.9 we obtain the second result with  $C_2 = \sqrt{2C_1}(1+2c_0)$ ,  $C_3 = \frac{2c(3c-1)}{c^2-1}$ , and  $C_4 = 2\sqrt{2}(1+2c_0)$ .

Lastly, under Assumption 3.1 (ii), (iv), by Theorem A.2, Proposition A.1.1, and the proof of Corollary A.1.1, the probability of  $E^c$  is

$$\begin{aligned} \Pr(E^c) &= \Pr\left(|\text{vech}(\hat{\Sigma} - \Sigma)|_\infty > \frac{1}{2\bar{G}s_\alpha(1+2c_0)^2}\right) \\ &\leq \frac{A_1 s_\alpha^{\tilde{\kappa}} p^2}{T^{\tilde{\kappa}-1}} + 2p(p+1) \exp(-A_2 T/s_\alpha^2) \end{aligned}$$

for some universal constants  $A_1$  and  $A_2$ .  $\square$

*Proof of Theorem 4.1.* By Fermat's rule, the sg-LASSO satisfies

$$\mathbf{X}^\top(\mathbf{X}\hat{\beta} - \mathbf{y})/T + \lambda z^* = 0, \quad z^* \in \partial\Omega(\hat{\beta}).$$

Rearranging this expression and multiplying by  $\hat{\Theta}$

$$\hat{\beta} - \beta^0 + \hat{\Theta}\lambda z^* = \hat{\Theta}\mathbf{X}^\top\mathbf{u}/T + (I - \hat{\Theta}\hat{\Sigma})(\hat{\beta} - \beta^0) + \hat{\Theta}\mathbf{X}^\top(\mathbf{m} - \mathbf{X}\beta^0)/T.$$

Plugging in  $\lambda z^*$  and normalizing by  $\sqrt{T}$

$$\begin{aligned} \sqrt{T}(\hat{\beta} - \beta^0 + b) &= \hat{\Theta}\mathbf{X}^\top\mathbf{u}/\sqrt{T} + \sqrt{T}(I - \hat{\Theta}\hat{\Sigma})(\hat{\beta} - \beta^0) + \hat{\Theta}\mathbf{X}^\top(\mathbf{m} - \mathbf{X}\beta^0)/\sqrt{T} \\ &= \frac{1}{\sqrt{T}} \sum_{t=1}^T u_t \Theta X_t + \frac{1}{\sqrt{T}} \sum_{t=1}^T u_t (\hat{\Theta} - \Theta) X_t + \sqrt{T}(I - \hat{\Theta}\hat{\Sigma})(\hat{\beta} - \beta^0) \\ &\quad + \hat{\Theta}\mathbf{X}^\top(\mathbf{m} - \mathbf{X}\beta^0)/\sqrt{T}. \end{aligned}$$

Next, we look at coefficients corresponding to  $G \subset [p]$

$$\begin{aligned}\sqrt{T}(\hat{\beta}_G - \beta_G^0 + b_G) &= \frac{1}{\sqrt{T}} \sum_{t=1}^T u_t \Theta_G X_t + \frac{1}{\sqrt{T}} \sum_{t=1}^T u_t (\hat{\Theta}_G - \Theta_G) X_t + \sqrt{T}(I - \hat{\Theta}\hat{\Sigma})_G(\hat{\beta} - \beta^0) \\ &\quad + \hat{\Theta}_G \mathbf{X}^\top (\mathbf{m} - \mathbf{X}\beta^0)/\sqrt{T} \\ &\triangleq I_T + II_T + III_T + IV_T.\end{aligned}$$

We will show that  $I_T \xrightarrow{d} N(0, \Xi_G)$  by the triangular array CLT, c.f., [Neumann \(2013\)](#), Theorem 2.1. To that end, first, by the Crámer-Wold theorem, it is sufficient to show that  $z^\top I_T \xrightarrow{d} z^\top N(0, \Xi_G)$  for every  $z \in \mathbf{R}^{|G|}$ . Second, under Assumptions 3.1 and 4.1 (i)-(ii)

$$\begin{aligned}\sum_{t=1}^T \mathbb{E} \left| \frac{z^\top \xi_t}{\sqrt{T}} \right|^2 &= \mathbb{E} |u_t z^\top \Theta_G X_t|^2 \\ &\leq C z^\top \Theta_G \Sigma \Theta_G^\top z \\ &= C z^\top (\Theta_G)_G z \\ &= O(1).\end{aligned}$$

Third, under Assumptions 3.1 (i), for every  $\epsilon > 0$

$$\begin{aligned}\sum_{t=1}^T \mathbb{E} \left[ \left| \frac{z^\top \xi_t}{\sqrt{T}} \right|^2 \mathbf{1} \left\{ \left| z^\top \xi_t \right| > \epsilon \sqrt{T} \right\} \right] &\leq \frac{\mathbb{E} |z^\top \xi_t|^q}{(\epsilon \sqrt{T})^{q-2}} \\ &= o(1),\end{aligned}$$

where we use the fact that by the Minkowski inequality and Assumptions 3.1 (i) and 4.1 (ii)

$$\begin{aligned}\mathbb{E} \|z^\top \xi_t\|_q &\leq \sum_{k \in G} |z_k| \sum_{j \in [p]} |\Theta_{k,j}| \|u_t X_{t,j}\|_q \\ &= O \left( |z|_1 \max_{k \in G} |\Theta_k|_1 \right) \\ &= O(1).\end{aligned}\tag{A.10}$$

Fourth, under stationarity

$$\text{Var} \left( \frac{1}{\sqrt{T}} \sum_{t=1}^T z^\top \xi_t \right) = \text{Var}(z^\top \xi_0) + 2 \sum_{t=1}^{T-1} \left( 1 - \frac{t}{T} \right) \text{Cov}(z^\top \xi_0, z^\top \xi_t)$$

and under Assumptions 3.1 (i) and 4.1 (iii), by Proposition [A.1.1](#) and the Minkowski

inequality

$$\begin{aligned}
\sum_{t=1}^{\infty} |\text{Cov}(z^{\top} \xi_0, z^{\top} \xi_t)| &\leq \|z^{\top} \xi_0\|_q^{q/(q-1)} \sum_{t=1}^{\infty} \|\mathbb{E}(z^{\top} \xi_t | \mathcal{M}_0) - \mathbb{E}(z^{\top} \xi_t)\|_1^{\frac{q-2}{q-1}} \\
&\leq \|z^{\top} \xi_0\|_q^{q/(q-1)} |z|_1^{\frac{q-2}{q-1}} \sum_{t=1}^{\infty} \tau_{T,t}^{\frac{q-2}{q-1}} \\
&= O(1).
\end{aligned}$$

By the Lebesgue dominated convergence, this shows that the long run variance exists

$$\lim_{T \rightarrow \infty} \text{Var} \left( \frac{1}{\sqrt{T}} \sum_{t=1}^T z^{\top} \xi_t \right) = z^{\top} \Xi_G z.$$

Let  $\mathcal{M}_t = \sigma(\xi_s : s \leq t)$ . Then, for every measurable function  $g : \mathbf{R}^h \rightarrow \mathbf{R}$  with  $\sup_x |g(x)| \leq 1$ , by [Dedecker and Doukhan \(2003\)](#), Proposition 1, for all  $h \in \mathbf{N}$  and all indices  $1 \leq t_1 < t_2 < \dots < t_h < t_h + r \leq t_h + s \leq T$

$$\begin{aligned}
&\left| \text{Cov} \left( g(z^{\top} \xi_{t_1} / \sqrt{T}, \dots, z^{\top} \xi_{t_h} / \sqrt{T}) z^{\top} \xi_{t_h} / \sqrt{T}, z^{\top} \xi_{t_h+r} / \sqrt{T} \right) \right| \\
&\leq \frac{1}{T} \int_0^{\gamma(\mathcal{M}_0, z^{\top} \xi_r)} Q_{z^{\top} \xi_0} \circ G_{z^{\top} \xi_r}(u) du \\
&\leq \frac{1}{T} \|\mathbb{E}(z^{\top} \xi_r | \mathcal{M}_0) - \mathbb{E}(z^{\top} \xi_r)\|_1^{\frac{q-2}{q-1}} \|z^{\top} \xi_0\|_q^{q/(q-1)} \\
&\leq \frac{1}{T} |z|_1^{\frac{q-2}{q-1}} \|z^{\top} \xi_0\|_q^{q/(q-1)} \tau_{T,r}^{\frac{q-2}{q-1}},
\end{aligned}$$

where the second line follows by stationarity and  $\sup_x |g(x)| \leq 1$ , the third since by Hölder's inequality and the change of variables

$$\int_0^{\|z^{\top} \xi_0\|_1} Q_{z^{\top} \xi_0}^{q-1} \circ G_{z^{\top} \xi_r}(u) du = \int_0^1 Q_{z^{\top} \xi_0}^q(u) du = \|z^{\top} \xi_0\|_q^q,$$

and the last by [Proposition A.1.1](#). Similarly,

$$\begin{aligned}
&\left| \text{Cov} \left( g(z^{\top} \xi_{t_1} / \sqrt{T}, \dots, z^{\top} \xi_{t_h} / \sqrt{T}), z^{\top} \xi_{t_h+r} / \sqrt{T} z^{\top} \xi_{t_h+s} / \sqrt{T} \right) \right| \\
&\leq \frac{1}{T} \int_0^{\gamma(\mathcal{M}_0, z^{\top} \xi_r z^{\top} \xi_s)} Q_g \circ G_{z^{\top} \xi_r z^{\top} \xi_s}(u) du \\
&\leq \frac{1}{T} \left\| \mathbb{E}(z^{\top} \xi_r z^{\top} \xi_s | \mathcal{M}_0) - \mathbb{E}(z^{\top} \xi_r z^{\top} \xi_s) \right\|_1 \\
&\leq \frac{1}{T} |z|_1^2 \tilde{\tau}_{T,r}.
\end{aligned}$$

Therefore, by [Neumann \(2013\)](#), Theorem 2.1,  $z^\top I_T \xrightarrow{d} z^\top N(0, \Xi_G)$  for every  $z \in \mathbf{R}^{|G|}$ .

Next,

$$\begin{aligned} |II_T|_\infty &= \left| (\hat{\Theta} - \Theta)_G \left( \frac{1}{\sqrt{T}} \sum_{t=1}^T u_t X_t \right) \right|_\infty \\ &\leq \|\hat{\Theta}_G - \Theta_G\|_\infty \left| \frac{1}{\sqrt{T}} \sum_{t=1}^T u_t X_t \right|_\infty \\ &= O_P \left( \frac{Sp^{1/\kappa}}{T^{1-1/\kappa}} \vee S\sqrt{\frac{\log p}{T}} \right) O_P \left( \frac{p^{1/\kappa}}{T^{1/2-1/\kappa}} + \sqrt{\log p} \right) \\ &= o_P(1), \end{aligned}$$

where the second line follows by  $|Ax|_\infty \leq \|A\|_\infty |x|_\infty$ , the third line by [Proposition A.3.2](#) and [Corollary A.1.1](#), and the last under [Assumption 4.1 \(v\)](#).

Likewise, using  $|Ax|_\infty \leq \max_{j,k} |A_{j,k}|_\infty |x|_1$ , by [Proposition A.3.2](#) and [Corollary 3.1](#)

$$\begin{aligned} |(I - \hat{\Theta}\hat{\Sigma})_G(\hat{\beta} - \beta^0)|_\infty &\leq \max_{j \in G} |(I - \hat{\Theta}\hat{\Sigma})_j|_\infty |\hat{\beta} - \beta^0|_1 \\ &= O_P \left( \frac{p^{1/\kappa}}{T^{1-1/\kappa}} \vee \sqrt{\frac{\log p}{T}} \right) O_P \left( \frac{s_\alpha p^{1/\kappa}}{T^{1-1/\kappa}} \vee s_\alpha \sqrt{\frac{\log p}{T}} \right). \end{aligned}$$

Under [Assumption 4.1 \(v\)](#), this shows that

$$\begin{aligned} |III_T|_\infty &= O_P \left( \frac{p^{1/\kappa}}{T^{1/2-1/\kappa}} \vee \sqrt{\log p} \right) O_P \left( \frac{s_\alpha p^{1/\kappa}}{T^{1-1/\kappa}} \vee s_\alpha \sqrt{\frac{\log p}{T}} \right) \\ &= o_P(1). \end{aligned}$$

Lastly, under [Assumption 4.1 \(vi\)](#)

$$\begin{aligned} |IV_T|_\infty &\leq \max_{j \in G} |\mathbf{X}\hat{\Theta}_j^\top|_2 \|\mathbf{m} - \mathbf{X}\beta^0\|_T \\ &= \max_{j \in G} \sqrt{\hat{\Theta}_j \hat{\Sigma} \hat{\Theta}_j^\top} o_P(1) \\ &= o_P(1), \end{aligned}$$

where the last line follows since  $\hat{\Theta}_j$  is consistent in the  $\ell_1$  norm while  $\hat{\Sigma}$  is consistent in the  $\ell_\infty$  norm under maintained assumptions.  $\square$

Next, we consider the regularized estimator of the variance of the regression error

$$\hat{\sigma}^2 = \|\mathbf{y} - \mathbf{X}\hat{\beta}\|_T^2 + \lambda\Omega(\hat{\beta}),$$

where  $\hat{\beta}$  is the sg-LASSO estimator. While the regularization is not needed to have a consistent variance estimator, the LASSO version of the regularized estimator ( $\alpha = 1$ ) is needed to establish the CLT for the debiased sg-LASSO estimator. The following result describes the converges of this variance estimator to its population counterpart  $\sigma^2 = \mathbb{E}\|\mathbf{u}\|_T^2$ .

**Proposition A.3.1.** *Suppose that Assumptions 3.1, 3.2, 3.3, and 3.4 are satisfied and that  $(u_t^2)_{t \in \mathbf{Z}}$  has a finite long run variance. Then*

$$\hat{\sigma}^2 = \sigma^2 + O_P \left( \frac{s_\alpha p^{1/\kappa}}{T^{1-1/\kappa}} \vee s_\alpha \sqrt{\frac{\log p}{T}} \right)$$

provided that  $\frac{s_\alpha p^{1/\kappa}}{T^{1-1/\kappa}} \vee s_\alpha \sqrt{\frac{\log p}{T}} = o(1)$ .

*Proof.* We have

$$\begin{aligned} |\hat{\sigma}^2 - \sigma^2| &= \left| \|\mathbf{u}\|_T^2 + 2\langle \mathbf{u}, \mathbf{m} - \mathbf{X}\hat{\beta} \rangle_T - \|\mathbf{m} - \mathbf{X}\hat{\beta}\|_T^2 + \lambda\Omega(\hat{\beta}) - \sigma^2 \right| \\ &\leq |\sigma^2 - \|\mathbf{u}\|_T^2| + 2\|\mathbf{u}\|_T \|\mathbf{m} - \mathbf{X}\hat{\beta}\|_T + 2\|\mathbf{X}(\hat{\beta} - \beta^0)\|_T^2 + 2\|\mathbf{m} - \mathbf{X}\beta^0\|_T^2 + \lambda\Omega(\hat{\beta}) \\ &\triangleq I_T + II_T + III_T + IV_T + V_T. \end{aligned}$$

By the Chebychev's inequality since the long-run variance exists, for every  $\varepsilon > 0$

$$\Pr \left( \left| \frac{1}{\sqrt{T}} \sum_{t=1}^T (u_t^2 - \sigma^2) \right| > \varepsilon \right) \leq \frac{1}{\varepsilon^2} \sum_{t \in \mathbf{Z}} \text{Cov}(u_0^2, u_t^2),$$

whence  $I_T = O_P\left(\frac{1}{\sqrt{T}}\right)$ . Therefore, by the triangle inequality and Corollary 3.1

$$\begin{aligned} II_T &= O_P(1) \|\mathbf{m} - \mathbf{X}\hat{\beta}\|_T \\ &\leq O_P(1) \left( \|\mathbf{m} - \mathbf{X}\beta^0\|_T + \|\mathbf{X}(\hat{\beta} - \beta^0)\|_T \right) = O_P \left( s_\alpha^{1/2} \lambda + \frac{s_\alpha^{1/2} p^{1/\kappa}}{T^{1-1/\kappa}} \vee \sqrt{\frac{s_\alpha \log p}{T}} \right). \end{aligned}$$

By Corollary 3.1 we also have

$$III_T + IV_T = O_P \left( \frac{s_\alpha p^{2/\kappa}}{T^{2-2/\kappa}} \vee \frac{s_\alpha \log p}{T} + s_\alpha \lambda^2 \right).$$

Lastly, another application of Corollary 3.1 gives

$$\begin{aligned} V_T &= \lambda\Omega(\hat{\beta} - \beta^0) + \lambda\Omega(\beta^0) \\ &= O_P \left( \lambda \left( \frac{s_\alpha p^{1/\kappa}}{T^{1-1/\kappa}} \vee s_\alpha \sqrt{\frac{\log p}{T}} \right) + \lambda s_\alpha \right). \end{aligned}$$

The result follows from combining all estimates together.  $\square$

Consider nodewise LASSO regressions in equation (5) for each  $j \in [p]$ . Put  $S = \max_{j \in G} S_j$ , where  $S_j$  is the support of  $\gamma_j$ .

**Proposition A.3.2.** *Suppose that Assumptions 3.1, 3.2, 3.3, and 3.4 are satisfied for each nodewise regression  $j \in G$  and that  $(V_{t,j}^2)_{t \in \mathbf{Z}}$  has a finite long-run variance for each  $j \in G$ . Then if  $S^\kappa p = o(T^{\kappa-1})$  and  $S = o(T^{1/2}/\log^{1/2} p)$*

$$\|\hat{\Theta}_G - \Theta_G\|_\infty = O_P \left( \frac{Sp^{1/\kappa}}{T^{1-1/\kappa}} \vee S \sqrt{\frac{\log p}{T}} \right)$$

and

$$\max_{j \in G} |(I - \hat{\Theta}\hat{\Sigma})_j|_\infty = O_P \left( \frac{p^{1/\kappa}}{T^{1-1/\kappa}} \vee \sqrt{\frac{\log p}{T}} \right).$$

*Proof.* By Corollary 3.1 and Proposition A.3.1 with  $\alpha = 1$  (corresponding to the LASSO estimator of  $\gamma_j$  and  $\sigma_j^2$ )

$$\begin{aligned} \|\hat{\Theta}_G - \Theta_G\|_\infty &= \max_{j \in G} |\hat{\Theta}_j - \Theta_j|_1 \\ &\leq \max_{j \in G} \left\{ |\hat{\gamma}_j|_1 \left| \hat{\sigma}_j^{-2} - \sigma_j^{-2} \right| + |\hat{\gamma}_j - \gamma_j|_1 |\sigma_j^{-2}| \right\} \\ &= O_P \left( \frac{Sp^{1/\kappa}}{T^{1-1/\kappa}} \vee S \sqrt{\frac{\log p}{T}} \right), \end{aligned}$$

where we use the fact that  $|G|$  is fixed and that  $\hat{\sigma}_j^2 \xrightarrow{p} \sigma_j^2$ .

Second, for each  $j \in G$ , by Fermat's rule,

$$\mathbf{X}_{-j}^\top (\mathbf{X}_j - \mathbf{X}_{-j} \hat{\gamma}_j) / T = \lambda_j z^*, \quad z^* \in \partial |\hat{\gamma}_j|_1,$$

where  $\hat{\gamma}_j^\top z^* = |\hat{\gamma}_j|_1$  and  $|z^*|_\infty \leq 1$ . Then

$$\begin{aligned} \mathbf{X}_j^\top (\mathbf{X}_j - \mathbf{X}_{-j} \hat{\gamma}_j) / T &= \|\mathbf{X}_j - \mathbf{X}_{-j} \hat{\gamma}_j\|_T^2 + \hat{\gamma}_j^\top \mathbf{X}_{-j}^\top (\mathbf{X}_j - \mathbf{X}_{-j} \hat{\gamma}_j) / T \\ &= \|\mathbf{X}_j - \mathbf{X}_{-j} \hat{\gamma}_j\|_T^2 + \lambda_j \hat{\gamma}_j^\top z^* = \hat{\sigma}_j^2, \end{aligned}$$

and whence

$$\begin{aligned} |(I - \hat{\Theta}\hat{\Sigma})_j|_\infty &= |I_j - (\mathbf{X}_j - \mathbf{X}_{-j} \hat{\gamma}_j)^\top \mathbf{X} / (T \hat{\sigma}_j^2)|_\infty \\ &= \max \left\{ |1 - \mathbf{X}_j^\top (\mathbf{X}_j - \mathbf{X}_{-j} \hat{\gamma}_j) / (T \hat{\sigma}_j^2)|, |\mathbf{X}_{-j}^\top (\mathbf{X}_j - \mathbf{X}_{-j} \hat{\gamma}_j) / (T \hat{\sigma}_j^2)|_\infty \right\} \\ &= \lambda_j |z^*|_\infty / \hat{\sigma}_j^2 = O_P \left( \frac{p^{1/\kappa}}{T^{1-1/\kappa}} \vee \sqrt{\frac{\log p}{T}} \right), \end{aligned}$$

where the last line follows since  $\hat{\sigma}_j^{-2} = O_P(1)$  and  $|z^*|_\infty \leq 1$ . The conclusion follows from the fact that  $|G|$  is fixed.  $\square$

## A.4 High-dimensional HAC estimator

In this section, we first derive the non-asymptotic Frobenius norm bound with explicit constants for a generic HAC estimator of the sample mean that holds uniformly over a class of distributions. This result is a counterpart to the asymptotic result of [Parzen \(1957\)](#) for the spectral density estimator evaluated at zero. Next, we characterize the convergence rate of the HAC estimator based on LASSO residuals.

We focus on the  $p$ -dimensional centered stochastic process  $(V_t)_{t \in \mathbf{Z}}$  and put

$$\Xi = \sum_{k \in \mathbf{Z}} \Gamma_k \quad \text{and} \quad \tilde{\Xi} = \sum_{|k| < T} K\left(\frac{k}{M_T}\right) \tilde{\Gamma}_k,$$

where  $\Gamma_k = \mathbb{E}[V_t V_{t+k}^\top]$  and  $\tilde{\Gamma}_k = \frac{1}{T} \sum_{t=1}^{T-k} V_t V_{t+k}^\top$ . Put also  $\Gamma = (\Gamma_k)_{k \in \mathbf{Z}}$  and let  $\langle \cdot, \cdot \rangle$  be the Frobenius inner product with corresponding Frobenius norm  $\|\cdot\|$ . The following assumption describes the relevant class of distributions and kernel functions.

**Assumption A.4.1.** *Suppose that (i)  $K : \mathbf{R} \rightarrow [-1, 1]$  is a Riemann integrable function such that  $K(0) = 1$ ; (ii) there exists some  $\varepsilon, \varsigma > 0$  such that  $|K(0) - K(x)| \leq L|x|^\varsigma$  for all  $|x| < \varepsilon$ ; (iii)  $(V_t)_{t \in \mathbf{Z}}$  is fourth-order stationary; (iv)  $\Gamma \in \mathcal{G}(\varsigma, B_1, B_2)$ , where*

$$\mathcal{G}(\varsigma, B_1, B_2) = \left\{ \sum_{k \in \mathbf{Z}} |k|^\varsigma \|\Gamma_k\| \leq B_1, \quad \sup_{k \in \mathbf{Z}} \sum_{l \in \mathbf{Z}} \sum_{t \in \mathbf{Z}} \sum_{j, h \in [p]} |\text{Cov}(V_{0,j} V_{k,h}, V_{t,j} V_{t+l,h})| \leq B_2 \right\}$$

for some  $B_1, B_2 > 0$ .

Condition (ii) describes the smoothness (or order) of the kernel in the neighborhood of zero.  $\varsigma = 1$  for the Bartlett kernel and  $\varsigma = 2$  for the Parzen, Tukey-Hanning, and Quadratic spectral kernels, see [Andrews \(1991\)](#). Since the bias of the HAC estimator is limited by the order of the kernel, it is typically not recommended to use the Bartlett kernel in practice. Higher-order kernels with  $\varsigma > 2$  do not ensure positive definiteness of the HAC estimator and require additional spectral regularization, see [Politis \(2011\)](#). Condition (iv) describes the class of autocovariances that vanish rapidly enough. Note that if (iv) holds for some  $\bar{\varsigma}$ , then it also holds for every  $\varsigma < \bar{\varsigma}$  and that if (ii) holds for some  $\tilde{\varsigma} > \varsigma$ , then it also holds for  $\tilde{\varsigma} = \varsigma$ . In practice, it is recommended to use second order kernel, to ensure that the HAC estimator is a positive definite matrix, see [Newey and West \(1987\)](#) and [Andrews \(1991\)](#). The covariance condition in (iv) can be justified under more primitive moment and summability conditions imposed on  $L_1$ -mixingale/ $\tau$ -dependence coefficients, see [Proposition A.1.1](#) and [Andrews \(1991\)](#), Lemma 1. The following result gives a nonasymptotic risk bound uniformly over the class  $\mathcal{G}$  and corresponds to the asymptotic convergence rates for the spectral density evaluated at zero derived in [Parzen \(1957\)](#).

**Proposition A.4.1.** Suppose that Assumption A.4.1 is satisfied. Then

$$\sup_{\Gamma \in \mathcal{G}(\varsigma, B_1, B_2)} \mathbb{E} \|\tilde{\Xi} - \Xi\|^2 \leq C_1 \frac{M_T}{T} + C_2 M_T^{-2\varsigma} + C_3 T^{-2(\varsigma \wedge 1)},$$

where  $C_1 = B_2 \left( \int |K(u)| du + o(1) \right)$ ,  $C_2 = 2 \left( B_1 L + \frac{2B_1}{\varepsilon^\varsigma} \right)^2$ , and  $C_3 = 2B_1^2$ .

*Proof.* By the triangle inequality, under Assumption A.4.1 (i)

$$\begin{aligned} \|\mathbb{E}[\tilde{\Xi}] - \Xi\| &= \left\| \sum_{|k| < T} K\left(\frac{k}{M_T}\right) \frac{T-k}{T} \Gamma_k - \sum_{k \in \mathbf{Z}} \Gamma_k \right\| \\ &\leq \sum_{|k| < T} \left| K\left(\frac{k}{M_T}\right) - K(0) \right| \|\Gamma_k\| + \frac{1}{T} \sum_{|k| < T} |k| \|\Gamma_k\| + \sum_{|k| \geq T} \|\Gamma_k\| \\ &\triangleq I_T + II_T + III_T. \end{aligned}$$

For the first term, we obtain

$$\begin{aligned} I_T &= \sum_{|k| < \varepsilon M_T} \left| K(0) - K\left(\frac{k}{M_T}\right) \right| \|\Gamma_k\| + \sum_{\varepsilon M_T \leq |k| < T} \left| K\left(\frac{k}{M_T}\right) - K(0) \right| \|\Gamma_k\| \\ &\leq L M_T^{-\varsigma} \sum_{|k| < \varepsilon M_T} |k|^\varsigma \|\Gamma_k\| + 2 \sum_{\varepsilon M_T \leq |k| < T} \|\Gamma_k\| \\ &\leq \frac{B_1 L}{M_T^\varsigma} + \frac{2}{\varepsilon^\varsigma M_T^\varsigma} \sum_{\varepsilon M_T \leq |k| < T} |k|^\varsigma \|\Gamma_k\| \\ &\leq \frac{B_1 L}{M_T^\varsigma} + \frac{2B_1}{\varepsilon^\varsigma M_T^\varsigma}, \end{aligned}$$

where the second sum is defined to be zero if  $T \leq \varepsilon M_T$ , the second line follows under Assumption A.4.1 (i)-(ii) and the last two under Assumption A.4.1 (iii). Next, if  $\varsigma \geq 1$ ,

$$\sum_{|k| < T} |k| \|\Gamma_k\| \leq \sum_{|k| < T} |k|^\varsigma \|\Gamma_k\|,$$

while if  $\varsigma \in (0, 1)$

$$\sum_{|k| < T} |k| \|\Gamma_k\| \leq T^{1-\varsigma} \sum_{|k| < T} |k|^\varsigma \|\Gamma_k\|.$$

Therefore, since  $\sum_{|k| \geq T} \|\Gamma_k\| \leq T^{-\varsigma} \sum_{|k| \geq T} |k|^\varsigma \|\Gamma_k\|$ , under Assumption A.4.1 (iv)

$$\begin{aligned} II_T + III_T &\leq \begin{cases} \frac{B_1}{T} & \varsigma \geq 1 \\ \frac{B_1}{T^\varsigma} & \varsigma \in (0, 1) \end{cases} \\ &= \frac{B_1}{T^{\varsigma \wedge 1}}. \end{aligned}$$

This shows that

$$\|\mathbb{E}[\tilde{\Xi}] - \Xi\| \leq \frac{B_1 L}{M_T^\varsigma} + \frac{2B_1}{\varepsilon^\varsigma M_T^\varsigma} + \frac{B_1}{T^{\varsigma \wedge 1}}. \quad (\text{A.11})$$

Next, under Assumption A.4.1 (i)

$$\begin{aligned} \mathbb{E}\|\tilde{\Xi} - \mathbb{E}[\tilde{\Xi}]\|^2 &= \sum_{|k| < T} \sum_{|l| < T} K\left(\frac{k}{M_T}\right) K\left(\frac{l}{M_T}\right) \mathbb{E}\left\langle \tilde{\Gamma}_k - \mathbb{E}\tilde{\Gamma}_k, \tilde{\Gamma}_l - \mathbb{E}\tilde{\Gamma}_l \right\rangle \\ &\leq \sum_{|k| < T} \left| K\left(\frac{k}{M_T}\right) \right| \sup_{|k| < T} \sum_{|l| < T} \left| \mathbb{E}\left\langle \tilde{\Gamma}_k - \mathbb{E}\tilde{\Gamma}_k, \tilde{\Gamma}_l - \mathbb{E}\tilde{\Gamma}_l \right\rangle \right|, \end{aligned}$$

where under Assumptions A.4.1 (iii)

$$\begin{aligned} T \left| \mathbb{E}\left\langle \tilde{\Gamma}_k - \mathbb{E}\tilde{\Gamma}_k, \tilde{\Gamma}_l - \mathbb{E}\tilde{\Gamma}_l \right\rangle \right| &\leq \frac{1}{T} \sum_{t=1}^{T-k} \sum_{r=1}^{T-l} \sum_{j,h \in [p]} |\text{Cov}(V_{t,j} V_{t+k,h}, V_{r,j} V_{r+l,h})| \\ &\leq \sum_{t \in \mathbf{Z}} \sum_{j,h \in [p]} |\text{Cov}(V_{0,j} V_{k,h}, V_{t,j} V_{t+l,h})|. \end{aligned}$$

Therefore, under Assumptions A.4.1 (i), (iv)

$$\mathbb{E}\|\tilde{\Xi} - \mathbb{E}[\tilde{\Xi}]\|^2 \leq M_T \left( \int |K(u)| du + o(1) \right) \frac{B_2}{T}. \quad (\text{A.12})$$

The result follows from combining estimates in equations (A.11) and (A.12).  $\square$

The risk bound in Proposition A.4.1 depends on  $B_1^2$  and  $B_2$  from Assumption A.4.1 (iv). Since the Frobenius norm scales with the dimension as  $O(p)$ , without making further (restrictive) assumptions, we will have  $B_1^2 = O(p^2)$ . Similar dependence on the dimension of the Frobenius norm for the HAC estimator has already been observed in Li and Liao (2019), Theorem 5 with a slightly different dependence on the bandwidth parameter  $M_T$ . It is likely that the entrywise maximum norm, scales better with the dimension. However, since we are only interested in conducting inference on the low-dimensional group of parameters of a fixed size, we will treat the HAC estimator without separating the "meat" from the "bread" of the sandwich and working with the Frobenius norm.

Note that by construction of the precision matrix  $\hat{\Theta}$ , its  $j^{th}$  row is  $\hat{\Theta}_j X_t = \hat{v}_{t,j} / \hat{\sigma}_j^2$ , where  $\hat{v}_{t,j}$  is the regression residual from the  $j^{th}$  nodewise LASSO regression and  $\hat{\sigma}_j^2$  is the corresponding estimator of the variance of the regression error. Therefore, the HAC estimator based on the LASSO residuals in Eq. 6 can be written as

$$\hat{\Xi}_G = \sum_{|k| < T} K\left(\frac{k}{M_T}\right) \hat{\Gamma}_k,$$

where  $\hat{\Gamma}_k$  has generic  $(j, h)$ -entry  $\frac{1}{T} \sum_{t=1}^{T-k} \hat{u}_t \hat{u}_{t+k} \hat{v}_{t,j} \hat{v}_{t+k,h} \hat{\sigma}_j^{-2} \hat{\sigma}_h^{-2}$ .

Similarly, we define

$$\tilde{\Xi}_G = \sum_{|k| < T} K\left(\frac{k}{M_T}\right) \tilde{\Gamma}_k,$$

where  $\tilde{\Gamma}_k$  has generic  $(j, h)$ -entry  $\frac{1}{T} \sum_{t=1}^{T-k} u_t u_{t+k} v_{t,j} v_{t+k,h} \sigma_j^{-2} \sigma_h^{-2}$  and note that the long-run variance  $\Xi_G$  has generic  $(j, h)$ -entry  $\mathbb{E}[u_t u_{t+k} v_{t,j} v_{t+k,h}] \sigma_j^{-2} \sigma_h^{-2}$ .

**Assumption A.4.2.** Suppose that uniformly over  $k \in \mathbf{Z}$  and  $j, h \in G$  (i)  $\mathbb{E}|u_0 u_k v_{0,j} v_{k,h}| < \infty$ ; (ii)  $\mathbb{E}|v_{0,j} u_k v_{k,h}|^2 < \infty$ ,  $\mathbb{E}|u_0 u_k v_{k,h}|^2 < \infty$ ,  $\mathbb{E}|u_0 v_{0,j} u_k|^2 < \infty$ , and  $\mathbb{E}|u_0 v_{0,j} v_{k,h}|^2 < \infty$ ; (iii)  $\mathbb{E}|u_0|^{2q} < \infty$  and  $\mathbb{E}|v_{0,j}|^{2q} < \infty$  for some  $q \geq 1$ .

*Proof of Theorem 4.2.* By Proposition A.4.1 with  $V_t = (u_t v_{t,j} / \sigma_j^2)_{j \in G}$

$$\|\hat{\Xi}_G - \Xi_G\| \leq \|\hat{\Xi}_G - \tilde{\Xi}_G\| + O_P\left(\sqrt{\frac{M_T}{T}} + M_T^{-\varsigma} + T^{-(\varsigma \wedge 1)}\right). \quad (\text{A.13})$$

Next,

$$\begin{aligned} \|\hat{\Xi}_G - \tilde{\Xi}_G\| &\leq \sum_{|k| < T} \left| K\left(\frac{k}{M_T}\right) \right| \|\hat{\Gamma}_k - \tilde{\Gamma}_k\| \\ &\leq |G| \sum_{|k| < T} \left| K\left(\frac{k}{M_T}\right) \right| \max_{j, h \in G} \left| \frac{1}{\hat{\sigma}_j^2 \hat{\sigma}_h^2 T} \sum_{t=1}^{T-k} \hat{u}_t \hat{u}_{t+k} \hat{v}_{t,j} \hat{v}_{t+k,h} - \frac{1}{\sigma_j^2 \sigma_h^2 T} \sum_{t=1}^{T-k} u_t u_{t+k} v_{t,j} v_{t+k,h} \right| \\ &\leq |G| \sum_{|k| < T} \left| K\left(\frac{k}{M_T}\right) \right| \max_{j, h \in G} \frac{1}{\hat{\sigma}_j^2 \hat{\sigma}_h^2} \left| \frac{1}{T} \sum_{t=1}^{T-k} \hat{u}_t \hat{u}_{t+k} \hat{v}_{t,j} \hat{v}_{t+k,h} - \frac{1}{T} \sum_{t=1}^{T-k} u_t u_{t+k} v_{t,j} v_{t+k,h} \right| \\ &\quad + |G| \max_{j, h \in G} \left| \frac{1}{\hat{\sigma}_j^2 \hat{\sigma}_h^2} - \frac{1}{\sigma_j^2 \sigma_h^2} \right| \sum_{|k| < T} \left| K\left(\frac{k}{M_T}\right) \right| \left| \frac{1}{T} \sum_{t=1}^{T-k} u_t u_{t+k} v_{t,j} v_{t+k,h} \right| \\ &\triangleq S_T^a + S_T^b. \end{aligned}$$

By Proposition A.3.1, since  $s_\alpha \sqrt{\frac{\log p}{T}} = o(1)$  and  $s_\alpha^\kappa p = o(T^{4\kappa/5-1})$ , under stated assumptions, we obtain  $\max_{j \in G} |\hat{\sigma}_j^2 - \sigma_j^2| = o_P(1)$ , and whence  $\max_{j \in G} \hat{\sigma}_j^{-2} = O_P(1)$ . Using  $\hat{a}\hat{b} - ab = (\hat{a} - a)b + a(\hat{b} - b) + (\hat{a} - a)(\hat{b} - b)$ , by Proposition A.3.1

$$S_T^b = O_P\left(\frac{s_\alpha p^{1/\kappa}}{T^{1-1/\kappa}} \vee s_\alpha \sqrt{\frac{\log p}{T}}\right) \sum_{|k| < T} \left| K\left(\frac{k}{M_T}\right) \right| \max_{j, h \in G} \left| \frac{1}{T} \sum_{t=1}^{T-k} u_t u_{t+k} v_{t,j} v_{t+k,h} \right|$$

Under Assumption A.4.1 (i) and A.4.2 (i)

$$\begin{aligned}
\mathbb{E} \left[ \sum_{|k| < T} \left| K \left( \frac{k}{M_T} \right) \right| \max_{j, h \in G} \left| \frac{1}{T} \sum_{t=1}^{T-k} u_t u_{t+k} v_{t,j} v_{t+k,h} \right| \right] &\leq O(M_T) \sup_{k \in \mathbf{Z}} \sum_{j, h \in G} \mathbb{E} \left| \frac{1}{T} \sum_{t=1}^{T-k} u_t u_{t+k} v_{t,j} v_{t+k,h} \right| \\
&\leq O(M_T) |G|^2 \sup_{k \in \mathbf{Z}} \max_{j, h \in G} \mathbb{E} |u_t u_{t+k} v_{t,j} v_{t+k,h}| \\
&= O(M_T),
\end{aligned}$$

and whence  $S_T^b = O_P \left( M_T \left( \frac{s_\alpha p^{1/\kappa}}{T^{1-1/\kappa}} \vee s_\alpha \sqrt{\frac{\log p}{T}} \right) \right)$ .

Next, we evaluate uniformly over  $|k| < T$

$$\begin{aligned}
&\left| \frac{1}{T} \sum_{t=1}^{T-k} \hat{u}_t \hat{u}_{t+k} \hat{v}_{t,j} \hat{v}_{t+k,h} - \frac{1}{T} \sum_{t=1}^{T-k} u_t u_{t+k} v_{t,j} v_{t+k,h} \right| \\
&\leq \left| \frac{1}{T} \sum_{t=1}^{T-k} (\hat{u}_t \hat{v}_{t,j} - u_t v_{t,j}) u_{t+k} v_{t+k,h} \right| + \left| \frac{1}{T} \sum_{t=1}^{T-k} u_t v_{t,j} (\hat{u}_{t+k} \hat{v}_{t+k,h} - u_{t+k} v_{t+k,h}) \right| \\
&+ \left| \frac{1}{T} \sum_{t=1}^{T-k} (\hat{u}_t \hat{v}_{t,j} - u_t v_{t,j}) (\hat{u}_{t+k} \hat{v}_{t+k,h} - u_{t+k} v_{t+k,h}) \right| \triangleq I_T + II_T + III_T.
\end{aligned}$$

We bound the first term as

$$\begin{aligned}
I_T &\leq \left| \frac{1}{T} \sum_{t=1}^{T-k} (\hat{u}_t - u_t) v_{t,j} u_{t+k} v_{t+k,h} \right| + \left| \frac{1}{T} \sum_{t=1}^{T-k} u_t (\hat{v}_{t,j} - v_{t,j}) u_{t+k} v_{t+k,h} \right| \\
&+ \left| \frac{1}{T} \sum_{t=1}^{T-k} (\hat{u}_t - u_t) (\hat{v}_{t,j} - v_{t,j}) u_{t+k} v_{t+k,h} \right| \triangleq I_T^a + I_T^b + I_T^c.
\end{aligned}$$

By the Cauchy-Schwartz inequality, under Assumptions of Corollary 3.1 for the sg-LASSO and Assumption A.4.2 (ii)

$$\begin{aligned}
I_T^a &= \left| \frac{1}{T} \sum_{t=1}^{T-k} \left( X_t^\top (\beta^0 - \hat{\beta}) + m_t - X_t^\top \beta_0 \right) v_{t,j} u_{t+k} v_{t+k,h} \right| \\
&\leq (\|\mathbf{X}(\hat{\beta} - \beta^0)\|_T + \|\mathbf{m} - \mathbf{X}\beta^0\|_T) \sqrt{\frac{1}{T} \sum_{t=1}^{T-k} v_{t,j}^2 u_{t+k}^2 v_{t+k,h}^2} \\
&= O_P \left( \frac{s_\alpha p^{1/\kappa}}{T^{1-1/\kappa}} \vee \sqrt{\frac{s_\alpha \log p}{T}} \right).
\end{aligned}$$

Similarly, under Assumptions of Corollary 3.1 for the nodewise LASSO and Assumption A.4.2 (ii)

$$I_T^b \leq \left( \|\mathbf{X}_{-j}(\hat{\gamma}_j - \gamma_j)\|_T + o_P(T^{-1/2}) \right) \sqrt{\frac{1}{T} \sum_{t=1}^{T-k} u_t^2 u_{t+k}^2 v_{t+k,h}^2} = O_P \left( \frac{S_j p^{1/\kappa}}{T^{1-1/\kappa}} \vee \sqrt{\frac{S_j \log p}{T}} \right).$$

Note that for arbitrary  $(\xi_t)_{t \in \mathbf{Z}}$  and  $q \geq 1$ , by Jensen's inequality

$$\mathbb{E} \left[ \max_{t \in [T]} |\xi_t| \right] \leq \left( \mathbb{E} \left[ \max_{t \in [T]} |\xi_t|^q \right] \right)^{1/q} \leq \left( \mathbb{E} \left[ \sum_{t=1}^T |\xi_t|^q \right] \right)^{1/q} = T^{1/q} (\mathbb{E} |\xi_t|^q)^{1/q}.$$

Then by the Cauchy-Schwartz inequality under Assumption A.4.2 (iii) and Corollary 3.1

$$\begin{aligned} I_T^c &\leq (\|\mathbf{X}(\hat{\beta} - \beta^0)\|_T + o_P(T^{-1/2})) (\|\mathbf{X}_{-j}(\hat{\gamma}_j - \gamma_j)\|_T + o_P(T^{-1/2})) \max_{t \in [T]} |u_t v_{t,h}| \\ &= O_P \left( \frac{s^2 p^{2/\kappa}}{T^{2-3/\kappa}} \vee \frac{s \log p}{T^{1-1/\kappa}} \right), \end{aligned}$$

where we use the fact that  $\kappa \leq q$ . Therefore, under maintained assumptions

$$I_T = O_P \left( \frac{sp^{1/\kappa}}{T^{1-1/\kappa}} \vee \sqrt{\frac{s \log p}{T}} + \frac{s^2 p^{2/\kappa}}{T^{2-3/\kappa}} \vee \frac{s \log p}{T^{1-1/\kappa}} \right)$$

and by symmetry

$$II_T = O_P \left( \frac{sp^{1/\kappa}}{T^{1-1/\kappa}} \vee \sqrt{\frac{s \log p}{T}} + \frac{s^2 p^{2/\kappa}}{T^{2-3/\kappa}} \vee \frac{s \log p}{T^{1-1/\kappa}} \right).$$

Lastly, by the Cauchy-Schwartz inequality

$$\begin{aligned} III_T &\leq \sqrt{\frac{1}{T} \sum_{t=1}^{T-k} (\hat{u}_t \hat{v}_{t,j} - u_t v_{t,j})^2 \frac{1}{T} \sum_{t=1}^{T-k} (\hat{u}_{t+k} \hat{v}_{t+k,h} - u_{t+k} v_{t+k,h})^2} \\ &\leq \sqrt{\frac{1}{T} \sum_{t=1}^T (\hat{u}_t \hat{v}_{t,j} - u_t v_{t,j})^2 \frac{1}{T} \sum_{t=1}^T (\hat{u}_t \hat{v}_{t,h} - u_t v_{t,h})^2}. \end{aligned}$$

For each  $j \in G$

$$\begin{aligned} \frac{1}{T} \sum_{t=1}^T (\hat{u}_t \hat{v}_{t,j} - u_t v_{t,j})^2 &\leq \frac{3}{T} \sum_{t=1}^T |\hat{u}_t - u_t|^2 v_{t,j}^2 + \frac{3}{T} \sum_{t=1}^T |\hat{v}_{t,j} - v_{t,j}|^2 u_t^2 \\ &\quad + \frac{3}{T} \sum_{t=1}^T |\hat{u}_t - u_t|^2 |\hat{v}_{t,j} - v_{t,j}|^2 \\ &\triangleq III_T^a + III_T^b + III_T^c. \end{aligned}$$

Since under Assumption A.4.2 (iii),  $\mathbb{E}|v_{t,j}|^{2q} < \infty$  and  $\mathbb{E}|u_t|^{2q} < \infty$ ,

$$III_T^a \leq 3 \max_{t \in [T]} |v_{t,j}|^2 (\|\mathbf{X}(\hat{\beta} - \beta^0)\|_T^2 + o_P(T^{-1/2})) = O_P \left( \frac{s_\alpha p^{2/\kappa}}{T^{2-3/\kappa}} \vee \frac{s_\alpha \log p}{T^{1-1/\kappa}} \right)$$

and

$$III_T^b \leq 3 \max_{t \in [T]} |u_t|^2 (\|\mathbf{X}_{-j}(\hat{\gamma}_j - \gamma_j)\|_T^2 + o_P(T^{-1/2})) = O_P \left( \frac{S_j p^{2/\kappa}}{T^{2-3/\kappa}} \vee \frac{S_j \log p}{T^{1-1/\kappa}} \right).$$

For the last term, since under Assumption 3.1 (ii),  $\sup_k \mathbb{E}|X_{t,k}|^{2\tilde{q}} < \infty$  and  $\kappa \geq \tilde{q}$ , by Corollary 3.1

$$\begin{aligned} III_T^c &\leq 3(\|\mathbf{X}(\hat{\beta} - \beta^0)\|_T^2 + o_P(T^{-1/2})) \max_{t \in [T]} |X_{t,-j}^\top(\hat{\gamma}_j - \gamma_j) + m_t - X_t^\top \beta^0|^2 \\ &\leq O_P \left( \frac{s_\alpha p^{2/\kappa}}{T^{2-2/\kappa}} \vee \frac{s_\alpha \log p}{T} \right) \left( 2 \max_{t \in [T]} |X_t|_\infty^2 |\hat{\gamma}_j - \gamma_j|_1^2 + 2T \|\mathbf{m} - \mathbf{X}^\top \beta^0\|_T^2 \right) \\ &= O_P \left( \left( \frac{s_\alpha p^{2/\kappa}}{T^{2-2/\kappa}} \vee \frac{s_\alpha \log p}{T} \right) \left( \frac{S^2 p^{2/\kappa}}{T^{2-2/\kappa}} \vee S^2 \frac{\log p}{T} \right) (pT)^{1/\kappa} \right) \\ &= O_P \left( \frac{s^3 p^{5/\kappa}}{T^{4-5/\kappa}} + \frac{s^3 p^{3/\kappa} \log p}{T^{3-3/\kappa}} + \frac{s^3 p^{1/\kappa} \log^2 p}{T^{2-1/\kappa}} \right) \\ &= O_P \left( \frac{s^3 p^{5/\kappa}}{T^{4-5/\kappa}} + \frac{s^3 p^{3/\kappa} \log p}{T^{3-3/\kappa}} \right), \end{aligned}$$

where we use the fact that  $\kappa > 2$ ,  $s = s_\alpha \vee S$ ,  $s^\kappa p = o(T^{4\kappa/5-1})$ , and  $\frac{s^2 \log p}{T} = o(1)$  as  $T \rightarrow \infty$ . Then for every  $j \in G$

$$\frac{1}{T} \sum_{t=1}^T (\hat{u}_t \hat{v}_{t,j} - u_t v_{t,j})^2 = O_P \left( \frac{sp^{2/\kappa}}{T^{2-3/\kappa}} \vee \frac{s \log p}{T^{1-1/\kappa}} + \frac{s^3 p^{5/\kappa}}{T^{4-5/\kappa}} + \frac{s^3 p^{3/\kappa} \log p}{T^{3-3/\kappa}} \right),$$

and whence

$$III_T = O_P \left( \frac{sp^{2/\kappa}}{T^{2-3/\kappa}} \vee \frac{s \log p}{T^{1-1/\kappa}} + \frac{s^3 p^{5/\kappa}}{T^{4-5/\kappa}} + \frac{s^3 p^{3/\kappa} \log p}{T^{3-3/\kappa}} \right).$$

Therefore, since  $\hat{\sigma}_j^2 \xrightarrow{P} \sigma_j^2$ , we obtain

$$\begin{aligned} S_T^a &= O_P \left( M_T \left( \frac{sp^{1/\kappa}}{T^{1-1/\kappa}} \vee \sqrt{\frac{s \log p}{T}} + \frac{s^2 p^{2/\kappa}}{T^{2-3/\kappa}} \vee \frac{s \log p}{T^{1-1/\kappa}} + \frac{s^3 p^{5/\kappa}}{T^{4-5/\kappa}} + \frac{s^3 p^{3/\kappa} \log p}{T^{3-3/\kappa}} \right) \right) \\ &= O_P \left( M_T \left( \frac{sp^{1/\kappa}}{T^{1-1/\kappa}} \vee \sqrt{\frac{s \log p}{T}} + \frac{s^2 p^{2/\kappa}}{T^{2-3/\kappa}} + \frac{s^3 p^{5/\kappa}}{T^{4-5/\kappa}} \right) \right), \end{aligned}$$

where the last line follows since  $s^\kappa p/T^{4\kappa/5-1} = o(1)$ . Combining this estimate with previously obtained estimate for  $S_T^b$

$$\|\hat{\Xi}_G - \tilde{\Xi}_G\| = O_P \left( M_T \left( \frac{sp^{1/\kappa}}{T^{1-1/\kappa}} \vee s\sqrt{\frac{\log p}{T}} + \frac{s^2 p^{2/\kappa}}{T^{2-3/\kappa}} + \frac{s^3 p^{5/\kappa}}{T^{4-5/\kappa}} \right) \right).$$

The result follows from combining this estimate with the estimate in equation (A.13).  $\square$

## A.5 Monte Carlo Simulation Design

To assess the predictive performance and the MIDAS weight recovery, we use the following DGP in our MC experiments

$$y_t = \rho_1 y_{t-1} + \rho_2 y_{t-2} + \sum_{k=1}^K \frac{1}{m} \sum_{j=1}^m \omega(j/m; \beta_k) x_{t-j/m, k} + u_t$$

where  $u_t \sim_{i.i.d.} N(0, \sigma_u^2)$  and  $\{x_{k,t-j/m} : k = 1, \dots, K\}$ . This corresponds to a target of interest  $y_t$  driven by two lags AR augmented with high frequency series, hence, the DGP is an ARDL-MIDAS model. We set  $\sigma_u^2 = 1$ ,  $\rho_1 = 0.3$ ,  $\rho_2 = 0.01$ , and take the number of relevant high frequency regressors  $K = 3$ . In some scenarios we also set  $\sigma_u^2 = 5$ . We are interested in quarterly/monthly data, and use four quarters of data for the high frequency regressors so that  $m = 12$ . We rely on a commonly used weighting scheme in the MIDAS literature, namely  $\omega(j/m; \beta_k)$  for  $k = 1, 2$  and  $3$  are determined by beta densities respectively equal to Beta(1, 3), Beta(2, 3), and Beta(2, 2).<sup>29</sup> The high frequency regressors are generated as either one of the following:

1.  $K$  i.i.d. realizations of the univariate autoregressive (AR) process

$$x_h = \rho x_{h-1} + \varepsilon_h,$$

where  $\rho = 0.2$  and either  $\varepsilon_h \sim_{i.i.d.} N(0, \sigma_\varepsilon^2)$ ,  $\sigma_\varepsilon^2 = 5$ , or  $\varepsilon_h \sim_{i.i.d.} \text{student-}t(5)$ , and  $h$  denotes the high-frequency sampling.

2. Multivariate vector autoregressive (VAR) process

$$X_h = \Phi X_{h-1} + \varepsilon_h,$$

where  $\varepsilon_h \sim_{i.i.d.} N(0, I_K)$ .

---

<sup>29</sup>See Ghysels, Sinko, and Valkanov (2006) or Ghysels and Qian (2019), among others, for further details.

The latter creates contemporaneously correlated high frequency regressors.<sup>30</sup> In the estimation procedure, we add 7 noisy covariates which are generated in the same way as the relevant covariates and use 5 low-frequency lags.

The empirical models use a dictionary which consists of Legendre polynomials up to degree  $L = 10$  shifted to  $[0, 1]$  interval with  $\omega(t; \beta_k)$  defined in equation (3) where  $\{w_l : l = 1, \dots, L\}$ . The sample size is  $T \in \{50, 100, 200\}$ . Throughout the experiment, we use 5000 simulation replications and 10-fold cross-validation to select the tuning parameter.

We assess the performance of different methods by varying assumptions on error terms of the high-frequency process  $\varepsilon_h$ , considering multivariate high-frequency process, changing the degree of Legendre polynomials  $L$ , increasing the noise level of the low-frequency process  $\sigma_u$ , using only half of the high-frequency lags in predictive regressions, and adding a larger number of noisy covariates. In the case of VAR high-frequency process, we set  $\Phi$  to be block-diagonal with the first  $5 \times 5$  block having entries 0.15 and the remaining  $5 \times 5$  block(s) having entries 0.075.

We estimate three different LASSO-type regression models. In the first model we keep the weighting function unconstrained, therefore, we estimate 12 coefficients per high-frequency covariate using unstructured LASSO estimator. We denote this model LASSO-U-MIDAS. In the second model we use MIDAS weights together with unstructured LASSO estimator; we call this model LASSO-MIDAS. In this case, we estimate  $L + 1$  number of coefficients per high-frequency covariate. The third model applies sg-LASSO estimator together with MIDAS weights. Groups are defined as in Section 2; each low-frequency lag and high-frequency covariate is a group, therefore, we have  $K+5$  number of groups. We set the relative weight  $\alpha$  to 0.65. This model is denoted sg-LASSO-MIDAS.

For regressions with aggregated data, we consider:

1. Flow aggregation (FLOW):  $x_{k,t}^A = \frac{1}{m} \sum_{j=1}^m w_k x_{k,t-j/m}$ .
2. Stock aggregation (STOCK):  $x_{k,t}^A = x_{k,t}$ .
3. Single high-frequency lag (MIDDLE):  $x_{k,t-(m-1)/m}$

In these cases, models are estimated using the OLS estimator.

To assess the small sample properties of the HAC estimator for the low-dimensional parameter in a high dimensional data setting we simplify the DGP to a linear regression

---

<sup>30</sup>In the AR case, we initiate the two processes from

$$x_0 \sim N\left(0, \frac{\sigma^2}{1 - \rho^2}\right), \quad y_0 \sim N\left(0, \frac{\sigma^2(1 - \rho_2)}{(1 + \rho_2)((1 - \rho_2)^2 - \rho_1^2)}\right).$$

In the VAR case, we use the same initial value for  $(y_t)$  and initiate  $X_0 \sim N(0, I_K)$ . We burn-in the first 200 observations in all cases.

model with covariates  $\{x_{t,j}, j \in [p]\}$  drawn independently from the AR(1) process

$$x_{t,j} = \rho x_{t-1,j} + \epsilon_{t,j},$$

where  $\rho$  is the persistence parameter. The regression error follows the AR(1) process

$$u_t = \rho u_{t-1} + \nu_t,$$

where  $\rho$  is the persistence parameter (the same as for covariates) and errors are either both  $\epsilon_{t,j}, \nu_t \sim_{i.i.d.} N(0, 1)$  or  $\epsilon_{t,j}, \nu_t \sim_{i.i.d.} \text{student-}t(5)$ . The vector of population regression coefficients  $\beta^0$  has the first five non-zero entries  $(5, 4, 3, 2, 1)$  and all remaining entries are zero, i.e.,

$$\beta^0 = (5, 4, 3, 2, 1, \underbrace{0, \dots, 0}_{p-5}).$$

The sample size is  $T = 500$  and the number of covariates is  $p \in \{20, 200\}$ . We consider the persistence parameter  $\rho = 0.8$ . We focus on the LASSO estimator to estimate coefficients  $\hat{\beta}$ . Throughout the experiment, we choose the LASSO tuning parameters using the data-driven rule borrowed from [Belloni and Chernozhukov \(2011\)](#):  $\lambda = 2c\hat{\sigma}\sqrt{T}\Phi^{-1}(1 - \alpha/2p)$ , where  $\Phi(\cdot)$  is a CDF of the standard normal distribution,  $\hat{\sigma}$  is a preliminary estimate of  $\sigma = \sqrt{\mathbb{E}u^2}$ , and we take the default choice of parameters  $c$  and  $\alpha$  for the LASSO model:  $c = 0.5$ ,  $\alpha = 0.1$ , see [Chernozhukov, Hansen, and Spindler \(2016\)](#).<sup>31</sup>

## A.6 Monte Carlo Simulations

---

<sup>31</sup>An alternative, less conservative, but computationally more intensive bootstrap-based algorithm is discussed in [Chernozhukov, Härdle, Huang, and Wang \(2019\)](#).

| T                              | FLOW                                       | STOCK | MIDDLE | LASSO-U | LASSO-M | SGL-M | FLOW  | STOCK  | MIDDLE | LASSO-U | LASSO-M | SGL-M |
|--------------------------------|--|-------|--------|---------|---------|-------|-------|--------|--------|---------|---------|-------|
| Baseline scenario              |  |       |        |         |         |       |       |        |        |         |         |       |
| 50                             | 2.847                                      | 3.839 | 4.660  | 4.213   | 2.561   | 2.188 | 2.081 | 2.427  | 2.702  | 2.334   | 2.066   | 1.749 |
|                                | 0.059                                      | 0.077 | 0.090  | 0.087   | 0.054   | 0.044 | 0.042 | 0.053  | 0.062  | 0.056   | 0.051   | 0.041 |
| 100                            | 2.110                                      | 2.912 | 3.814  | 2.244   | 1.579   | 1.473 | 1.504 | 1.900  | 2.155  | 1.761   | 1.535   | 1.343 |
|                                | 0.041                                      | 0.057 | 0.076  | 0.045   | 0.032   | 0.030 | 0.030 | 0.038  | 0.043  | 0.034   | 0.030   | 0.026 |
| 200                            | 1.882                                      | 2.772 | 3.681  | 1.539   | 1.302   | 1.230 | 1.357 | 1.714  | 1.986  | 1.414   | 1.238   | 1.192 |
|                                | 0.037                                      | 0.056 | 0.072  | 0.031   | 0.026   | 0.025 | 0.027 | 0.035  | 0.040  | 0.029   | 0.025   | 0.024 |
| High-frequency process: VAR(1) |  |       |        |         |         |       |       |        |        |         |         |       |
|                                | Legendre degree $L = 3$                    |       |        |         |         |       |       |        |        |         |         |       |
| 50                             | 1.869                                      | 2.645 | 2.863  | 2.135   | 1.726   | 1.533 | 2.847 | 3.839  | 4.660  | 4.213   | 2.339   | 1.979 |
|                                | 0.039                                      | 0.053 | 0.057  | 0.046   | 0.036   | 0.032 | 0.059 | 0.077  | 0.090  | 0.087   | 0.050   | 0.041 |
| 100                            | 1.453                                      | 2.073 | 2.245  | 1.575   | 1.373   | 1.284 | 2.110 | 2.912  | 3.814  | 2.244   | 1.503   | 1.386 |
|                                | 0.028                                      | 0.042 | 0.046  | 0.031   | 0.028   | 0.025 | 0.041 | 0.057  | 0.076  | 0.045   | 0.031   | 0.029 |
| 200                            | 1.283                                      | 1.921 | 2.040  | 1.348   | 1.240   | 1.201 | 1.882 | 2.772  | 3.681  | 1.539   | 1.277   | 1.196 |
|                                | 0.026                                      | 0.038 | 0.041  | 0.026   | 0.024   | 0.023 | 0.037 | 0.056  | 0.072  | 0.031   | 0.025   | 0.024 |
|                                | Legendre degree $L = 10$                   |       |        |         |         |       |       |        |        |         |         |       |
|                                | Low frequency noise level $\sigma_u^2 = 5$ |       |        |         |         |       |       |        |        |         |         |       |
| 50                             | 2.847                                      | 3.839 | 4.660  | 4.213   | 2.983   | 2.583 | 9.598 | 10.429 | 10.726 | 9.799   | 8.732   | 7.785 |
|                                | 0.059                                      | 0.077 | 0.090  | 0.087   | 0.063   | 0.053 | 0.196 | 0.211  | 0.213  | 0.198   | 0.180   | 0.159 |
| 100                            | 2.110                                      | 2.912 | 3.814  | 2.244   | 1.719   | 1.633 | 7.319 | 8.177  | 8.880  | 8.928   | 7.359   | 6.606 |
|                                | 0.041                                      | 0.057 | 0.076  | 0.045   | 0.035   | 0.032 | 0.147 | 0.163  | 0.176  | 0.179   | 0.147   | 0.135 |
| 200                            | 1.882                                      | 2.772 | 3.681  | 1.539   | 1.348   | 1.300 | 6.489 | 7.699  | 8.381  | 7.275   | 6.391   | 5.919 |
|                                | 0.037                                      | 0.056 | 0.072  | 0.031   | 0.027   | 0.026 | 0.127 | 0.154  | 0.165  | 0.146   | 0.126   | 0.117 |
|                                | Half high-frequency lags                   |       |        |         |         |       |       |        |        |         |         |       |
|                                | Number of covariates $p = 50$              |       |        |         |         |       |       |        |        |         |         |       |
| 50                             | 2.750                                      | 2.730 | 3.562  | 2.455   | 2.344   | 1.905 |       |        |        | 5.189   | 3.610   | 2.658 |
|                                | 0.058                                      | 0.056 | 0.070  | 0.050   | 0.048   | 0.038 |       |        |        | 0.104   | 0.075   | 0.054 |
| 100                            | 2.134                                      | 2.167 | 3.082  | 1.899   | 1.718   | 1.468 | 5.582 | 5.633  | 6.298  | 3.527   | 2.034   | 1.753 |
|                                | 0.043                                      | 0.043 | 0.061  | 0.038   | 0.034   | 0.030 | 0.117 | 0.113  | 0.126  | 0.075   | 0.042   | 0.036 |
| 200                            | 1.833                                      | 1.971 | 2.808  | 1.400   | 1.356   | 1.225 | 2.679 | 3.573  | 4.399  | 1.867   | 1.413   | 1.319 |
|                                | 0.036                                      | 0.039 | 0.055  | 0.028   | 0.027   | 0.024 | 0.053 | 0.071  | 0.090  | 0.038   | 0.028   | 0.026 |

Table A.1: Forecasting accuracy results – See Table A.2

| T                              | FLOW  | STOCK | MIDDLE | LASSO-U | LASSO-M | SGL-M | FLOW  | STOCK  | MIDDLE | LASSO-U | LASSO-M | SGL-M |
|--------------------------------|-------|-------|--------|---------|---------|-------|---|--------|--------|---------|---------|-------|
| <u>Baseline scenario</u>       |       |       |        |         |         |       | $\varepsilon_h \sim i.i.d.$ student- $t(5)$ |        |        |         |         |       |
| 50                             | 3.095 | 3.793 | 4.659  | 4.622   | 3.196   | 2.646 | 2.257                                       | 2.391  | 2.649  | 2.357   | 2.131   | 1.786 |
|                                | 0.067 | 0.078 | 0.094  | 0.094   | 0.064   | 0.055 | 0.046                                       | 0.054  | 0.057  | 0.050   | 0.047   | 0.038 |
| 100                            | 2.393 | 2.948 | 3.860  | 2.805   | 2.113   | 1.888 | 1.598                                       | 1.840  | 2.068  | 1.824   | 1.653   | 1.433 |
|                                | 0.048 | 0.060 | 0.078  | 0.058   | 0.044   | 0.038 | 0.032                                       | 0.037  | 0.043  | 0.036   | 0.033   | 0.029 |
| 200                            | 2.122 | 2.682 | 3.597  | 1.971   | 1.712   | 1.604 | 1.452                                       | 1.690  | 1.969  | 1.544   | 1.383   | 1.302 |
|                                | 0.042 | 0.055 | 0.072  | 0.039   | 0.034   | 0.032 | 0.030                                       | 0.035  | 0.041  | 0.032   | 0.028   | 0.026 |
| High-frequency process: VAR(1) |       |       |        |         |         |       | Legendre degree $L = 3$                     |        |        |         |         |       |
| 50                             | 2.086 | 2.418 | 2.856  | 2.208   | 1.828   | 1.612 | 3.095                                       | 3.793  | 4.659  | 4.622   | 2.987   | 2.451 |
|                                | 0.044 | 0.050 | 0.057  | 0.049   | 0.039   | 0.033 | 0.067                                       | 0.078  | 0.094  | 0.094   | 0.061   | 0.050 |
| 100                            | 1.571 | 1.906 | 2.341  | 1.671   | 1.430   | 1.329 | 2.393                                       | 2.948  | 3.860  | 2.805   | 2.020   | 1.796 |
|                                | 0.031 | 0.039 | 0.047  | 0.033   | 0.028   | 0.026 | 0.048                                       | 0.060  | 0.078  | 0.058   | 0.042   | 0.037 |
| 200                            | 1.397 | 1.720 | 2.168  | 1.428   | 1.307   | 1.248 | 2.122                                       | 2.682  | 3.597  | 1.971   | 1.680   | 1.560 |
|                                | 0.028 | 0.034 | 0.043  | 0.028   | 0.026   | 0.024 | 0.042                                       | 0.055  | 0.072  | 0.039   | 0.033   | 0.031 |
| Legendre degree $L = 10$       |       |       |        |         |         |       | Low frequency noise level $\sigma_u^2 = 5$  |        |        |         |         |       |
| 50                             | 3.095 | 3.793 | 4.659  | 4.622   | 3.528   | 2.948 | 9.934                                       | 10.566 | 10.921 | 9.819   | 9.037   | 8.091 |
|                                | 0.067 | 0.078 | 0.094  | 0.094   | 0.071   | 0.059 | 0.213                                       | 0.212  | 0.216  | 0.198   | 0.184   | 0.168 |
| 100                            | 2.393 | 2.948 | 3.860  | 2.805   | 2.271   | 2.079 | 7.576                                       | 8.130  | 8.854  | 9.190   | 7.743   | 6.876 |
|                                | 0.048 | 0.060 | 0.078  | 0.058   | 0.047   | 0.042 | 0.150                                       | 0.166  | 0.180  | 0.188   | 0.160   | 0.141 |
| 200                            | 2.122 | 2.682 | 3.597  | 1.971   | 1.777   | 1.693 | 6.830                                       | 7.580  | 8.351  | 7.648   | 6.820   | 6.258 |
|                                | 0.042 | 0.055 | 0.072  | 0.039   | 0.035   | 0.034 | 0.135                                       | 0.152  | 0.168  | 0.156   | 0.136   | 0.124 |
| Half high-frequency lags       |       |       |        |         |         |       | Number of covariates $p = 50$               |        |        |         |         |       |
| 50                             | 3.014 | 2.773 | 3.638  | 2.455   | 2.509   | 2.201 |   |        |        | 5.222   | 3.919   | 3.002 |
|                                | 0.063 | 0.056 | 0.072  | 0.050   | 0.051   | 0.046 |   |        |        | 0.105   | 0.081   | 0.061 |
| 100                            | 2.344 | 2.087 | 3.116  | 1.899   | 2.101   | 1.774 | 5.978                                       | 5.556  | 6.536  | 3.948   | 2.665   | 2.232 |
|                                | 0.046 | 0.041 | 0.063  | 0.038   | 0.043   | 0.036 | 0.121                                       | 0.112  | 0.132  | 0.083   | 0.053   | 0.044 |
| 200                            | 2.119 | 1.985 | 2.988  | 1.400   | 1.761   | 1.590 | 2.974                                       | 3.422  | 4.412  | 2.355   | 1.938   | 1.725 |
|                                | 0.041 | 0.040 | 0.061  | 0.028   | 0.035   | 0.032 | 0.059                                       | 0.070  | 0.087  | 0.048   | 0.040   | 0.035 |

Table A.2: Nowcasting accuracy results

The table reports simulation results for nowcasting accuracy. We report eight different scenarios for the DGP: baseline scenario (upper-left block) DGP is with the low-frequency noise level  $\sigma_u^2 = 1$  which we keep for all other scenarios except where we change it to  $\sigma_u^2 = 5$ , the degree of Legendre polynomial  $L=5$ , and Gaussian high-frequency error term. All remaining blocks report results for different DGPs: e.g. in the upper-right block, we report results where the noise term of high-frequency covariates is i.i.d. student- $t(5)$ . Each block reports results for LASSO-U-MIDAS (LASSO-U), LASSO-MIDAS (LASSO-M) and sg-LASSO-MIDAS (SGL-M) estimators (the last three columns). In addition, we report results for predictive regressions using aggregated data where we use different aggregation schemes: 1) flow aggregation (FLOW), stock aggregation (STOCK) and taking the middle value of high-frequency covariates (MIDDLE). We vary the sample size  $T$  from 50 to 200. Each entry in the odd row is the average mean squared forecast error, and each entry in the even row is the simulation standard error.

|                   | LASSO-U  | LASSO-M | SGL-M | LASSO-U | LASSO-M | SGL-M | LASSO-U | LASSO-M | SGL-M |
|-------------------|--|---------|-------|---------|---------|-------|---------|---------|-------|
|                   | T=50   |         |       | T=100   |         |       | T=200   |         |       |
| Baseline scenario |  |         |       |         |         |       |         |         |       |
| Beta(1, 3)        | 1.955  | 0.887   | 0.652 | 1.846   | 0.287   | 0.247 | 1.804   | 0.138   | 0.106 |
|                   | 0.002  | 0.012   | 0.010 | 0.002   | 0.004   | 0.004 | 0.001   | 0.002   | 0.002 |
| Beta(2, 3)        | 1.211  | 0.739   | 0.625 | 1.157   | 0.351   | 0.268 | 1.128   | 0.199   | 0.118 |
|                   | 0.001  | 0.008   | 0.008 | 0.001   | 0.004   | 0.004 | 0.001   | 0.002   | 0.002 |
| Beta(2, 2)        | 1.062  | 0.593   | 0.537 | 1.019   | 0.231   | 0.216 | 0.995   | 0.106   | 0.092 |
|                   | 0.001  | 0.007   | 0.007 | 0.001   | 0.003   | 0.003 | 0.001   | 0.001   | 0.001 |
|                   | $\varepsilon_h \sim i.i.d. \text{ student-}t(5)$ |         |       |         |         |       |         |         |       |
| Beta(1, 3)        | 2.005  | 1.688   | 1.290 | 1.953   | 1.064   | 0.624 | 1.885   | 0.471   | 0.401 |
|                   | 0.002  | 0.012   | 0.014 | 0.002   | 0.011   | 0.009 | 0.002   | 0.005   | 0.005 |
| Beta(2, 2)        | 1.237  | 1.126   | 0.993 | 1.218   | 0.848   | 0.614 | 1.185   | 0.506   | 0.440 |
|                   | 0.001  | 0.007   | 0.010 | 0.001   | 0.007   | 0.007 | 0.001   | 0.005   | 0.004 |
| Beta(2, 2)        | 1.084  | 0.969   | 0.874 | 1.070   | 0.691   | 0.518 | 1.047   | 0.369   | 0.356 |
|                   | 0.001  | 0.006   | 0.008 | 0.001   | 0.006   | 0.006 | 0.001   | 0.004   | 0.004 |
|                   | high-frequency process: VAR(1)                   |         |       |         |         |       |         |         |       |
| Beta(1, 3)        | 1.935  | 1.271   | 0.939 | 1.890   | 0.772   | 0.492 | 1.842   | 0.419   | 0.288 |
|                   | 0.003  | 0.016   | 0.015 | 0.002   | 0.010   | 0.008 | 0.002   | 0.005   | 0.004 |
| Beta(2, 3)        | 1.177  | 0.864   | 0.811 | 1.155   | 0.610   | 0.505 | 1.136   | 0.468   | 0.359 |
|                   | 0.002  | 0.011   | 0.012 | 0.002   | 0.008   | 0.008 | 0.001   | 0.005   | 0.005 |
| Beta(2, 2)        | 1.036  | 0.706   | 0.729 | 1.023   | 0.477   | 0.458 | 1.008   | 0.326   | 0.299 |
|                   | 0.002  | 0.009   | 0.011 | 0.002   | 0.007   | 0.007 | 0.001   | 0.004   | 0.004 |
|                   | Legendre degree $L = 3$                          |         |       |         |         |       |         |         |       |
| Beta(1, 3)        | 1.955  | 0.727   | 0.484 | 1.846   | 0.248   | 0.178 | 1.804   | 0.123   | 0.081 |
|                   | 0.002  | 0.010   | 0.008 | 0.002   | 0.004   | 0.003 | 0.001   | 0.002   | 0.001 |
| Beta(2, 3)        | 1.211  | 0.642   | 0.491 | 1.157   | 0.313   | 0.201 | 1.128   | 0.181   | 0.094 |
|                   | 0.001  | 0.008   | 0.007 | 0.001   | 0.004   | 0.003 | 0.001   | 0.002   | 0.001 |
| Beta(2, 2)        | 1.062  | 0.508   | 0.414 | 1.019   | 0.200   | 0.156 | 0.995   | 0.094   | 0.069 |
|                   | 0.001  | 0.007   | 0.006 | 0.001   | 0.003   | 0.003 | 0.001   | 0.001   | 0.001 |

Table A.3: Shape of weights estimation accuracy I.

The table reports results for shape of weights estimation accuracy for the first four DGPs of Table A.1-A.2 using LASSO-U, LASSO-M and SGL-M estimators for the weight functions Beta(1, 3), Beta(2, 3) and Beta(2, 2) with sample size  $T = 50, 100$  and  $200$ . Entries in odd rows are the average point-wise mean squared error, and in even rows the simulation standard error.

|  | LASSO-U        |                |                | LASSO-M        |                |                | SGL-M          |                |                |       |
|--|----------------|----------------|----------------|----------------|----------------|----------------|----------------|----------------|----------------|-------|
|  | T=50           |                |                | T=100          |                |                | T=200          |                |                |       |
| Legendre degree $L = 10$                 |                |                |                |                |                |                |                |                |                |       |
| Beta(1, 3)                               | 1.955<br>0.002 | 1.155<br>0.013 | 0.952<br>0.011 | 1.846<br>0.002 | 0.378<br>0.006 | 0.386<br>0.006 | 1.804<br>0.001 | 0.163<br>0.001 | 0.179<br>0.002 | 0.003 |
| Beta(2, 3)                               | 1.211<br>0.001 | 0.902<br>0.008 | 0.885<br>0.009 | 1.157<br>0.001 | 0.423<br>0.005 | 0.370<br>0.005 | 1.128<br>0.001 | 0.225<br>0.001 | 0.162<br>0.002 | 0.002 |
| Beta(2, 2)                               | 1.062<br>0.001 | 0.747<br>0.007 | 0.775<br>0.008 | 1.019<br>0.001 | 0.293<br>0.004 | 0.314<br>0.005 | 0.995<br>0.001 | 0.126<br>0.001 | 0.135<br>0.002 | 0.002 |
| low frequency noise level $\sigma_1 = 5$ |                |                |                |                |                |                |                |                |                |       |
| Beta(1, 3)                               | 2.022<br>0.001 | 1.736<br>0.012 | 1.389<br>0.017 | 1.972<br>0.002 | 1.290<br>0.011 | 0.757<br>0.011 | 1.893<br>0.002 | 0.716<br>0.008 | 0.355<br>0.006 |       |
| Beta(2, 3)                               | 1.244<br>0.001 | 1.132<br>0.008 | 1.060<br>0.013 | 1.220<br>0.001 | 0.929<br>0.007 | 0.700<br>0.009 | 1.186<br>0.001 | 0.657<br>0.006 | 0.385<br>0.006 |       |
| Beta(2, 2)                               | 1.089<br>0.001 | 0.980<br>0.007 | 0.936<br>0.012 | 1.069<br>0.001 | 0.781<br>0.007 | 0.604<br>0.008 | 1.042<br>0.001 | 0.509<br>0.005 | 0.315<br>0.005 |       |
| Half high-frequency lags                 |                |                |                |                |                |                |                |                |                |       |
| Beta(1, 3)                               | 1.997<br>0.001 | 1.509<br>0.011 | 1.083<br>0.011 | 1.925<br>0.001 | 0.882<br>0.008 | 0.686<br>0.006 | 1.878<br>0.001 | 0.571<br>0.004 | 0.535<br>0.004 |       |
| Beta(2, 3)                               | 1.243<br>0.001 | 1.121<br>0.006 | 1.026<br>0.007 | 1.221<br>0.001 | 0.913<br>0.005 | 0.828<br>0.006 | 1.202<br>0.001 | 0.729<br>0.004 | 0.716<br>0.004 |       |
| Beta(2, 2)                               | 1.090<br>0.001 | 0.998<br>0.005 | 0.955<br>0.007 | 1.074<br>0.001 | 0.838<br>0.005 | 0.813<br>0.005 | 1.059<br>0.001 | 0.719<br>0.004 | 0.740<br>0.004 |       |
| Number of covariates $p = 50$            |                |                |                |                |                |                |                |                |                |       |
| Beta(1, 3)                               | 2.031<br>0.001 | 1.563<br>0.010 | 1.038<br>0.011 | 1.931<br>0.002 | 0.620<br>0.007 | 0.401<br>0.005 | 1.841<br>0.001 | 0.223<br>0.002 | 0.174<br>0.002 |       |
| Beta(2, 3)                               | 1.250<br>0.001 | 1.067<br>0.006 | 0.883<br>0.007 | 1.206<br>0.001 | 0.606<br>0.006 | 0.436<br>0.005 | 1.156<br>0.001 | 0.296<br>0.003 | 0.196<br>0.002 |       |
| Beta(2, 2)                               | 1.095<br>0.000 | 0.923<br>0.005 | 0.782<br>0.006 | 1.062<br>0.001 | 0.461<br>0.005 | 0.360<br>0.004 | 1.023<br>0.001 | 0.178<br>0.001 | 0.153<br>0.002 |       |

Table A.4: Shape of weights estimation accuracy II. – See Table A.3

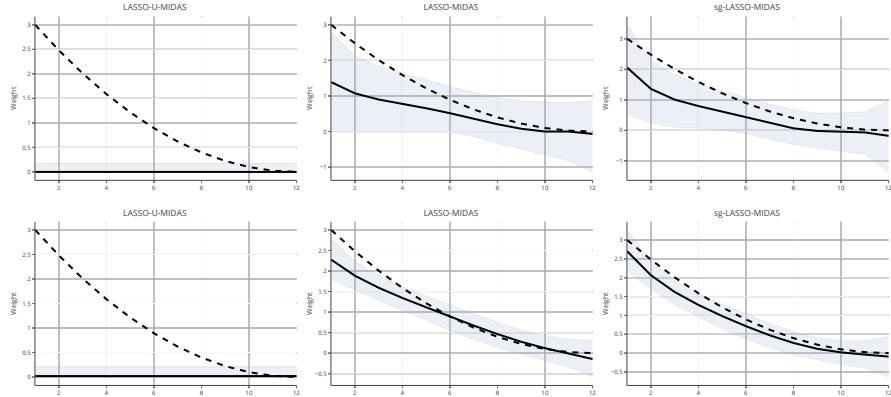


Figure A.1: The figure shows the fitted Beta(1,3) weights. We plot the estimated weights for the LASSO-U-MIDAS, LASSO-MIDAS and sg-LASSO-MIDAS estimators for the baseline DGP scenario. The first row plots weights for the sample size  $T = 50$ , the second row plot weights for the sample size  $T = 200$ . Black solid line is the median estimate of the weights function, black dashed line is the population weight function, and the grey area is the 90% confidence interval.

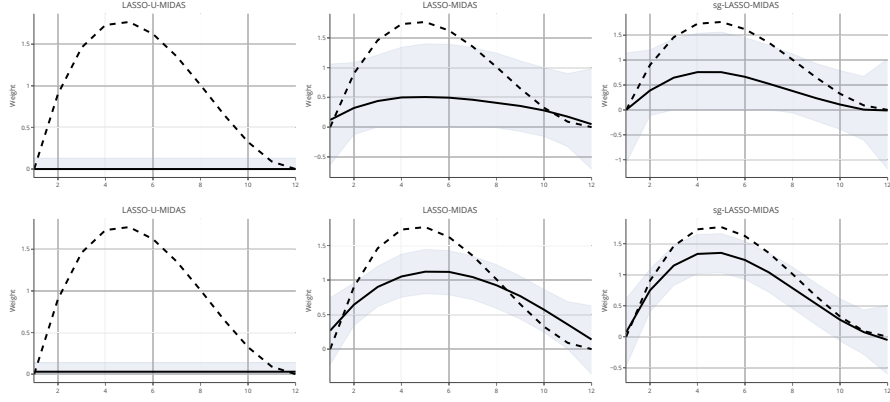


Figure A.2: The figure shows the fitted Beta(2,3) weights. We plot the estimated weights for the LASSO-U-MIDAS, LASSO-MIDAS and sg-LASSO-MIDAS estimators for the baseline DGP scenario. The first row plots weights for the sample size  $T = 50$ , the second row plot weights for the sample size  $T = 200$ . Black solid line is the median estimate of the weights function, black dashed line is the population weight function, and the grey area is the 90% confidence interval.

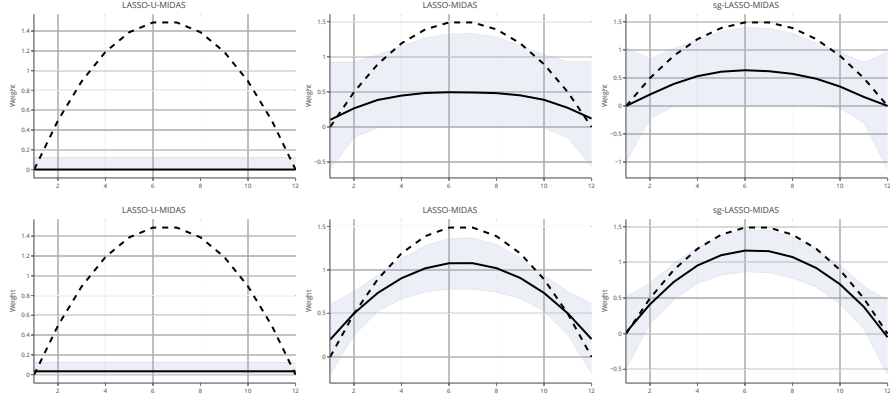


Figure A.3: The figure shows the fitted Beta(2,2) weights. We plot the estimated weights for the LASSO-U-MIDAS, LASSO-MIDAS and sg-LASSO-MIDAS estimators for the baseline DGP scenario. The first row plots weights for the sample size  $T = 50$ , the second row plot weights for the sample size  $T = 200$ . Black solid line is the median estimate of the weights function, black dashed line is the population weight function, and the grey area is the 90% confidence interval.

|                   | Average coverage (av. cov) |       |                           |       | Confidence interval length |       |                           |       |
|-------------------|----------------------------|-------|---------------------------|-------|----------------------------|-------|---------------------------|-------|
|                   | Active set of $\beta_0$    |       | Inactive set of $\beta_0$ |       | Active set of $\beta_0$    |       | Inactive set of $\beta_0$ |       |
| $M_T \setminus p$ | 20                         | 200   | 20                        | 200   | 20                         | 200   | 20                        | 200   |
| 10                | 0.929                      | 0.941 | 0.937                     | 0.950 | 0.355                      | 0.336 | 0.343                     | 0.312 |
| 20                | 0.940                      | 0.953 | 0.946                     | 0.954 | 0.372                      | 0.357 | 0.350                     | 0.313 |
| 40                | 0.947                      | 0.967 | 0.949                     | 0.959 | 0.389                      | 0.390 | 0.349                     | 0.310 |
| 60                | 0.952                      | 0.976 | 0.952                     | 0.965 | 0.403                      | 0.420 | 0.345                     | 0.307 |
| 80                | 0.957                      | 0.981 | 0.955                     | 0.972 | 0.417                      | 0.446 | 0.341                     | 0.304 |
| 100               | 0.962                      | 0.985 | 0.958                     | 0.978 | 0.429                      | 0.471 | 0.338                     | 0.301 |
| 120               | 0.965                      | 0.987 | 0.961                     | 0.983 | 0.441                      | 0.493 | 0.334                     | 0.299 |
| 140               | 0.969                      | 0.989 | 0.964                     | 0.985 | 0.452                      | 0.514 | 0.331                     | 0.296 |
| 160               | 0.972                      | 0.991 | 0.966                     | 0.987 | 0.463                      | 0.534 | 0.328                     | 0.294 |

Table A.5: HAC inference simulation results table – The table reports average coverage (first four columns) and average length of confidence intervals (last four columns) for active and inactive sets of  $\beta_0$ . The data is generated using Gaussian distribution. We report results for a set of truncation parameter  $M_T$  values. The long run variance is computed using Quadratic spectral kernel.

|                   | Average coverage (av. cov) |       |                           |       | Confidence interval length |       |                           |       |
|-------------------|----------------------------|-------|---------------------------|-------|----------------------------|-------|---------------------------|-------|
|                   | Active set of $\beta_0$    |       | Inactive set of $\beta_0$ |       | Active set of $\beta_0$    |       | Inactive set of $\beta_0$ |       |
| $M_T \setminus p$ | 20                         | 200   | 20                        | 200   | 20                         | 200   | 20                        | 200   |
| 10                | 0.944                      | 0.961 | 0.947                     | 0.958 | 0.376                      | 0.364 | 0.354                     | 0.325 |
| 20                | 0.953                      | 0.970 | 0.954                     | 0.961 | 0.397                      | 0.388 | 0.362                     | 0.324 |
| 40                | 0.961                      | 0.979 | 0.958                     | 0.966 | 0.422                      | 0.431 | 0.360                     | 0.320 |
| 60                | 0.968                      | 0.986 | 0.963                     | 0.971 | 0.443                      | 0.468 | 0.356                     | 0.317 |
| 80                | 0.973                      | 0.990 | 0.967                     | 0.978 | 0.463                      | 0.501 | 0.352                     | 0.314 |
| 100               | 0.977                      | 0.992 | 0.972                     | 0.984 | 0.481                      | 0.531 | 0.348                     | 0.311 |
| 120               | 0.980                      | 0.993 | 0.975                     | 0.988 | 0.498                      | 0.558 | 0.345                     | 0.308 |
| 140               | 0.983                      | 0.995 | 0.977                     | 0.990 | 0.514                      | 0.584 | 0.342                     | 0.305 |
| 160               | 0.984                      | 0.995 | 0.979                     | 0.991 | 0.529                      | 0.608 | 0.339                     | 0.302 |

Table A.6: HAC inference simulation results table – The table reports average coverage (first four columns) and average length of confidence intervals (last four columns) for active and inactive sets of  $\beta_0$ . The data is generated using student-t(5) distribution. We report results for a set of truncation parameter  $M_T$  values. The long run variance is computed using Quadratic spectral kernel.

## A.7 Detailed data description

To compute the main results reported in Table 3, we use thirty monthly macro series, eight quarterly survey covariates, and six news attention series which are aggregated using Legendre polynomials.<sup>32</sup> Thirty predictors are real-time macro series that are either directly taken from FRED-MD dataset, or are calculated by using FRED-MD series, denoted by FRED-MD and FRED-MD (calc.) respectively in the *Source* column of the data description table A.7 below. Note that for all monthly macro data, we use real-time vintages, which effectively means that we take all macro series with one month delay. For example, if we nowcast the first quarter of GDP one month ahead, we use data up to the end of February, and thus all macro series that enter the model are available up to the end of January. We then use Legendre polynomials of degree three for all covariates to aggregate twelve lags of monthly macro data. In particular, let  $x_{t+(h+1-j)/m,k}$  be  $k$ -th  $\in \{1, \dots, 30\}$  covariate at quarter  $t$ ,  $j = 1, \dots, 12$ ,  $m = 3$ , and  $h = 2$ , minus additional lag to account for the publication delay of macro series. Therefore, for macro series the first lag index is:  $(h + 1 - j - 1)/m = (2 + 1 - 1 - 1)/3 = 1/3$ . We then collect all lags in  $X_{tk}$  vector, i.e.

$$X_{tk} = (x_{t+1/3,k}, x_{t+0/3,k}, \dots, x_{t-11/3,k})$$

and aggregate  $X_{tk}$  using dictionary  $W$  consisting of Legendre polynomials,  $X_{tk}W$ . In this case,  $X_{tk}W$  is defined as a single group for the sg-LASSO estimator.

Furthermore, we use data from the Survey of Professional Forecasters (SPF) - nowcasts and forecasts - aggregated using Legendre polynomial of degree three. More precisely, denote  $x_{mean,t}^h$  and  $x_{median,t}^h$  the mean and median forecast at the horizon  $h$ . We collect all mean and median forecast horizons that do not have missing entries,  $h = 0, 1, 2, 3$ , in the  $X_t$  vector

$$X_t = (x_{mean,t}^0, x_{mean,t}^1, x_{mean,t}^2, x_{mean,t}^3, x_{median,t}^0, x_{median,t}^1, x_{median,t}^2, x_{median,t}^3),$$

and aggregate this data using the same dictionary  $W$ , i.e.  $X_tW$ , and define  $X_tW$  as a single group for the sg-LASSO. Note that SPF data is quarterly; therefore, we aggregate it cross-sectionally rather than time series.

Lastly, we take six news attention series from <http://structureofnews.com/>, see Table A.7, and, as for macro series, use Legendre polynomials of degree three to aggregate twelve monthly lags of each attention news series. However, in this case, news attention series is used without a publication delay, that is, for the one-month horizon, we take the series up to the end of the second month.

We compute the predictions by using the expanding window scheme. The first nowcast is for the 2002 Q1, the effective sample size is from 1990 February to 2001 November, and the prediction is computed using 2002 February data. We calculate predictions until

---

<sup>32</sup>We transform all macro covariates using transformations suggested by McCracken and Ng (2016), see Table A.7. We then standardize all covariates before the aggregation step.

the sample is exhausted, which is 2017 Q2, the last date for which news attention data is available.

|    | id  | Source                               | T-code |
|----|---|--------------------------------------|--------|
| 1  | Commodities                                 | Bybee, Kelly, Manela, and Xiu (2019) | 1      |
| 2  | Government budgets                          | Bybee, Kelly, Manela, and Xiu (2019) | 1      |
| 3  | Oil market                                  | Bybee, Kelly, Manela, and Xiu (2019) | 1      |
| 4  | Recession                                   | Bybee, Kelly, Manela, and Xiu (2019) | 1      |
| 5  | Savings & loans                             | Bybee, Kelly, Manela, and Xiu (2019) | 1      |
| 6  | Mortgages                                   | Bybee, Kelly, Manela, and Xiu (2019) | 1      |
| 7  | IP: Business Equipment                      | FRED-MD                              | 5      |
| 8  | IP: Fuels                                   | FRED-MD                              | 5      |
| 9  | IP: Manufacturing (SIC)                     | FRED-MD                              | 5      |
| 10 | IP: Durable Consumer Goods                  | FRED-MD                              | 5      |
| 11 | Civilians Unemployed - Less Than 5 Weeks    | FRED-MD                              | 5      |
| 12 | All Employees: Financial Activities         | FRED-MD                              | 5      |
| 13 | All Employees: Government                   | FRED-MD                              | 5      |
| 14 | Initial Claims                              | FRED-MD                              | 5      |
| 15 | All Employees: Total nonfarm                | FRED-MD                              | 5      |
| 16 | All Employees: Service-Providing Industries | FRED-MD                              | 5      |
| 17 | All Employees: Mining and Logging: Mining   | FRED-MD                              | 5      |
| 18 | Unemployment Rate                           | FRED-MD                              | 2      |
| 19 | All Employees: Manufacturing                | FRED-MD                              | 5      |
| 20 | Housing Starts, Midwest                     | FRED-MD                              | 4      |
| 21 | Housing Starts, West                        | FRED-MD                              | 4      |
| 22 | Housing Starts: Total New Privately Owned   | FRED-MD                              | 4      |
| 23 | Retail and Food Services Sales              | FRED-MD                              | 5      |
| 24 | New Orders for Durable Goods                | FRED-MD                              | 5      |
| 25 | MZM Money Stock                             | FRED-MD                              | 6      |
| 26 | Personal Cons. Expend.: Chain Index         | FRED-MD                              | 6      |
| 27 | CPI: All Items                              | FRED-MD                              | 6      |
| 28 | S&P: Industrials                            | FRED-MD                              | 5      |
| 29 | 3-Month AA Fin. Comm. Paper Rate            | FRED-MD                              | 2      |
| 30 | Crude Oil                                   | FRED-MD                              | 6      |
| 31 | 5-Year Treasury                             | FRED-MD                              | 2      |
| 32 | 3-Month Commercial Paper - FEDFUNDS         | FRED-MD                              | 1      |
| 33 | Moodys Baa Corporate Bond - FEDFUNDS        | FRED-MD                              | 1      |
| 34 | 10-Year Treasury                            | FRED-MD                              | 2      |
| 35 | S&P 500                                     | FRED-MD                              | 5      |
| 36 | Moodys Baa - Aaa Corporate Bond Spread      | FRED-MD (calc.)                      | 1      |
| 37 | Survey of professional forecasters          | Phil. Fed                            | 1      |

Table A.7: Data description table – The *id* column gives mnemonics according to data source, which is given in the second column *Source*. The column *T-code* denotes the data transformation applied to a time-series, which are: (1) not transformed, (2)  $\Delta x_t$ , (3)  $\Delta^2 x_t$ , (4)  $\log(x_t)$ , (5)  $\Delta \log(x_t)$ , (6)  $\Delta^2 \log(x_t)$ .

## A.8 Additional results for empirical application

### A.8.1 Full-sample nowcasting results

As for the main results, we benchmark our predictions with the simple random walk (RW) model. We implemented the following alternative machine learning nowcasting methods. The first method is the PCA factor-augmented autoregression, where we estimate the first principal component of a monthly macro panel and use it together with four autoregressive lags. We denote this model PCA-OLS. We then consider three alternative penalty functions for the same linear model: Ridge, LASSO and Elastic Net. For these methods, we leave high-frequency lags unrestricted, and thus we call these methods the unrestricted MIDAS (U-MIDAS). Lastly, we use sg-LASSO estimator, where we also aggregate high-frequency lags using MIDAS weights. The weight function is approximated by using Legendre polynomials of degree three. For each method, we use four lags of GDP and twelve lags of each high-frequency covariates. The first prediction is for the 2002 Q1, and we use expanding window scheme up until 2017 Q2. In this case, we use larger samples to estimate all models, and thus the effective sample starts from 1960 February. For each quarter, we take predictors that do not have missing values. In addition, we compute corporate bond spread and discard NONBORRES series due to a possible break in this series, see [Uematsu and Tanaka \(2019\)](#). In total, the number of covariates (without taking into account lags) ranges from 94 to 114.

In Table A.8, we report out-of-sample nowcasting results for one-month horizon using real-time data vintages. We report root mean squared forecast error relative to the RW model (column Rel-RMSE) and the Diebold Mariano predictive accuracy test statistic (DM). In addition to models we implemented, we compare GDP growth nowcasts provided by the New York Fed (denoted NY Fed). The column DM-stat-1 reports Diebold Mariano test statistic where we compare NY Fed predictions with other methods, and the column DM-stat-2 compares sg-LASSO-MIDAS with alternative methods.

Using full-sample data, sg-LASSO-MIDAS model also gives smaller forecast errors when compared with NY Fed predictions, however, the gains are not statistically significant. Nonetheless, sg-LASSO-MIDAS model nowcasts give significantly smaller prediction errors compared with other alternative machine learning methods.



Figure A.4: Sparsity pattern for 50 most selected covariates.

|                     | Rel-RMSE | DM-stat-1 | DM-stat-2 |
|---------------------|----------|-----------|-----------|
| RW                  | 2.606    | 2.370     | 3.318     |
| PCA-OLS             | 0.849    | 0.854     | 1.975     |
| Ridge-U-MIDAS       | 0.838    | 0.763     | 1.974     |
| LASSO-U-MIDAS       | 0.853    | 0.967     | 2.039     |
| Elastic Net-U-MIDAS | 0.833    | 0.699     | 1.888     |
| sg-LASSO-MIDAS      | 0.750    | -0.739    |           |
| NY Fed              | 0.790    |           | 0.739     |

Table A.8: Nowcast comparison table – Forecast horizon is one month ahead. Column *Rel-RMSE* reports root mean squared forecasts error relative to the RW model. Column *DM-stat-1* reports Diebold and Mariano (1995) test statistic of all models relative to NY Fed nowcasts, while column *DM-stat-2* reports the Diebold Mariano test statistic relative to sg-LASSO-MIDAS model. Out-of-sample period: 2002 Q1 to 2017 Q2.

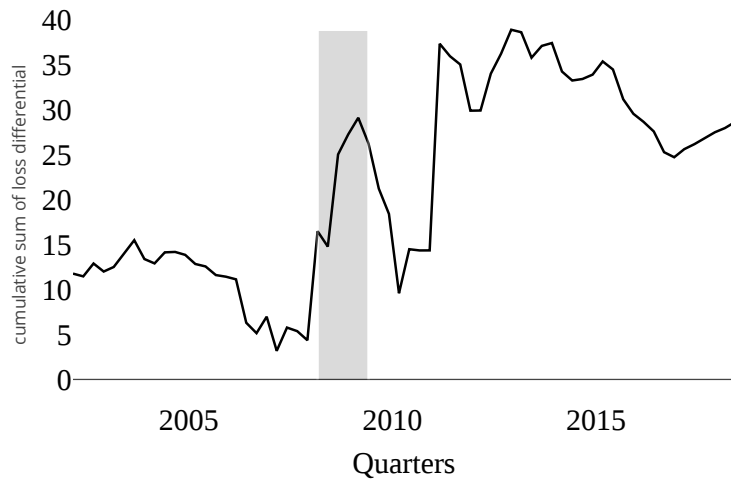


Figure A.5: Cumulative sum of loss differential. Gray shaded area — NBER recession period.

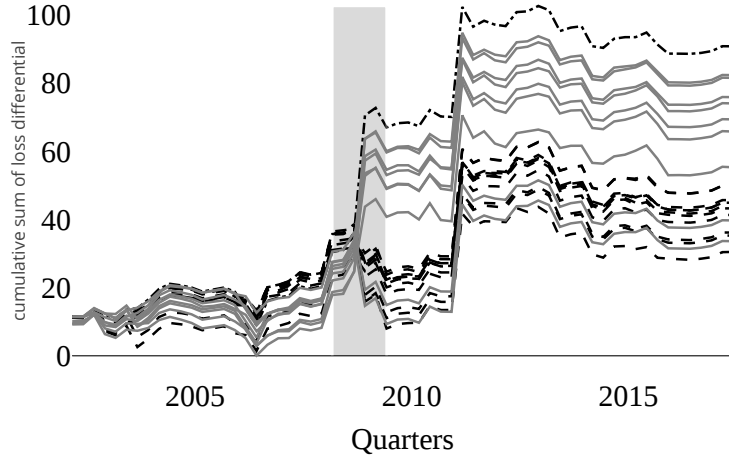


Figure A.6: Cumulative sum of loss differentials (cumsfe) of New York Fed nowcasts compared with sg-LASSO-MIDAS model with textual analysis based data for different  $\alpha \in [0, 1]$  value. Dashed black lines are cumsfe's for  $\alpha \in [0, 0.5]$ , gray solid lines -  $\alpha \in (0.5, 1]$  excluding 0.65, and dash-dotted black line - cumsfe for  $\alpha = 0.65$ . Gray shaded area — NBER recession period.

Table A.9: Significance test table

| $M_T$              | 10     | 20     | 30     |
|--------------------|--------|--------|--------|
| Commodities        | 3.152  | 3.271  | 3.024  |
| Government budgets | 16.461 | 13.512 | 13.680 |
| Oil market         | 11.216 | 9.796  | 12.068 |
| Recession          | 5.843  | 4.720  | 4.132  |
| Savings & loans    | 1.900  | 2.275  | 2.440  |
| Mortgages          | 1.923  | 2.728  | 3.031  |

Table A.10: Significance test table – Wald test statistic values for news attention series for a set of truncation parameter  $M_T$  values. The number of lags in the HAC estimator correspond to  $M_T$ . The critical value at 5% is 9.488.